Pathways in pluripotency and differentiation of embryonic cells

Leonie du Puy

ISBN 978-90-393-5246-5
Copyright © 2009 Leonie du Puy

Printed in the Netherlands by Digital Printing Partners, Houten
Printing of this thesis was financially supported by the J.E. Jurriaanse Stiching

Cover design and layout by Marije Brouwer and Harry Otter, Division Multimedia, Faculty of Veterinary Medicine
Cover Illustration: embryonic day 7 porcine blastocyst

The research described in this thesis was performed at the Department of Farm Animal Health, Faculty of Veterinary Medicine, Utrecht University, the Netherlands

Pathways in pluripotency and differentiation of embryonic cells

Pluripotentie en differentiatie van embryonale cellen
(met een samenvatting in het Nederlands)

Proefschrift

ter verkrijging van de graad van doctor aan de Universiteit Utrecht
op gezag van de rector magnificus, prof. dr. J.C. Stoof,
ingevolge het besluit van het college voor promoties
in het openbaar te verdedigen op donderdag 7 januari 2010
des ochtends te 10.30 uur

door

Leonie du Puy

geboren op 18 april 1981 te IJzendijke

Promotores: Prof. dr. B. Colenbrander
Prof. dr. H.P. Haagsman

Co-promoter: Dr. B.A.J. Roelen

Contents

Chapter 1	General introduction	1
Chapter 2	Characterization and culture of the pluripotent cell population of porcine blastocysts	21
Chapter 3	Differentiation of porcine ICM cells into proliferating neural cells	43
Chapter 4	Cazip, a novel protein expressed in the developing heart and nervous system	65
Chapter 5	Early embryonic expression pattern of Sarcosin in mice and its localization and knock-down in differentiating C2C12 myoblasts	83
Chapter 6	Summarizing Discussion	105
Chapter 7	Summary in Dutch	117
	Acknowledgements	125
	Curriculum Vitae	127
	List of publications	128

Chapter 1

General introduction

General introduction

Embryonic stem (ES) cells have the ability to self-renew while keeping their undifferentiated state and are pluripotent, meaning that they are able to give rise to all cell types found in the adult organism. These cells are generated from the inner cell mass (ICM) of embryos at the blastocyst-stage of development. ES cell lines are the result of over 50 years of research, starting with the discovery of the mouse strain 129/Sv in which testicular teratocarcinomas occur at high frequency [1]. Teratocarcinomas contain a population of cells named embryonal carcinoma (EC) cells that are pluripotent, as injection of these cells into blastocysts led to the formation of chimeras with tumor-derived cells in tissue-types of all three germ layers [2]. Cell lines from EC cells were first cultured as ascites, transplanted every two to three weeks into a new host. Later, *in vitro* cultures were developed using a feeder-cell layer of mitotically inactivated fibroblasts (MEFs) [3, 4]. As teratocarcinomas can be induced *in vivo* by transplantation of an early mouse embryo to extra-uterine sites of another mouse, attempts were made to culture embryonic cells directly from a preimplantation mouse embryo. By applying the same conditions used to culture EC cells, the first ES cell lines were generated independently by two groups in 1981 [5, 6]. The ultimate proof of pluripotency was given in 1984 when it was demonstrated that these cells contributed to the germ line after injection into a blastocyst [7].

Still, it took till 1998 before the first human ES cell line was generated [8]. With this, the definition of an ES cell line was set: an ES cell line must be derived from a preimplantation embryo, be capable of unlimited self-renewal and able to differentiate into derivatives of the three germ layers. Though for ethical reasons not possible in humans, forming germ-line chimeras after tetraploid complementation is the decisive test whether a cell line is truly pluripotent. *In vitro* however, human ES cells are capable of differentiating into cells expressing markers of germ cells, providing some evidence for the germline potential of these cells [9]. To this day ES cell lines, meeting the mentioned criteria and proven to contribute to the germline have been generated from mouse and rat, the latter needing special culture conditions using small molecule inhibitors [10, 11]. Numerous groups have reported the isolation and culture of what have been presented as “ES-like” cell lines from various species (Figure 1, [11-27]). These cell lines were not demonstrated to be pluripotent àn capable of unlimited self-renewal: germline chimera production after long-term culture has never been reported, hence the name “ES-like” cell lines. In this chapter the potential use of farm animal-derived ES cell lines, with an emphasis on the pig, and the difficulties involved in generating these cell lines are discussed.

species characteristics	human [8]	mouse [5-7]	monkey [12-14]	rat [10-11]	cow [15-17]	horse [18, 19]	sheep [20]	Goat [21]	pig [20, 22-27]
SSEA1 expression	neg	pos	pos	pos	pos [17] neg [16]	pos	n.r.	n.r.	pos, in less than 5% of the cells [22]
SSEA3 expression	pos	neg	pos	n.r.	neg [17]	neg [18]	n.r.	n.r.	n.r.
SSEA4 expression	pos	neg	pos	neg	pos [16] neg [17]	pos [19] neg [18]	n.r.	n.r.	n.r.
TRA-1-60 expression	pos	neg	pos	neg	n.r.	pos [19]	n.r.	n.r.	n.r.
TRA-1-81 expression	pos	neg	pos	n.r.	n.r.	pos [19]	n.r.	n.r.	n.r.
Oct4 expression	pos	pos	pos	pos	pos [16, 17]	pos	n.r.	n.r.	n.r.
Nanog expression	pos	pos	pos	pos	n.r.	n.r.	n.r.	n.r.	n.r.
Alkaline phosphatase activity	pos	pos	pos	pos	neg [15] pos [16, 17]	pos [18] pos, tested with ICC [19]	n.r.	pos	pos [23]
LIF depency	neg	pos	neg	pos	n.r., but differentiation without feeders in presence of LIF [17] n.r., but cultured in presence of LIF [16] n.r., but cultured on feeders without LIF [15]	n.r., but differentiation without feeders in the presence of LIF [18] n.r., but differentiation on feeders in absence of LIF [19]	n.r.	n.r.	No delay of ES-like cell differentiation by LIF stimulation [24] High LIF concentrations delay proliferation decline [22]
Maximum number of passages	since 1998	since 1981	Rhesus monkey > 1 year [12] Common Marmoset > 1 year [13] Cynomolgous monkey > 6 months [14]	> 60 passages [10] > 6 months [11]	>20 passages [17] >1 year [15] >1 year, passage every 14 days [16]	≥ 56 passages, weekly passage [18] >28 passages [19]	< 3 passages	< 8 passages	> 35 passages, morphological analysis [23 <11 passages (3 months) [25]

***in vitro* lineage differentiation**	3 lineages	3 lineages	3 lineages	n.r.	ectoderm; morphological, RT-PCR and ICC analysis [17] 3 lineages; morphological and ICC analysis [16]	2 lineages (ectoderm, mesoderm); morphological, RT-PCR and ICC analysis [18] 3 lineages, RT-PCR and ICC analysis [19]	n.r.	ectoderm; morphological and ICC analysis	3 lineages; morphological analysis [27]
Embryoid body formation	pos	pos	pos	Pos [18] n.r. [19]	pos [16, 17]	pos	n.r.	pos	pos [25, 27]
teratocarcinoma formation	pos	pos	pos	pos	n.r.	No teratocarcinoma formation in SCID mice [19]	n.r.	n.r.	No teratoma formation in athymic mice [20] Teratoma formation in nude mice after injection of passage 3 and 4 ES like cells [25]
Chimera formation	n/a	germline chimeras	n.r.	pos	After injection of passage 3 ES-like cells into morulas transgenic chimeric blastocysts were obtained *in vitro* [16] Passage 3 transgenic ES-like cells led to chimeric calves with transgenic oocytes [15]	n.r.	n.r.	n.r.	Tested, but no chimerism detected [20, 26, 27] Chimeric piglets but no germline chimerism [23]

Figure 1: Characteristics of ES-like cell lines generated from various species.
References are indicated between brackets. Abbreviations: n.r., not reported; n/a, not applicable; pos, positive; neg, negative; ICC, immunocytochemistry; LIF, leukemia inhibitory factor.

Potential of farm animal-derived ES cell lines

One of the major potentials of human ES cells is their possible clinical application in stem cell-based therapies to treat medical disorders by replacement of lost or damaged tissue. Pigs, and ES cell lines derived from these species, can be very useful in testing the safety and feasibility of these therapies in human medicine. In this regard, pigs have greater similarities in anatomy, physiology, immunology and life span with humans than mice [28, 29]. Also, use of porcine cells would circumvent the ethical concerns raised by research in humans and monkeys and the physiological concerns as lifespan and genetic background raised by research in mice. Therefore we have focused our research on the derivation of porcine ES cell lines.

Via genetically modified cells and somatic cell nuclear transfer (SCNT) transgenic farm animals can be generated. For example, sheep were generated that produced a human therapeutic protein in their milk [30], pigs with organs less likely to be rejected after xenotransplantation [31] and sheep likely to be more resistant to prion diseases [32]. However, homologous recombination is not very efficient in primary somatic cells and the success rate of nuclear transfer leading to viable offspring is small [33, 34]. On the other hand, transgenic mice can be made with high efficiency through gene targeting of ES cells, injection of these cells in blastocysts and the subsequent generation of germline chimeras. Therefore, ES cell lines from domestic animal species would greatly facilitate gene targeting of these animals and simplify the use of this application in biomedical sciences.

The current world production of meat is accompanied by high energy demands and global pollution, and animal welfare has also been considered an issue of concern. A possible alternative for conventional meat production is the generation of in vitro meat. In vitro meat, also known as engineered meat or cultured meat, is an edible meat product produced from animal muscle cells cultured *in vitro*. In vitro meat could serve as a solution for above mentioned problems. For the production of in vitro meat, cells are needed that are able to self-renew in culture and upon stimulation differentiate into skeletal muscle cells and fuse to form muscle fibers. Self-renewal of the cells is important to ensure that no animals need to be sacrificed for the repeated isolation of cells to produce muscle fibers. Therefore, the possibility of generating and culturing stem cells from farm animal species needs to be investigated

Besides these practical examples of the use of ES cells from livestock species, more basic questions are in need of being answered. Apparent differences exist between mouse and human ES cell lines, the embryos they are derived from, and the cell signalling pathways responsible for their pluripotency and self-renewal (Table 1, [35-41]). Possibly, the dissimilarities between mouse and human ES cells result from differences in early embryonic development between these species. Therefore, it would be of interest to determine the signalling pathways responsible for pluripotency and

self-renewal in farm animal ES cells, and the embryos they are derived from, and to evaluate how these cells compare to mouse and human ES cells.

Table 1 Differences between human and Mouse ES cell lines [a,b]

ES cell line	Origin	Differentiation capacity	Signal transduction pathways involved in self-renewal and differentiation
mouse	derived from *in vivo* embryos derived from inbred strains derived from the ICM of blastocysts	Not capable of differentiation into the extra-embryonic lineages [41]	LIF dependent [35] BMP inhibits (neural) differentiation [38] and supports self-renewal [37]
Human	derived from *in vitro* embryos outbred (donated IVF embryos) derived from the epiblast of early embryonic disc stage embryos	Capable of differentiating into the extra-embryonic lineages [40]	LIF independent [36] BMP induces differentiation into the extra-embryonic lineages [39,40]

[a]References are indicated in brackets, [b]Abbreviations: ICM, inner cell mass; IVF, in vitro fertilization; LIF, leukemia inhibitory factor.

Developmental stage optimal for pluripotent cell isolation

The optimal time window for pluripotent cell isolation from embryos to generate ES cell lines of farm animal species is not known. In mice, pluripotent embryonic cell lines can be generated from ICM cells of pre-implantation blastocysts and from epiblast cells of post-implantation embryos (EpiSCs), although germline transmission of these epiblast-derived cell lines was not observed [42, 43].

Remarkable differences exist between peri-implantation development of mice, man and ungulates. Development from the zygote up to the segregation of the trophectoderm and ICM development is rather similar, though there are some differences in time span between fertilization and blastocyst formation (Table 2, [44-54]). After blastocyst formation, the polar trophectoderm (adjacent to the ICM) in mice starts to proliferate, giving rise to the ectoplacental cone and formation of an egg cylinder. In human embryos an embryonic disc is formed (Figure 2). In both species the blastocyst subsequently penetrates the endometrium, a process called invasive implantation. In pigs the polar trophectoderm (Rauber's layer) degenerates after zona shedding, uncovering the embryonic disc; the blastocyst expands to a spherical structure and this expansion is followed by a rapid elongation of the trophectoderm.

Table 2: Key time points during embryonic development[a]

	morula (dpc)	blastocyst formation (dpc)	onset of elongation (dpc)	implantation (dpc)()[b]	primitive mesoderm formation (dpc)	primitive streak formation (dpc)	gestation time (dpc)
Human [44][c]	3-4	4-5	n/a	7-10 (invasive)	12	13-14	280
Murine [45]c	2	3.5	n/a	4.5 (invasive)	n/a	6.5	19
Bovine [46-48][c]	4-5	6-7	13	21-22 (non invasive)	14	14-15	285
Caprine [46,47][c]	4-5	6	13	19-20 (non invasive)	13-15	14-16	150
Ovine [4, 49, 50][c]	3-4	6	11	15-18 (non invasive)	12-13	13-14	150
Equine [46,51][c]	4-5	6-8	n/a	36-38 (non invasive)	12	13-14	340
Porcine [47, 52-54][c]	3-4	4-5	9-12	14-18 (non invasive)	9	11-13	115

[a]dpc, days post conception; n/a, not applicable. [b]Method of implantation. [c]Referencs are indicated in brackets.

The blastocyst transforms into a filamentous conceptus that can be more than 1000 mm in length [54]. The rapid change in morphology of the blastocyst from tubular (10 mm) to filamentous conceptus (100 mm) occurs within a few hours and the trophoblast elongates at a rate of 30-45 mm/h. This rapid elongation is a consequence of extensive cellular remodelling and not of cellular hyperplasia. Elongation of the trophoblast is necessary for maternal recognition of pregnancy as this increases the uterine surface area stimulated by the blastocyst [55]. Thus, while in mice and man blastocyst formation is rapidly followed by invasive implantation of the blastocyst into the uterine wall, in farm animal species the preimplantation period is extended. Following trophectoderm differentiation, the second event in embryogenesis is the formation of the primitive endoderm layer. Cells of this layer will participate in formation of the extra-embryonic structures. Next, mesoderm formation starts and the primitive streak is formed. In man, pigs, domestic ruminants and horses primitive mesoderm cells migrate between the trophectoderm and the primitive endoderm; they will form the yolk sac by fusion with the primitive endoderm and the chorion by fusion with the trophoblast.

Aggregates of these primitive mesoderm cells are located at a single pole of the epiblast and appear before any sign of primitive streak formation [48, 50, 53]. This is in contrast to mesoderm formation in rodents, where extra-embryonic mesoderm is formed from cells migrating through the primitive streak.

How these differences in early embryonic development between species influence the generation of ES cell lines is unknown. Studying primary ICM cultures of farm animal embryos of different stages in early development will help to identify the developmental stage for ES cell line generation from embryos of these species.

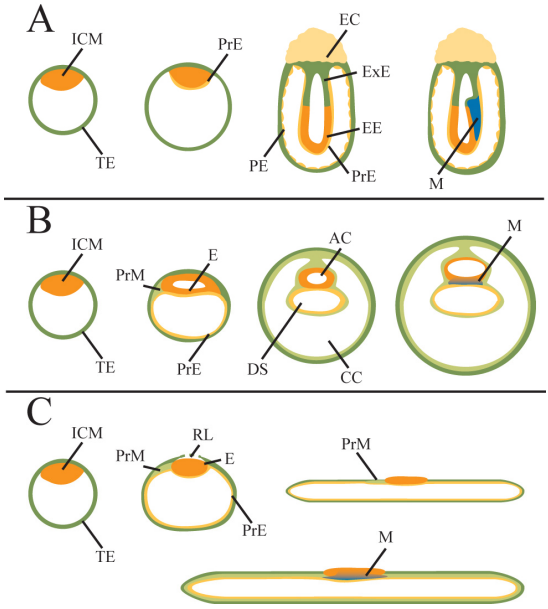

Figure 2: Illustration of the early embryonic development of mice, man, ruminants and pigs. Early embryonic development of A: mice, B: Man, and C: ruminants and pigs. Illustration not to scale. ICM, inner cell mass; TE, trophectoderm; PrE, primitive endoderm; EC, ectoplacental cone; PE, parietal endoderm; EE, embryonic ectoderm; M, mesoderm; ExE, extra-embryonic ectoderm; E, epiblast; PrM, primitive mesoderm; AC, amniotic cavity; CC, chorionic cavity; DS, definitive yolk sac; RL, Rauber's layer.

Culture conditions

For the generation of mouse and human ES and EC cell lines, a feeder layer of mitotically inactivated embryonic fibroblasts has been of critical importance. Commonly used feeder cells are primary mouse embryonic fibroblasts (MEFs) and the

immortalized mouse embryonic fibroblast STO cell line. Feeder layers provide a microenvironment that suppresses differentiation during stem cell proliferation. Feeder cells secrete ligands of signalling pathways such as fibroblast growth factors (FGFs), transforming growth factor (TGF) betas, Wnts and leukaemia inhibitory factor (LIF) and these signalling pathways play different roles in the self-renewal and differentiation of mouse and human ES cells. Murine ES cells can be cultured in an undifferentiated state in feeder-free conditions in the presence of recombinant LIF [35]. LIF activates the JAK-STAT pathway [56] and the ERK-MEK-ras-raf pathway [57]. Although human ES cells express a functional LIF-STAT3 signalling pathway, these cells are not dependent on LIF and addition of LIF to feeder-free culture conditions does not maintain the pluripotency of human ES cells [36].

Besides LIF, undifferentiated growth of mouse ES cells is dependent on fetal calf serum. Without serum, mouse ES cells differentiate along the neural pathway. This inhibitory effect of serum on neural differentiation is induced by bone morphogenetic proteins (BMPs) through the expression of *inhibitor of differentiation* (Id) genes via the SMAD pathway [38, 58]. Mouse ES cells can be cultured in an undifferentiated state in the absence of feeders and serum when LIF and BMP4 are present in the medium. In human ES cells however, BMPs induce differentiation towards extra-embryonic lineages [37, 40]. Moreover, presence of the BMP inhibitor NOGGIN together with high levels of basic fibroblast growth factor (bFGF) maintain human ES cells in an undifferentiated state under feeder-free conditions [39, 59]. These results illustrate that there are a number of differences between human ES and mouse ES cells. Surprisingly, mouse EpiSCs remained pluripotent using human ES cell culture conditions but not using mouse ES cell culture conditions [42, 43].

LIF and bFGF have been most often used in attempts to generate ES cell lines from farm animal species (Fig 1 and references therein), but the addition of these growth factors to the culture medium has not been sufficient to generate ES cell lines from these species. It would be interesting to explore whether porcine ICM/epiblast cells can be cultured *in vitro* in a pluripotent state by stimulating signalling pathways that have been demonstrated to be important for maintenance of human ES and mEpiSCs.

Another challenge in the derivation and culture of ES cells is the sub-culturing of these cells. Autocrine and paracrine signalling between ES/embryonic cells influence pluripotency and differentiation [60]. Disruption of colonies to a single cell suspension often leads to differentiation and this is probably due to a loss of contact and communication between ES/embryonic cells. While mouse ES cells are generally less sensitive to single cell dissociation using enzymes such as trypsin or collagenase, human ES cells are often passaged mechanically keeping cell-cell contact intact as much as possible. Medium conditioned by EC cells promoted the generation of mouse ES cell lines [5], and the derivation of ES cell lines from single blastomeres was done

by co-culturing these blastomeres with existing ES cell lines [61, 62], demonstrating the importance of signalling between ES cells. Bovine ES-like cell lines have been reported that were sensitive to enzymatic passaging [16], and medium conditioned by mouse ES cells had a positive effect on the self-renewal capacity of goat ES-like cells, although these cells were lost after eight passages [21]. The sub-culturing method that will enable the undifferentiated growth of ES cells from farm animal species still needs to be established.

Cellular markers of pluripotency

To identify undifferentiated ES cells in initial cultures and to characterize newly generated ES cell lines it is important to have reliable cellular markers for pluripotency. Several mouse and human gene products important for the maintenance of a pluripotent cell population have been identified, the key players being the transcription factors OCT4, NANOG and SOX2 [63-68].

The OCT4 homologue has also been identified in other mammalian species and its expression pattern has been studied in bovine, porcine and caprine embryos [69-73]. In all three species, OCT4 expression was observed in the trophectoderm as well as in the epiblast of early blastocysts. This is in contrast to the expression pattern in mice, where OCT4 expression is rapidly down-regulated in the trophectoderm and is restricted to the epiblast upon blastocyst formation. In human embryos OCT4 expression becomes restricted to the ICM after blastocyst formation and this restriction coincides with optimal derivation efficiencies of human ES cell lines from these ICMs [74]. The developmental stage at which OCT4 expression is restricted to the pluripotent cell mass of porcine embryos is unknown, and whether restriction of OCT4 expression to the ICM is of influence on the establishment of farm animal ES cell lines needs to be examined.

NANOG, a homeodomain-containing transcription factor, is expressed in pluripotent ES cells, the inner cells of the late mouse morula, the ICM of preimplantation embryos and in primordial germ cells. Forced NANOG expression in mouse ES cells circumvents the LIF dependency of these cells [67, 68]. NANOG protein expression has been described in *in vitro* produced bovine blastocysts and in preimplantation goat embryos [71, 73]. In bovine embryos NANOG protein was restricted to the ICM of blastocyst stage embryos; in porcine oocytes and embryos NANOG protein expression was undetectable [73]. In goat, NANOG mRNA was first detected at the eight cell stage and in later stages NANOG was highly expressed in the ICM and to a much lower extent in the trophectoderm. A similar pattern was described for NANOG protein. NANOG protein expression in the trophectoderm was located mainly in the nucleoli, possibly indicating a mechanism of inactivation [71].

Transcription factors and their effectors, other than NANOG and OCT4, contribute to the long-term, undifferentiated culture of ES cells (reviewed in [75]). Over-expression in embryonic fibroblasts of four exogenous factors (OCT4, SOX2, C-MYC and KLF4) reprograms these cells to a pluripotent state and enables these cells to self-renew [76-78]. For this, the cells must be cultured in medium that sustains the growth of ES cells. Porcine fibroblasts can also be reprogrammed using above mentioned factors [79-81]. However, these induced pluripotent stem cells (iPS) lose their pluripotency and self-renewal capacity upon removal of these exogenous factors, suggesting that unidentified growth factors are required in the culture medium in order to maintain porcine iPS in a pluripotent state.

Overall, validated pluripotent cell lines from livestock species will greatly enrich our knowledge about differences in early embryonic development between species and in signal transduction pathways involved in pluripotency and differentiation of early embryonic cells. Both characterizing the temporal-spatial expression of OCT4, NANOG and SOX2 in farm animal embryos, and studying the function of different signalling pathways in the survival and self-renewal of cultures of primary ICM cells will help to identify the conditions needed to generate ES cell lines from these species.

Muscle differentiation

ES cells differentiated to the muscle-lineage can potentially be of therapeutic use in tissue regeneration. For example, in mice, intra-muscular transplantation of a cell population derived from differentiating ES cells resulted in engraftment of muscle fibers and enhanced muscle contraction [82]. Also, differentiation of ES cells into the muscle-lineage can be studied to identify novel genes important in muscle differentiation and genetically modified ES cells could be used as *in vitro* models for muscle diseases [83]. For the production of in vitro meat, stem cells have to be triggered to differentiate into the muscle lineage in a controlled and efficient manner. As most *in vitro* differentiation processes of stem cells to a certain specialized lineage follow the same path as the *in vivo* formation of that tissue during embryonic development, a proper understanding of how muscle differentiation is organized is therefore essential.

Skeletal muscle formation

Embryonic skeletal muscle derives from somites, blocks of segmented paraxial mesoderm at either side of the neural tube. Somites arise in a cranio-caudal direction: the somites bud off from the anterior part of the paraxial mesoderm at regular intervals in a bilaterally symmetric manner to form a series of repeating epithelial structures.

During maturation the somite becomes subdivided into compartments: the dermomyotome that will give rise to the dermis of the skin and which will form skeletal and smooth muscle tissue, and the sclerotome that will give rise to the vertebral column and ribs (Figure 3) [84]. Subdivision of these somite compartments and the onset of myogenesis are regulated by signals from the surrounding neural tube, notochord and ectoderm. Sonic Hedgehog (SHH) and Noggin signals from the notochord are responsible for the epithelial to mesenchymal transition that forms the sclerotome, while dorsal Wnt signals from the neural tube and surface ectoderm play a role in the establishment of the dermomyotome (for review and references therein: [85]).

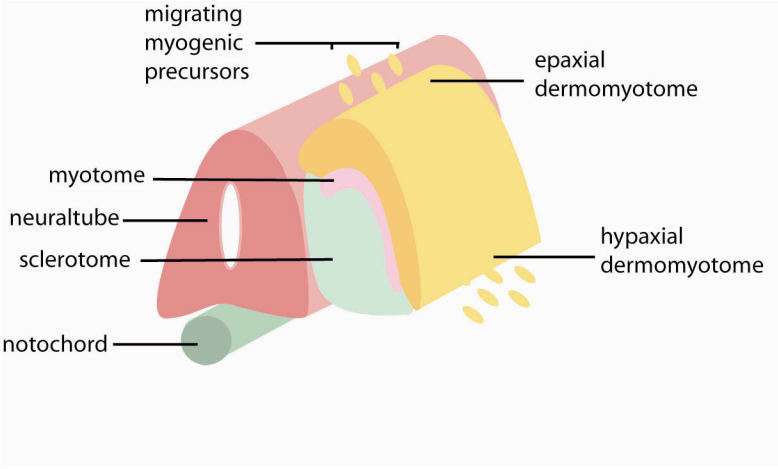

Figure 3: Illustration of the mammalian somite.

The epaxial part of the dermomyotome gives rise to the deep back muscles while the rest of the body muscle is derived from the hypaxial dermomyotome. At the start of myogenesis, myogenic progenitors migrate from the dermomyotome to the site of muscle formation (myotome, limb region, hypoglossal chord, diaphragm, tongue). Myogenic progenitor cells in the somite are characterized by the expression of the transcription factors paired box gene 3 (Pax3) and 7 (Pax7). Commitment to the myogenic lineage of these progenitors is initiated through expression of the myogenic regulatory factors (MRFs) myogenic factor 5 (Myf5), Myf6, also known als myogenic regulatory factor 4 (Mrf4), myogenic differentiation 1 (MyoD) and myogenin (MyoG). Signals as Wnt signalling, SHH and FGFs from the surrounding tissues regulate the

expression of these myogenic regulatory factors (for review and references therein [86]).

Cardiac muscle formation

Myocardial progenitor cells do not originate from the somite, but migrate from the primitive streak to positions under the head folds, forming two groups of cells on either side of the midline (the primary heart fields). These groups of cells fuse to form the cardiac crescent that will construct the linear heart tube. Another group of progenitor cells located in the secondary heart field add to the developing outflow tract of the heart tube. The heart tube undergoes cardiac looping to shape the heart, with the posterior region moving anteriorly. Through this looping and by expansion of the myocardium the heart chambers are formed (for review and references therein: [87]). Induction of the cardiomyogenic program in the cardiac crescent occurs through activation of transcription factors including the gata binding proteins Gata4/Gata5/Gata6, NK2 transcription factor related, locus 5 (Nkx2-5), the myocyte enhancer factors 2b and 2c (Mef2b and Mef2c), heart and neural crest derivatives expressed 1 and 2 (Hand1/Hand2), islet 1 (Isl1) and T-box 5 and 20 (Tbx5/Tbx20)). Induction of cardiac differentiation through activation of these factors is orchestrated by BMP and FGF8 signalling while Wnt signalling is inhibitory (for review and references therein: [88]).

Building blocks of the heart and skeletal muscle

Heart and skeletal muscle anatomy differ in some aspects. Skeletal muscle is formed through fusing myoblasts (individual skeletal muscle cells) that form the muscle myofibers, and a single myofiber therefore contains multiple nuclei. Cardiac myofibers on the other hand are composed of single cells that are connected to each other through intercalated discs. While the myofibers are linear and aligned longitudinally in skeletal muscle, myofibers in the cardiac muscle are branched.

The units of skeletal and heart muscle cells that are responsible for contraction are the sarcomeres (Figure 4). The borders of the individual sarcomeres are named the z-bands and constitute of alfa-actinin proteins in which the ends of the actin and titin filaments of opposite orientation are anchored. Under the light microscope sarcomeres appear striated and the I-band is isotropic in polarized light. The I-band region of the sarcomere spans from the z-band to the myosin filaments and contain the actin filaments together with nebulin and titin, which are thought to act as length-regulators of the actin filaments. Adjacent to the I-band is the A-band region (because it is anisotropic in polarized light), composed of myosin filaments with the M-line in the middle. The M-line is the anchoring point of titin filaments opposite of the z-band and is composed of myomesin and M-protein [89]. While many proteins have been

identified as part of the sarcomere, the mechanism of assembly of this structure is largely unknown.

Taken together there is a considerable overlap in the regulatory developmental pathways and in structure of cardiac and skeletal muscle. The identification of new genes such as Cazip, possibly involved in skeletal muscle and/or heart development and studies into the functional role of muscle proteins such as SARCOSIN are important for the understanding of the molecular program underlying embryonic development of these tissues. This knowledge will help to develop methods for the efficient differentiation of stem cells into the cardiac and skeletal muscle lineage.

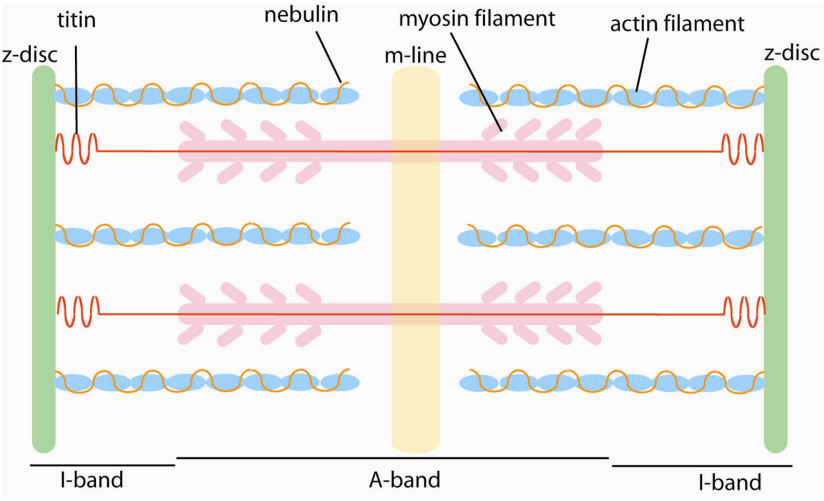

Figure 4: Illustration of sarcomere.

Thesis outline

The main subjects of this thesis are *in vivo* and *in vitro* pluripotency and cellular differentiation. The pig is an important large-animal model in biomedical research which can be used to study the potential application of ES cells in cell-based therapies. Therefore, the first two experimental chapters focus on the culture of porcine pluripotent embryonic cells from blastocyst-stage embryos. Chapter 2 aims to identify the optimal developmental stage for porcine pluripotent cell isolation. For this, we have analyzed the spatial and temporal expression pattern of genes involved in pluripotency in porcine blastocysts. Next, porcine pluripotent cells of blastocysts of various

embryonic days were isolated and cultured using media that stimulate different signalling pathways known to be involved in ES cell self-renewal. In chapter 3 we investigate an expandable population of neural cells from cultured porcine ICM cells and differentiation *in vitro*. Differentiation of genetically modified ES cells can be used as *in vitro* models for monogenic cardiovascular and muscular diseases. Also, to serve as a source for in vitro meat, porcine stem cells have to differentiate into muscle cells *in vitro*. Often *in vitro* differentiation from stem cells into a specific cell-type is induced by the same signalling pathways and down-stream elements as the development of a specific lineage *in vivo*. Therefore experimental chapters 4 and 5 focus on the development and differentiation of muscle tissue. The expression pattern of a novel protein which we named CAZIP indicated that this protein is potentially involved in the development and function of the heart and nervous system (chapter 4). Using RNA interference, the functional role of SARCOSIN, a protein exclusively expressed in sarcomeric muscle was examined and the results of this study are reported in chapter 5. Finally, in chapter 6 we discuss the findings reported in this thesis in the light of current scientific knowledge about pluripotency and self-renewal of embryonic cells and muscle development and differentiation.

REFERENCES

1. Stevens LC, Little CC. Spontaneous testicular teratomas in an inbred strain of mice. Proc Natl Acad Sci U S A. 1954;40:1080-1087.
2. Mintz B, Illmensee K. Normal genetically mosaic mice produced from malignant teratocarcinoma cells. Proc Natl Acad Sci U S A. 1975;72:3585-3589.
3. Kahan BW, Ephrussi B. Developmental potentialities of clonal in vitro cultures of mouse testicular teratoma. J Natl Cancer Inst. 1970;44:1015-1036.
4. Martin GR, Evans MJ. The morphology and growth of a pluripotent teratocarcinoma cell line and its derivatives in tissue culture. Cell. 1974;2:163-172.
5. Martin GR. Isolation of a pluripotent cell line from early mouse embryos cultured in medium conditioned by teratocarcinoma stem cells. Proc Natl Acad Sci U S A. 1981;78:7634-7638.
6. Evans MJ, Kaufman MH. Establishment in culture of pluripotential cells from mouse embryos. Nature. 1981;292:154-156.
7. Bradley A, Evans M, Kaufman MH, et al. Formation of germ-line chimaeras from embryo-derived teratocarcinoma cell lines. Nature. 1984;309:255-256.
8. Thomson JA, Itskovitz-Eldor J, Shapiro SS, et al. Embryonic stem cell lines derived from human blastocysts. Science. 1998;282:1145-1147.
9. Clark AT, Bodnar MS, Fox M, et al. Spontaneous differentiation of germ cells from human embryonic stem cells in vitro. Hum Mol Genet. 2004;13:727-739.
10. Li P, Tong C, Mehrian-Shai R, et al. Germline competent embryonic stem cells derived from rat blastocysts. Cell. 2008;135:1299-1310.
11. Buehr M, Meek S, Blair K, et al. Capture of authentic embryonic stem cells from rat blastocysts. Cell. 2008;135:1287-1298.

12. Thomson JA, Kalishman J, Golos TG, et al. Isolation of a primate embryonic stem cell line. Proc Natl Acad Sci U S A. 1995;92:7844-7848.
13. Thomson JA, Kalishman J, Golos TG, et al. Pluripotent cell lines derived from common marmoset (Callithrix jacchus) blastocysts. Biol Reprod. 1996;55:254-259.
14. Suemori H, Tada T, Torii R, et al. Establishment of embryonic stem cell lines from cynomolgus monkey blastocysts produced by IVF or ICSI. Dev Dyn. 2001;222:273-279.
15. Cibelli JB, Stice SL, Golueke PJ, et al. Transgenic bovine chimeric offspring produced from somatic cell-derived stem-like cells. Nat Biotechnol. 1998;16:642-646.
16. Wang L, Duan E, Sung LY, et al. Generation and characterization of pluripotent stem cells from cloned bovine embryos. Biol Reprod. 2005;73:149-155.
17. Saito S, Sawai K, Ugai H, et al. Generation of cloned calves and transgenic chimeric embryos from bovine embryonic stem-like cells. Biochem Biophys Res Commun. 2003;309:104-113.
18. Saito S, Ugai H, Sawai K, et al. Isolation of embryonic stem-like cells from equine blastocysts and their differentiation in vitro. FEBS Lett. 2002;531:389-396.
19. Li X, Zhou SG, Imreh MP, et al. Horse embryonic stem cell lines from the proliferation of inner cell mass cells. Stem Cells Dev. 2006;15:523-531.
20. Piedrahita JA, Anderson GB, BonDurant RH. On the isolation of embryonic stem cells: comparative behavior of murine, porcine and ovine embryos. Theriogenology. 1990;34:879-901.
21. Tian HB, Wang H, Sha HY, et al. Factors derived from mouse embryonic stem cells promote self-renewal of goat embryonic stem-like cells. Cell Biol Int. 2006;30:452-458.
22. Wianny F, Perreau C, Hochereau de Reviers MT. Proliferation and differentiation of porcine inner cell mass and epiblast in vitro. Biol Reprod. 1997;57:756-764.
23. Chen LR, Shiue YL, Bertolini L, et al. Establishment of pluripotent cell lines from porcine preimplantation embryos. Theriogenology. 1999;52:195-212.
24. Moore K, Piedrahita JA. Effects of heterologous hematopoietic cytokines on in vitro differentiation of cultured porcine inner cell masses. Mol Reprod Dev. 1996;45:139-144.
25. Hochereau-de Reviers MT, Perreau C. In vitro culture of embryonic disc cells from porcine blastocysts. Reprod Nutr Dev. 1993;33:475-483.
26. Anderson GB, Choi SJ, Bondurant RH. Survival of porcine inner cell masses in culture and after injection into blastocysts. Theriogenology. 1994;42:204-212.
27. Gerfen RW, Wheeler MB. isolation of embryonic cell-lines from porcine blastocysts. animal biotechnology. 1995;6:1-14.
28. Matsunari H, Nagashima H. Application of genetically modified and cloned pigs in translational research. The Journal of reproduction and development. 2009;55:225-230.
29. Ibrahim Z, Busch J, Awwad M, et al. Selected physiologic compatibilities and incompatibilities between human and porcine organ systems. Xenotransplantation. 2006;13:488-499.
30. McCreath KJ, Howcroft J, Campbell KH, et al. Production of gene-targeted sheep by nuclear transfer from cultured somatic cells. Nature. 2000;405:1066-1069.
31. Phelps CJ, Koike C, Vaught TD, et al. Production of alpha 1,3-galactosyltransferase-deficient pigs. Science. 2003;299:411-414.
32. Denning C, Burl S, Ainslie A, et al. Deletion of the alpha(1,3)galactosyl transferase (GGTA1) gene and the prion protein (PrP) gene in sheep. Nat Biotechnol. 2001;19:559-562.
33. Denning C, Priddle H. New frontiers in gene targeting and cloning: success, application and challenges in domestic animals and human embryonic stem cells. Reproduction. 2003;126:1-11.
34. Templeton NS, Roberts DD, Safer B. Efficient gene targeting in mouse embryonic stem cells. Gene Ther. 1997;4:700-709.

35. Williams RL, Hilton DJ, Pease S, et al. Myeloid leukaemia inhibitory factor maintains the developmental potential of embryonic stem cells. Nature. 1988;336:684-687.
36. Daheron L, Opitz SL, Zaehres H, et al. LIF/STAT3 signaling fails to maintain self-renewal of human embryonic stem cells. Stem cells (Dayton, Ohio). 2004;22:770-778.
37. Qi X, Li TG, Hao J, et al. BMP4 supports self-renewal of embryonic stem cells by inhibiting mitogen-activated protein kinase pathways. Proc Natl Acad Sci U S A. 2004;101:6027-6032.
38. Finley MF, Devata S, Huettner JE. BMP-4 inhibits neural differentiation of murine embryonic stem cells. J Neurobiol. 1999;40:271-287.
39. Xu RH, Peck RM, Li DS, et al. Basic FGF and suppression of BMP signaling sustain undifferentiated proliferation of human ES cells. Nat Methods. 2005;2:185-190.
40. Xu RH, Chen X, Li DS, et al. BMP4 initiates human embryonic stem cell differentiation to trophoblast. Nat Biotechnol. 2002;20:1261-1264.
41. Tesar PJ. Derivation of germ-line-competent embryonic stem cell lines from preblastocyst mouse embryos. Proc Natl Acad Sci U S A. 2005;102:8239-8244.
42. Brons IG, Smithers LE, Trotter MW, et al. Derivation of pluripotent epiblast stem cells from mammalian embryos. Nature. 2007;448:191-195.
43. Tesar PJ, Chenoweth JG, Brook FA, et al. New cell lines from mouse epiblast share defining features with human embryonic stem cells. Nature. 2007;448:196-199.
44. Drews U. Color atlas of embryology. New York: Thieme Medical Publishers;. 1995:40-64.
45. Hogan BB, R. Costantini, F. Lacy, E. Manipulating the mouse embryo, a laboratory manual. Second edition. Cold Spring Harbor Laboratory Press. 1994:21-69.
46. Senger PL. Pathways to pregnancy and parturition. Second edition. Washington: Current Conceptions, Inc;. 1997.
47. Guillomot M. Cellular interactions during implantation in domestic ruminants. J Reprod Fertil Suppl. 1995;49:39-51.
48. Maddox-Hyttel P, Alexopoulos NI, Vajta G, et al. Immunohistochemical and ultrastructural characterization of the initial post-hatching development of bovine embryos. Reproduction. 2003;125:607-623.
49. Spencer TE, Johnson GA, Bazer FW, et al. Implantation mechanisms: insights from the sheep. Reproduction. 2004;128:657-668.
50. Guillomot M, Turbe A, Hue I, et al. Staging of ovine embryos and expression of the T-box genes Brachyury and Eomesodermin around gastrulation. Reproduction. 2004;127:491-501.
51. Ender. Endoderm cells of the equine yolk sac from day 7 until formation of the definitive yolk sac placenta. Equine vet. J., Supll. 1993;15:3-9.
52. Prelle K, Holtz W, Osborn M. Immunocytochemical analysis of vimentin expression patterns in porcine embryos suggests mesodermal differentiation from day 9 after conception. Anat Histol Embryol. 2001;30:339-344.
53. Flechon JE, Degrouard J, Flechon B. Gastrulation events in the prestreak pig embryo: ultrastructure and cell markers. Genesis. 2004;38:13-25.
54. Marrable AW. The embryonic pig. Pitman Medical;. 1971:37-49.
55. Geisert RD, Brookbank JW, Roberts RM, et al. Establishment of pregnancy in the pig: II. Cellular remodeling of the porcine blastocyst during elongation on day 12 of pregnancy. Biol Reprod. 1982;27:941-955.
56. Niwa H, Burdon T, Chambers I, et al. Self-renewal of pluripotent embryonic stem cells is mediated via activation of STAT3. Genes Dev. 1998;12:2048-2060.
57. Burdon T, Stracey C, Chambers I, et al. Suppression of SHP-2 and ERK signalling promotes self-renewal of mouse embryonic stem cells. Dev Biol. 1999;210:30-43.
58. Ying QL, Nichols J, Chambers I, et al. BMP induction of Id proteins suppresses differentiation and sustains embryonic stem cell self-renewal in collaboration with STAT3. Cell. 2003;115:281-292.

59. Wang G, Zhang H, Zhao Y, et al. Noggin and bFGF cooperate to maintain the pluripotency of human embryonic stem cells in the absence of feeder layers. Biochem Biophys Res Commun. 2005;330:934-942.
60. Davey RE, Zandstra PW. Spatial organization of embryonic stem cell responsiveness to autocrine gp130 ligands reveals an autoregulatory stem cell niche. Stem cells (Dayton, Ohio). 2006;24:2538-2548.
61. Chung Y, Klimanskaya I, Becker S, et al. Embryonic and extraembryonic stem cell lines derived from single mouse blastomeres. Nature. 2005;439:216-219.
62. Klimanskaya I, Chung Y, Becker S, et al. Human embryonic stem cell lines derived from single blastomeres. Nature. 2006;444:481-485.
63. Palmieri SL, Peter W, Hess H, et al. Oct-4 transcription factor is differentially expressed in the mouse embryo during establishment of the first two extraembryonic cell lineages involved in implantation. Dev Biol. 1994;166:259-267.
64. Niwa H, Miyazaki J, Smith AG. Quantitative expression of Oct-3/4 defines differentiation, dedifferentiation or self-renewal of ES cells. Nat Genet. 2000;24:372-376.
65. Rosner MH, Vigano MA, Ozato K, et al. A POU-domain transcription factor in early stem cells and germ cells of the mammalian embryo. Nature. 1990;345:686-692.
66. Hansis C, Grifo JA, Krey LC. Oct-4 expression in inner cell mass and trophectoderm of human blastocysts. Mol Hum Reprod. 2000;6:999-1004.
67. Chambers I, Colby D, Robertson M, et al. Functional expression cloning of Nanog, a pluripotency sustaining factor in embryonic stem cells. Cell. 2003;113:643-655.
68. Mitsui K, Tokuzawa Y, Itoh H, et al. The homeoprotein Nanog is required for maintenance of pluripotency in mouse epiblast and ES cells. Cell. 2003;113:631-642.
69. van Eijk MJ, van Rooijen MA, Modina S, et al. Molecular cloning, genetic mapping, and developmental expression of bovine POU5F1. Biol Reprod. 1999;60:1093-1103.
70. Vejlsted M, Offenberg H, Thorup F, et al. Confinement and clearance of OCT4 in the porcine embryo at stereomicroscopically defined stages around gastrulation. Mol Reprod Dev. 2006;73:709-718.
71. He S, Pant D, Schiffmacher A, et al. Developmental expression of pluripotency determining factors in caprine embryos: Novel pattern of NANOG protein localization in the nucleolus. Mol Reprod Dev. 2006;73:1512-1522.
72. Kirchhof N, Carnwath JW, Lemme E, et al. Expression pattern of Oct-4 in preimplantation embryos of different species. Biol Reprod. 2000;63:1698-1705.
73. Kuijk EW, Du Puy L, Van Tol HT, et al. Differences in early lineage segregation between mammals. Dev Dyn. 2008;237:918-927.
74. Chen AE, Egli D, Niakan K, et al. Optimal timing of inner cell mass isolation increases the efficiency of human embryonic stem cell derivation and allows generation of sibling cell lines. Cell Stem Cell. 2009;4:103-106.
75. Niwa H. How is pluripotency determined and maintained? Development (Cambridge, England). 2007;134:635-646.
76. Takahashi K, Yamanaka S. Induction of pluripotent stem cells from mouse embryonic and adult fibroblast cultures by defined factors. Cell. 2006;126:663-676.
77. Yu J, Vodyanik MA, Smuga-Otto K, et al. Induced pluripotent stem cell lines derived from human somatic cells. Science. 2007;318:1917-1920.
78. Takahashi K, Tanabe K, Ohnuki M, et al. Induction of pluripotent stem cells from adult human fibroblasts by defined factors. Cell. 2007;131:861-872.
79. Esteban MA, Xu J, Yang J, et al. Generation of induced pluripotent stem cell lines from tibetan miniature pig. J Biol Chem. 2009;284:17634-17640.
80. Wu Z, Chen J, Ren J, et al. Generation of Pig-Induced Pluripotent Stem Cells with a Drug-Inducible System. J Mol Cell Biol. 2009;Published ahead of print.

81. Ezashi T, Telugu BP, Alexenko AP, et al. Derivation of induced pluripotent stem cells from pig somatic cells. Proc Natl Acad Sci U S A. 2009;106:10993-10998.
82. Darabi R, Gehlbach K, Bachoo RM, et al. Functional skeletal muscle regeneration from differentiating embryonic stem cells. Nature medicine. 2008;14:134-143.
83. Beqqali A, Kloots J, Ward-van Oostwaard D, et al. Genome-wide transcriptional profiling of human embryonic stem cells differentiating to cardiomyocytes. Stem cells (Dayton, Ohio). 2006;24:1956-1967.
84. Pourquie O. Vertebrate somitogenesis. Annu Rev Cell Dev Biol. 2001;17:311-350.
85. Kalcheim C, Ben-Yair R. Cell rearrangements during development of the somite and its derivatives. Curr Opin Genet Dev. 2005;15:371-380.
86. Bryson-Richardson RJ, Currie PD. The genetics of vertebrate myogenesis. Nat Rev Genet. 2008;9:632-646.
87. Harvey RP. Patterning the vertebrate heart. Nat Rev Genet. 2002;3:544-556.
88. Brand T. Heart development: molecular insights into cardiac specification and early morphogenesis. Dev Biol. 2003;258:1-19.
89. Clark KA, McElhinny AS, Beckerle MC, et al. Striated muscle cytoarchitecture: an intricate web of form and function. Annu Rev Cell Dev Biol. 2002;18:637-706.

Chapter 2

Characterization and culture of the pluripotent cell population of porcine blastocysts

Leonie du Puy [(1)], Susana M. Chuva de Sousa Lopes [(2)], Henk P. Haagsman [(3)], Bernard A.J. Roelen[(1)].

[1] Department of Farm Animal Health, Faculty of Veterinary Medicine, Utrecht University, Utrecht, The Netherlands ; [2] Department of Anatomy & Embryology, Leiden University Medical Center, Leiden, The Netherlands; [3] Department of Infectious Diseases and Immunology, Faculty of Veterinary Medicine, Utrecht University, Utrecht, The Netherlands.

Submitted for publication

Abstract

To derive porcine embryonic stem (ES) cell lines, the time-window during which porcine embryos contain pluripotent cells that are susceptible to undifferentiated self-renewal *in vitro* must be identified. Therefore we have studied the spatial and temporal expression pattern of key factors in pluripotency and lineage segregation of blastocyst-stage porcine embryos between embryonic day (E) 6.5 and E10.5 using whole mount *in situ* hybridization, quantitative real time PCR and whole mount immunofluorescence. The results demonstrated that *NANOG* and *SOX2* are expressed in both the ICM and epiblast, while *OCT4* expression becomes restricted to the epiblast at E9.5. Growth factors which sustain the undifferentiated growth of human ES cells and mouse epiblast stem cells (EpiSCs) were tested for their ability to sustain undifferentiated self-renewal of porcine ICM and epiblast cells *in vitro*. Cultures of ICM cells resulted in a higher percentage of primary colonies with an ES-like morphology compared to primary cultures derived from epiblast cells. However, the cells rapidly differentiated in cell types of mesodermal-, ectodermal-, and endodermal origin, as characterized by PCR. These results demonstrate that porcine ICM and epiblast cells can not be cultured *in vitro* using human ES cell culture conditions.

Introduction

Embryonic stem (ES) cells have the capacity to self-renew indefinitely *in vitro* without losing their potential to differentiate into all cell types of the embryo proper. ES cells are derived from the inner cell mass (ICM) of early embryos and were first generated from mouse blastocysts of the 129/Sv strain in 1981 [1, 2]. Fourteen years later the first non-human primate ES cell lines were derived, followed by human and rat ES cell lines in 1998 and 2008 respectively [3-6]. To this date ES cells that have a demonstrated capacity of occupying the germline after injection into blastocyst-stage embryos (germline transmission) have not been reported for any other species besides mice and rat.

The lifespan and physiology of pigs is far more comparable to that of humans compared with the lifespan and physiology of mice [7]. This would make ES cell lines from pigs useful to test the applicability and safety of employing human ES cells in medicine to replace lost or damaged tissues. Numerous attempts have been made to generate ES cell lines from pigs but all have been rather unsuccessful in deriving a well characterized self- renewing pluripotent cell line [8-16]. The difficulties in deriving porcine ES cell lines remain in identifying the time-window during which pig embryos contain pluripotent cells that are susceptible to *in vitro* culture without losing their

pluripotency and self-renewal. In addition, the culture conditions to sustain self-renewal of pluripotent porcine ES cells have remained unclear.

The developmental stage of the embryo is important in ES cell line derivation. Mouse ES cell lines are most easily derived from ICM cells of pre-implantation blastocysts of embryonic day (E) 3.5 although pluripotent cells have been derived from post implantation epiblasts of mouse embryos (EpiSCs) (E5.5) [17, 18]. Human ES cell lines are derived most efficiently from E6 blastocysts [19]. One of the reasons of the difficulty of establishing porcine ES cell lines can be the differences in embryology. The time-window between blastocyst formation and gastrulation is much larger in porcine embryos (E5.5-E11) compared to mouse embryos (E3.5-E6.5). While mouse embryos invasively implant into the uterine wall around E5, porcine embryos do not implant until several days after they arrive in the uterus and instead the trophectoderm undergoes rapid elongation. Also the timing and formation of the primitive endoderm and mesoderm layers differ between mice, men and pigs [20-26]. It is unclear during which embryonic period porcine ICM or epiblast cells are most susceptible to give rise to an undifferentiated culture *in vitro*.

Secretion of (growth) factors by mitotically inactivated mouse embryonic fibroblasts (MEFs) has been of critical importance for the derivation of both mouse and human ES cell lines. Interestingly, different signaling pathways maintain the undifferentiated state of human and mouse ES cells. In mouse ES cells, leukemia inhibitory factor (LIF) and bone morphogenetic proteins (BMP) are important for self-renewal [27, 28]. In contrast, inhibition of BMP signaling using NOGGIN, together with basic fibroblast growth factor (bFGF) maintain human ES cells in an undifferentiated state [29]. However, culture media supplemented with the growth factors LIF or bFGF did not sustain undifferentiated growth of porcine ICM cells [13, 30, 31]. Surprisingly, mouse EpiSCs remained pluripotent using human ES cell culture conditions but not using mouse ES cell culture conditions [17, 18]. This suggests that human ES cells resemble EpiSCs and are derived from embryos that are at a later developmental stage compared to the blastocysts of which mouse ES cells are derived. Therefore it would be interesting to culture porcine epiblast cells using human ES cell culture conditions.

Here the development of the pluripotent cell population in porcine embryos is studied and compared with the development of the pluripotent cell population in human and mouse embryos as described in literature. For this, porcine blastocysts were flushed from the uterus between E6.5 and E10.5 and their temporal and spatial expression patterns of key transcription factors (OCT4, NANOG, SOX2) important for maintenance of the pluripotent cell population in mice and human (for review and references therein: [32]) were analyzed. To explore the possibility that porcine pluripotent cells resemble human ES cells or mouse EpiSC in culture, ICM cells from early blastocyst-stage embryos (E6.5-8.5) and epiblast cells from late blastocyst-stage

embryos (E9.5-E10.5) were cultured using conditions which stimulate the signaling pathways that maintain human ES cell and mouse EpiSC pluripotency and self-renewal *in vitro*.

Material and Methods:

Embryo collection and ICM culture

Normal cycling sows were examined for the onset of estrous and upon detection were artificially inseminated with fresh boar semen of proven fertility and the following morning was considered embryonic day 0.5 (E0.5). E6.5-E10.5 embryos were flushed from the uteri of slaughtered sows with phosphate buffered saline (PBS, Sigma-aldrich, Zwijndrecht, The Netherlands) containing 0.1% fetal bovine serum (FBS, Invitrogen, Carlsbad, USA) and penicillin and streptomyocin. All procedures performed were approved by the institutional animal experiments ethical committee.

Isolation of the ICM or epiblast was done mechanically using tungsten needles. The isolated ICM or epiblast was placed on irradiated mouse embryonic fibroblasts (MEFs) in basic culture medium (b.c.m.) consisting of Knockout (KO) DMEM, 10% KO serum replacement, 10% human plasmanate (Sanquin, Amsterdam, The Netherlands), 1x non essential amino acid, 2 mM Glutamax, 0.1 mM beta-mercapthoethanol, 50 U/ml penicillin, 50 µg/ml streptomyocin (all from Invitrogen, Breda, The Netherlands). Extra growth factors were added to the culture medium: either 4-10 ng/ml basic fibroblast growth factor (bFGF) (Peprotech, London, UK; and Invitrogen) alone or in combination with 10 ng/ml ACTIVIN (Peprotech) or 100 ng/ml NOGGIN (Peprotech). In some experiments the ICM/epiblast cells were cultured on matrigel (BD Biosciences, Breda, The Netherlands) in modified TeSR medium (StemCell technologies, Grenoble, France). Four to eight days after initial plating, ICM-derived clumps were dissociated mechanically using a pulled glass-capillar from the embryo outgrowths and replated separately on a fresh mouse feeder layer. The resulting colonies were further propagated on mouse feeders every four to six days, but the cultures were refreshed daily with culture medium. Passaging was done mechanically, or using a combined method of exposure to collagenase IV (1 mg/ml, Invitrogen) for 7 minutes at room temperature followed by mechanical slicing. Cell culture was carried out at 37.5ºC and 5% CO_2.

RNA isolation and quantitative real-time PCR

Total RNA was extracted from embryonic cells using the RNeasy microkit (Qiagen, Valencia, California, USA). An on-column DNAse treatment (Qiagen) was performed before reverse transcription of the total RNA using Superscript II reverse transcription-polymerase (Invitrogen) and random primers (Invitrogen) according to the supplier's

protocol. For reverse transcriptase-polymerase chain reaction (RT-PCR) primers were designed using Primer 3 software [33] or based on literature [33-36] (Table 1). PCR was carried out using Taq DNA polymerase (Invitrogen) and 1 µl of cDNA under the following conditions: initial denaturation for 5 min at 95ºC, followed by 40 cycles of 15 sec at 95ºC, 30 sec at the corresponding annealing temperature (Table 1) and 30 sec at 72ºC. The final step consisted of 7 min extension at 72ºC. PCR products were separated on 1% agarose gels and visualized with ethidium bromide against a 100 bp ladder. To verify the specificity, the PCR products were sequenced.

Table 1. Primers used for RT-PCR and Q-PCR.

Gene [reference nr]	5' forward primer 5' reverse primer	Ta (°C)	amplicon size (bp)
GAPDH **[34]**	TCGGAGTGAACGGATTTG CCTGGAAGATGGTGATGG	51.1	219
PGK1 **[34]**	AGATAACGAACAACCAGAGG TGTCAGGCATAGGGATACC	56.4	126
UBIQUITIN **[34]**	TTCGTGAAGACCTTGACTG GGACTCCTTCTGGATGTTG	51.1	186
NANOG **[35]**	CCTCCATGGATCTGCTTATTC CATCTGCTGGAGGCTGAGGT	63.0	210
OCT4 **[35]**	GTTCTCTTTGGGAAGGTGTT ACACGCGGACCACATCCTTC	55.4	313
SOX2 **[36]**	CTGCGAGCGCTGCAGATGAA CCTCCGGGCAGTGTGTACTTATCCT	60.0	101
GATA4 **[35]**	ATGAAGCTCCATGGTGTCCC ACTGCTGGAGTTGCTGGAAG	55.8	162
CK18 **[35]**	ATGAAGAAGAACCACGAGGAGGAA TGTCTGCCATGATCTTGCTGAGG	54.8	118
CDX2 **[35]**	GTCACCAGAGCTTCTCTGGG AGACCAACAACCCAAACAGC	52.9	144
MYF5 **[35]**	TGCCATCCGCTACATTGAGAG GTTCTTTCGGGACCAGACAGG	55.4	160
MYOD	TCCGCGACGTAGATTTG ACGGGAAGTGCGAGTGTT	60.1	177
DESMIN	CCGAGATCTACGAGGAGGAG GTCTGAAAGAAGAAGCCGAGA	55.0	161

Quantitative real-time PCR was performed using SYBRGreen Mastermix on a MyIQ Real-Time PCR detection system (Bio-Rad, Veenendaal, The Netherlands). Thermal cycling conditions consisted of initial denaturation at 95ºC for 3 min, followed by 40 cycles of 30 sec at 95ºC, 30 sec at the corresponding annealing temperature (Table 1) and 30 sec at 72ºC. A melting curve was produced to verify single PCR product amplification. Efficiency of the PCR reaction was tested using a standard curve synthesized from either a dilution series of cDNA or PCR product. Data were analyzed with iQ5 software (Bio-Rad).

Whole mount in situ hybridization.

Whole mount *in situ* hybridisation was performed as described previously [37]. For the generation of DIG-labelled anti-sense RNA probes, purified PCR product was generated to be used as a template, using *OCT4* (forward: 5' CTGCAGAAGTGGGTGGAGGAAC 3' and reverse: 5' GCTGCTGGGCGATGTGGCTGAT 3') and *NANOG* (forward: 5' TTCCTTCCTCCATGGATCTG 3' and reverse: 5'TCTGCTGGAGGCTGAGGTA 3') specific primers that contained the T7 promoter sequence (TAATACGACTCACTATAGGGAGACCACA) at the 5'end of the reverse primer. RNA probes were synthesized using T7 (antisense) polymerase and DIG labelled nucleotides according to the manufacturer's protocol (Roche Applied Sciences, Almere, The Netherlands). Embryos were imaged using a Zeiss Axioplan SZX9 coupled to a Leica DFC480 digital camera. After whole mount in situ hybridization, embryos were first dehydrated through a graded series of ethanol and embedded in plastic (Technovit 8100, Heraeus, Hanau, Germany) at 4ºC overnight. Sections (10 µm) were counterstained with neural red and mounted with Depex (Merck, Darmstadt, Germany)

Alkaline phosphatase staining

For detection of alkaline phosphatase activity, cells were fixed 10 min in 4% paraformaldehyde (PFA, Klinipath, Duiven, The Netherlands) at RT and subsequently incubated for 15 minutes at RT in NBT/BCIP (Roche) diluted 50 times in buffer composed of 0.1M Tris-HCL (pH 9.5), 0.1M NaCl and 0.05M $MgCl_2$.

Whole mount immunofluorescence

Whole embryos were fixed in 4% PFA for 10 min at RT and permeabilized using 0.5% Triton X100 (Sigma-Aldrich) in PBS for 15 min. Aspecific binding was blocked using 10% FBS in PBS containing 0.1% Triton X100 for 2.5 hrs at RT. Embryos were incubated overnight with primary antibodies in blocking solution at 4°C and subsequently washed 4 times 30 min in blocking solution at RT. Secondary antibody incubation was 2 hrs at RT followed by 4 wash steps of 30 min each. Embryos were

next transferred to blocking solution containing nuclear stain (TO-PRO, Invitrogen) for 1 hr at RT and mounted in Vectashield mounting medium (Vector Laboratories, Inc. Burlingame, USA). Primary antibodies included: anti-OCT4 goat polyclonal 4 µg/ml (Abcam, Cambridge, UK; AB27985) and anti-SOX2 mouse monoclonal 10 µg/ml (R&D systems, Abingdon, UK; MAB2018), anti-GATA4 mouse monoclonal 4 µg/ml (Santa Cruz, Heidelberg, Germany; SC2531) and anti-NANOG rabbit polyclonal, 5 µg/ml (Peprotech, London, UK 500-P236). Secondary antibodies used were goat anti-mouse Alexa488-conjugated, goat anti-rabbit Alexa568-conjugated and bovine anti-goat Cy3-conjugated (1:200, Invitrogen). Embryos were imaged using confocal microscopy.

Results

ICMs of porcine blastocyst-stage embryos epithelialize around E9.5

To assess the morphology and characterize the expression patterns of genes important for pluripotency in porcine blastocyst-stage embryos, uteri of pregnant sows were flushed and embryos between E6.5 and E10.5 were recovered. At E6.5, embryos of most litters had hatched from the zona pellucida (40 out of 56 embryos flushed). E6.5 embryos were approximately 200 µm in diameter and the ICM was clearly visible as a dark clump of cells (Fig 1A).

Diameter of E7.5 and E8.5 embryos were doubled in size compared to embryos of E6.5 and the trophectoderm was darker and more dense. The ICM was not epithelialized and protruded from the blastocyst while still being covered by the trophectoderm (Rauber's layer) (Fig 1B, C). At E9.5 the ICM was epithelialized, forming an epiblast covered by Rauber's layer. At this stage embryos were approximately 700 µm in diameter (Fig 1D). At E10.5 a layer of primitive endoderm was microscopically distinguishable and the trophectoderm had expanded further, resulting in a blastocyst of spherical shape with a diameter of over 2500 µm (Fig 1E). Whole mount *in situ* hybridization demonstrated that both *NANOG* and *OCT4* mRNAs were expressed in the epiblasts of E10.5 embryos, but not in the trophectoderm and the primitive endoderm cells (Fig 1F-I).

OCT4 downregulated in the trophectoderm around E9.5

To further study the gene expression pattern of factors involved in pluripotency (*NANOG, OCT4* and *SOX2*) and lineage segregation (*CDX2, GATA4*), quantitative real-time PCR analysis was performed on blastocysts between E6.5 and E10.5. For this, the ICM/epiblast was mechanically separated from the trophectoderm with the use of tungsten needles.

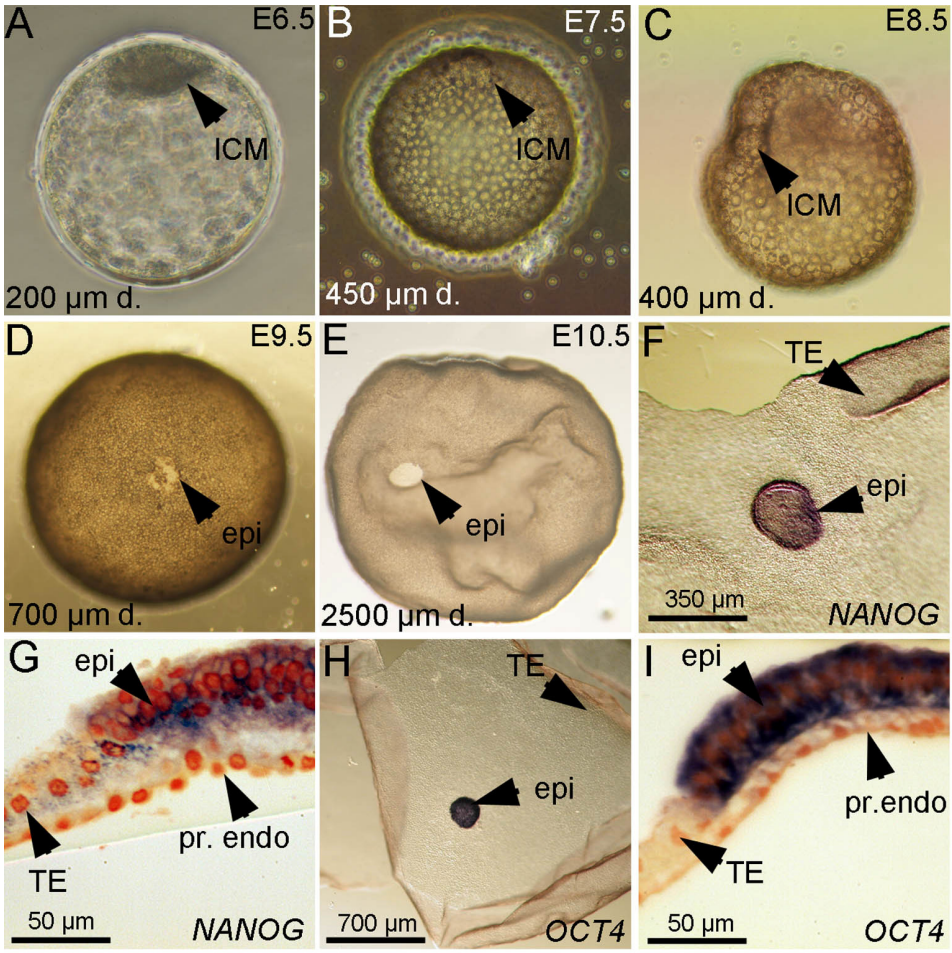

Fig 1: Porcine embryos at different stages of embryonic development
Morphology of porcine embryos at different embryonic days (E) 6.5 (A), E7.5 (B), E8.5 (C), E9.5 (D) and E10.5 (E). Whole mount *in situ* hybridization with digoxigenin-UTP labeled *NANOG* (F) and *OCT4* (H) riboprobe was performed on porcine embryos of E10.5 and subsequently sectioned (G: *NANOG*, I: *OCT4*). ICM: inner cell mass, epi: epiblast, te: trophectoderm, d.: diameter.

Gene expression levels were analyzed separately for each embryonic day and therefore gene expression levels between embryos of different embryonic age could not be compared.

Cytokeratin 18 (*CK18*) mRNA, of which the product is an intermediate filament expressed in the extra-embryonic tissues of early embryos, was equally

expressed in the trophectoderm and ICM both in E6.5 and E7.5 embryos. From E8.5 onwards, *CK18* mRNA expression was down-regulated in the ICM/epiblast compared to the trophectoderm (Fig 2A).

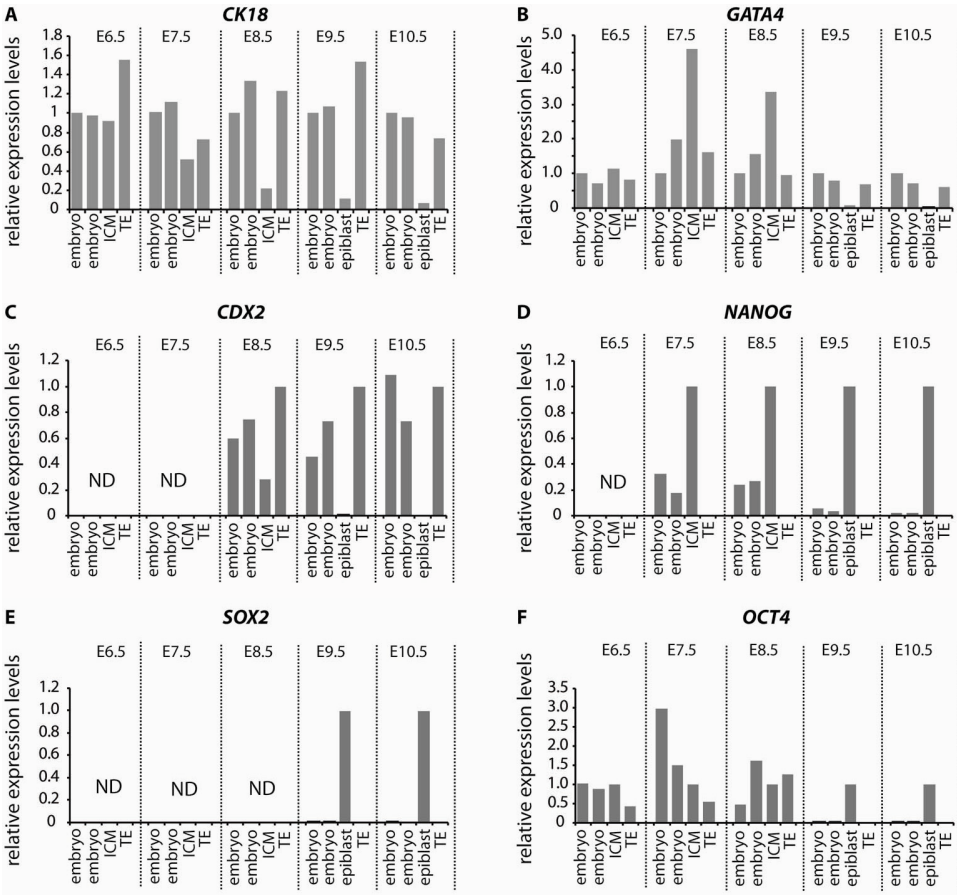

Fig 2: Quantitative real-time PCR analysis
Relative mRNA expression levels of *CK18* (A), *GATA4* (B), *CDX2* (C), *NANOG* (D), *SOX2* (E) and *OCT4* (F) in single embryos and pooled ICM and trophectoderm of 2 embryos, measured by quantitative real-time PCR. Gene expression levels were analyzed separately for each embryonic day and therefore gene expression levels between embryos of different embryonic age are not compared. Expression levels were normalized to the housekeeping genes *GAPDH, PGK1* and *UBIQUITIN* and presented relative to the expression level of the first embryo measured (A, B), or to the trophectoderm expression level (C) or to the expression levels of the ICM/epiblast (D, E, F). E: embryonic day; ND: not detectable; ICM: inner cell mass; TE: trophectoderm.

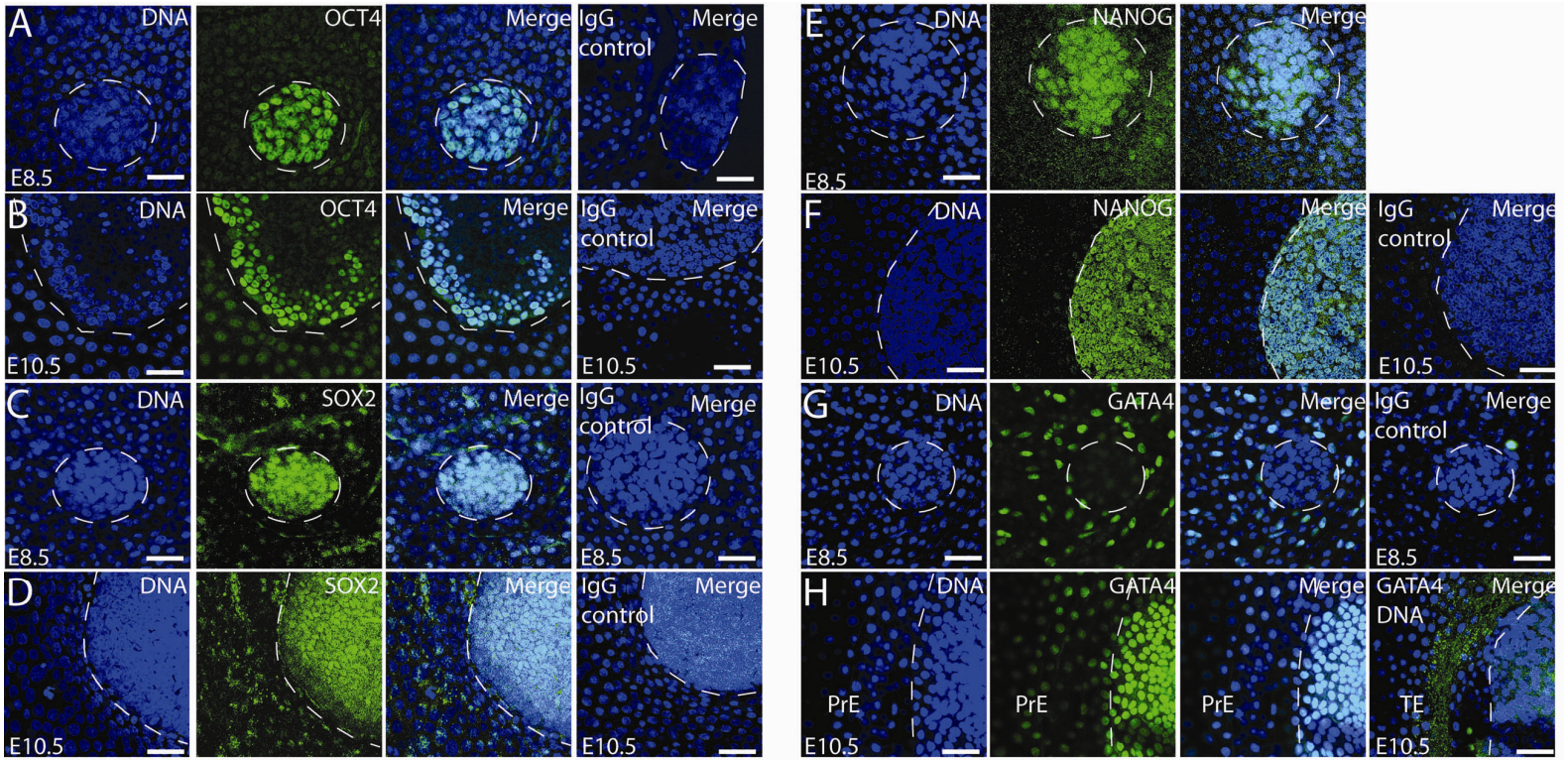

Fig 3: Whole mount immunofluorescence on porcine blastocysts

Confocal images of immunostainings of OCT4 (A-B), SOX2 (C-D), NANOG (E-F) and GATA4 (G-H) protein in porcine blastocysts of embryonic day 8.5 (E8.5) and E10.5. ICM (E8.5) and epiblast (E10.5) are encircled by a dashed line. DNA staining using ToPro is presented in blue and immunostaining in green followed by the merge of these two. Control embryos were incubated with the appropriate IgG control (green). In panel H, GATA4 staining is visible in the nuclei of primitive endoderm (PrE) cells covering the epiblast while the epiblast cells and trophectoderm (TE) cells are negative. Scale bar = 50 µm.

GATA4 mRNA, coding for a transcription factor involved in endoderm specification, was expressed in both the trophectoderm and ICM of E6.5-E8.5 embryos. In epiblasts of E9.5 and E10.5 embryos *GATA4* mRNA expression levels were down-regulated compared to the extra-embryonic tissues (Fig 2B). Messenger-RNA expression levels of the trophectoderm lineage segregation transcription factor *CDX2* were below the detection limit in tissues of E6.5 and E7.5 embryos. *CDX2* mRNA expression levels were readily detectable in the trophectoderm of E8.5-E10.5 embryos while below the detection limit in the ICM/epiblast (Fig 2C).

In tissues of E6.5 embryos, *NANOG* mRNA expression levels were below the detection limit (Fig 2D). *NANOG* mRNA, encoding for a transcription factor involved in pluripotency and specifically expressed in the ICM of mouse-blastocysts, was highly expressed in the ICM/epiblast of E7.5-E10.5 embryos. For *SOX2*, also encoding for a transcription factor involved in pluripotency, expression levels were below the detection limit in tissues from E6.5-E8.5 embryos but *SOX2* mRNA was highly expressed in the epiblast of E9.5 and E10.5 embryos (Fig 2E). Finally, mRNA expression levels of the transcription factor *OCT4* were analyzed. *OCT4* mRNA was expressed in both the trophectoderm and ICM of E6.5 to E8.5 embryos and restricted to the epiblast in embryos of E9.5 and E10.5 (Fig 2F). To examine protein expression, immunostainings were performed on E8.5 embryos (ICM-stage) and E10.5 embryos (epiblast-stage) (Fig 3). At both embryonic stages, OCT4 was expressed in the nuclei of trophectoderm cells although a much stronger OCT4 staining was observed in the nuclei of the ICM and epiblast (Fig 3, A and B). SOX2 protein expression patterns confirmed the result of the PCR study that SOX2 expression is restricted to the ICM and epiblast (Fig 3, C and D). NANOG protein was expressed in all nuclei of the ICM and epiblast but not in the endoderm and trophectoderm (Fig 3 E and F). GATA4 protein was expressed in the nuclei of cells located between trophectoderm cells in E8.5 embryos, but not in the nuclei of ICM cells (Fig 3G). In E10.5 embryos GATA4 was expressed the nuclei of the primitive endoderm cells, but not in the nuclei of trophectoderm and epiblast cells (Fig 3H).

Human ES cell culture conditions do not sustain undifferentiated growth of porcine ICM and epiblast cells.

To test whether conditions that sustain human ES cells/mouse EpiSC culture also sustained undifferentiated growth of porcine pluripotent cells, a total of 83 embryos were flushed and ICMs from early blastocyst-stage embryos (E6.5-8.5) and epiblasts from late blastocyst-stage embryos (E9.5-E10.5) were mechanically isolated. ICM/epiblast cells were either cultured using a MEF-feeder layer in basic culture medium supplemented with bFGF alone or in combination with ACTIVIN or NOGGIN [29, 38, 39]; or on Matrigel coated dishes and modified TeSR-medium [40] (Table 2).

Table 2. Schematic overview of porcine embryonic cell culture

Embryonic day (E.)	Culture conditions (*)	nr. of ICMs/epiblasts in culture (§)	nr. of primary colonies with ES-like morphology/ total nr of primary colonies (§)	morphology of the colonies after 0-4 cultural passages			
				endoderm-like	mesoderm-like	ectoderm-like	mixed
E6.5	MEF with b.c.m.	6	2/6	5/6	-	-	1/6
	MEF with b.c.m. + bFGF	20	9/19	5/19	2/19	4/19	8/19
	MEF with b.c.m. + bFGF + Activin	6	2/5	2/5	1/5	-	2/5
	MEF with b.c.m. + bFGF+ Noggin	5	1/4	1/4	-	2/4	1/4
	Matrigel with mTeSR	5	1/5	3/5	-	-	2/5
E7.5	MEF with b.c.m. + bFGF	4	4/4	-	-	4/4	-
E8.5	Matrigel with mTeSR	4	1/3	2/3	-	1/3	-
Total:		**50**	**20/46 (43%)a**	**18/46 (39%)**	**3/46 (7%)**	**11/46 (24%)**	**14/46 (30%)**
E9.5	MEF with b.c.m.	4	1/4	1/4	1/4	1/4	1/4
	MEF with b.c.m. + bFGF	4	1/4	2/4	-	-	2/4
	MEF with b.c.m. + bFGF + Activin	4	2/4	-	-	-	4/4
	MEF with b.c.m. + bFGF+ Noggin	4	0/4	3/4	-	-	1/4
E10.5	MEF with b.c.m.	5	0/4				5/5
	MEF with b.c.m. + bFGF	4	1/4				4/4
	MEF with b.c.m. + bFGF + Activin	4	0/4	2/4	-	-	2/4
	MEF with b.c.m. + bFGF+ Noggin	4	0/4	-	-	-	4/4
Total:		**33**	**5/33 (15%)b**	**8/33 (24%)**	**1/33 (3%)**	**1/33 (3%)**	**23/33 (70%)**

***** MEF: mouse embryonic fibroblasts, b.c.m: basic culture medium; bFGF: basic fibroblast growth factor
§ nr: number
a: $p<0.01$ versus b

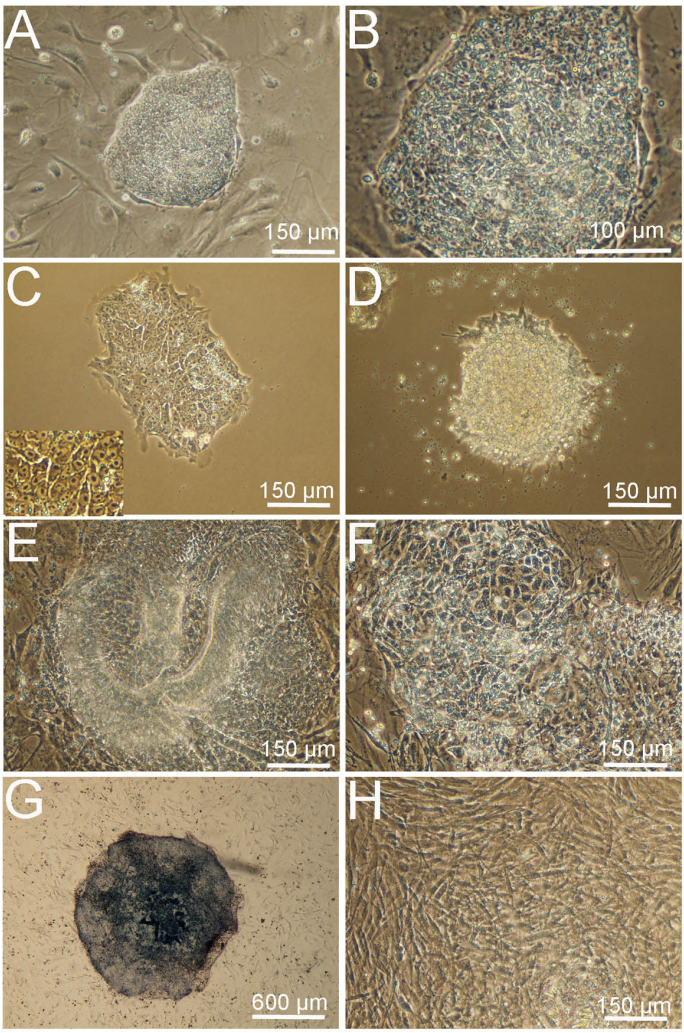

Fig 4: Outgrowths of ICM and epiblast cells in culture
Primary colony of cultured ICM cells with an ES-like morphology grown of a feeder layer of mouse embryonic fibroblasts in basic culture medium (A, B). Primary colony of cultured ICM cells with an ES-like morphology grown on a matrigel-coated dish in modified TeSR medium, insert shows higher magnification (C). Outgrowth of cell-colony represented in panel C after 4 days in culture (D). Representative picture of ectoderm-like cells that form neural rosette-like structures after 3 cultural passages on a feederlayer of mouse embryonic fibroblasts in basic culture medium (E). Representative picture of endoderm-like cells differentiated from ICM cells after 3 cultural passages on a feeder layer of mouse embryonic fibroblasts in basic culture medium (F). Alkaline phosphatase staining of endoderm-like cells grown on a feeder layer of mouse embryonic fibroblasts (G) Representative picture of mesoderm-like cells differentiated from ICM cells after 4 cultural passages on a feeder layer of mouse embryonic fibroblasts in basic culture medium (H).

The percentage of primary colonies with an ES-like morphology (small cells with large nuclei, unclear cell-cell boundaries and a well-defined colony border, Fig 4A-C); was significantly higher (43%) for ICM-cultures from early blastocysts compared to epiblast-cultures (15%) from late blastocysts. No effect of media was observed (Table 2). None of the culture media tested sustained the undifferentiated self-renewal of pluripotent porcine cells. Cellular outgrowths of the two colonies with an ES-like morphology cultured in modified TeSR medium were unable to attach to the culture dish (Fig 4 C, D). Outgrowths of ES-like colonies on MEF feeder-layers did attach, but differentiated after attachment.

Colonies were scored by their morphology as either of endoderm-, ectoderm- or mesoderm-like origin or a mixture of these cell types until passage 4 (Table 2). Cells of ectoderm-like colonies formed three-dimensional rosette-like structures (Fig 4E), endoderm-like cells formed round and flat colonies with individual cells with a cobble-stone appearance and had alkaline phosphatase activity (Fig 4F-G). Cells from mesoderm-like colonies were longitudinal in shape and colony borders were almost indistinguishable from the feeders (Fig 4H). On a single occasion beating cardiomyocytes were observed after 15 days of culture. A relatively large percentage of both ICM- and epiblast- derived colonies had an endoderm-like morphology (39% and 24% respectively). No correlation was observed between the media used and the differentiated cell-type formed.

To confirm the morphological observations, PCR analysis was done on cDNA isolated from cells of ES-, endoderm-, and mesoderm-like colonies. Cells from ES-like colonies expressed far higher levels of *OCT4*, *NANOG* and *SOX2* mRNA (Fig 5A-C) compared to cells cultured from primary endoderm and cells from ICM/epiblast derived endoderm-like colonies. On the other hand, cells cultured from primary endoderm and cells from ICM/epiblast derived endoderm-like colonies expressed higher levels of *GATA4* mRNA compared to cells ES-like colonies (Fig 5D). *CK18* mRNA expression levels were similar for cells from ES-like colonies, cells cultured from primary endoderm, and cells from ICM/epiblast derived endoderm-like colonies (Fig 5E). Normal RT-PCR analysis demonstrated gene-expression of the mesodermal markers *DESMIN*, *MYF5* and *MYOD* by cells from mesoderm-like colonies but not by cells from ectoderm-like colonies (Fig 5F). Previous results identified that rosette-like structures were of ectodermal-origin [41].

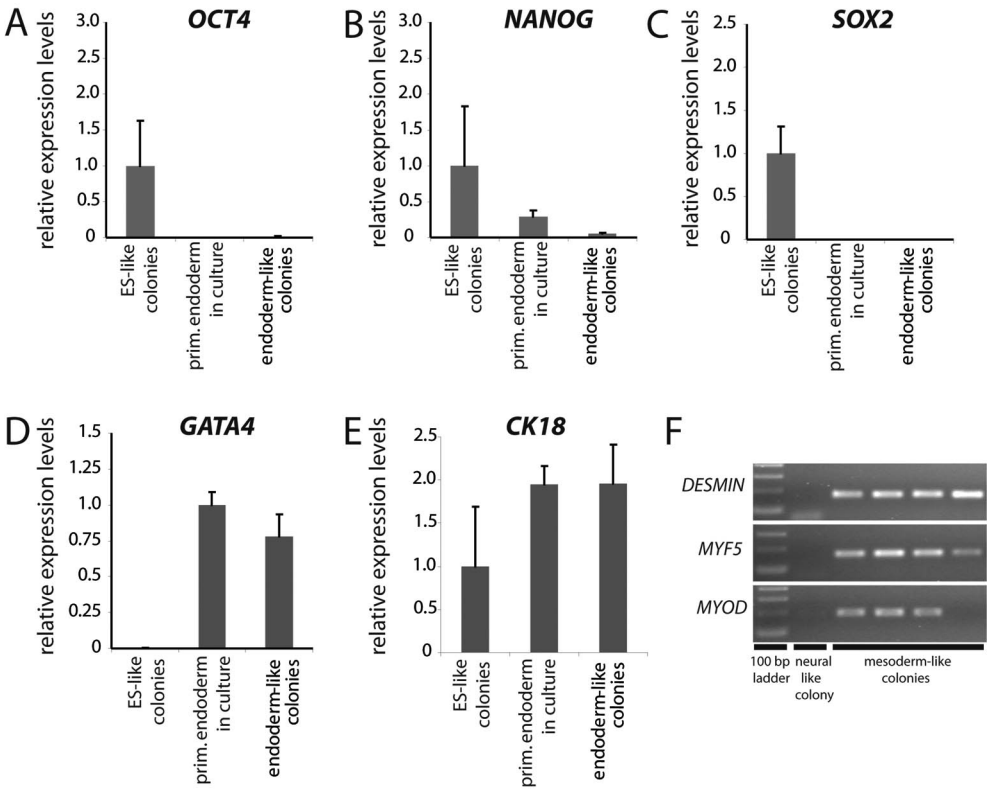

Fig 5: Characterization of cells in culture
Quantitative real-time PCR analysis on cDNA isolated from cells of ES-, and endoderm-like colonies and of primary endoderm in culture. Expression levels of *OCT4* (A), *NANOG* (B), *SOX2* (C), *GATA4* (D) and *CK18* (E) are presented relative to the expression level of ES-like colonies (A-C, E) or to primary endoderm in culture (D). Expression levels were measured and averaged for 3 cell culture samples per cell type. Error bars represent standard error of the mean. Expression levels are normalized to the housekeeping genes *GAPDH, PGK1* and *UBIQUITIN*. Normal PCR analysis of gene expression of *DESMIN, MYF5* and *MYOD* by mesoderm-like colonies (F).

Discussion

In mouse embryos the ICM forms a columnar layer of epithelialized cells at E4.5 just prior to implantation and porcine blastocysts containing an epiblast were first observed by us at E9.5. For gene-expression analysis of blastocysts between E6.5 and E10.5 the ICM/epiblast and trophectoderm were mechanically separated, although we cannot

exclude that some residual trophectoderm cells were present in the isolated ICMs of early embryos. Expression analysis of the trophectoderm specific transcription factor *CDX2* suggests that separation of the trophectoderm and ICM/epiblast was performed accurately. In several experiments gene expression levels measured by quantitative real-time PCR were below the detection limit proving that these genes are expressed at very low levels in these samples. GATA4, a transcription factor involved in primitive endoderm specification, was expressed in cells lining the ICM and in extra-embryonic tissue of early stage porcine blastocysts and was confined to the extra-embryonic lineages in E9.5-E10.5 embryos. During early mouse embryonic development GATA4 is expressed in the ICM of blastocyst stage embryos (E3.5) but becomes restricted to the primitive endoderm upon lineage segregation [42]. *CK18* mRNA expression is restricted to the extra-embryonic lineages in pig embryos of E8.5 and onwards. A similar expression pattern was observed in human embryos, where CK18 protein was observed in the outer cells of the compacting morula and in the trophectoderm and outer cells of the ICM in expanded blastocysts [43].

As in human and mouse embryos [43-45], both NANOG and SOX2 expression was restricted to the ICM/epiblast of porcine embryos. In mouse blastocysts, expression in the ICM of NANOG and the primitive endoderm marker GATA6 is heterogeneous and complementary [46]. In E8.5 porcine blastocysts all ICM cells are GATA4 negative showing that segregation of the primitive endoderm lineage from the ICM is completed, therefore it is not surprising that NANOG protein is expressed in all nuclei of E8.5 porcine ICM cells. Just prior to gastrulation *NANOG* expression in mouse embryos is localized in the emerging streak area of E6.5 embryos. In porcine embryos, *NANOG* mRNA was first detected at E7.5 and epiblasts still uniformly expressed NANOG five days after blastocyst formation (E10.5). At this stage, no morphological signs of gastrulation were observed. In mice, trophectoderm specification is regulated by CDX2 expression and OCT4 down-regulation in the outer cells of morula-stage embryos [47]. In pigs however, OCT4 is still expressed in trophectoderm of early blastocysts [35, 48]. Here we detected *OCT4* mRNA expression both in the trophectoderm and ICM of E6.5-E8.5 embryos, but the expression was down-regulated in the trophectoderm around E9. At E10.5 residual OCT4 protein was still detected in the nuclei of the trophectoderm. This suggests that in pigs OCT4 down-regulation, together with CDX2 expression, is sufficient for trophectoderm specification.

Summarized, epithelialization of the ICM coincides with OCT4 down-regulation in the trophectoderm around E9 and both NANOG and SOX2 are continuously expressed in the ICM/epiblast. The period between blastocyst development (E6) and epiblast formation (E9) in the pig is comparable to the period during which mouse ES cells are most easily derived (E3.5-E4.5). Mouse EpiSCs have been derived from postimplantation embryos just prior to gastrulation (E4.5-E5.5) and

this period is comparable to E9-E11 of porcine embryonic development. In human blastocysts restriction of OCT4 to the ICM, which occurs at day 6 post fertilization, coincides with a peak of human ES cell line derivation efficiency [19].

In human ES cells pluripotency is maintained by the combined actions of ACTIVIN regulated gene-expression through SMAD2/3 activation, NOGGIN induced inhibition of BMP signaling and bFGF induced activation of the mitogen activated protein kinase (MAPK) pathway [29, 38, 39, 49]. The findings that both mouse and rat EpiSCs can be maintained pluripotent *in vitro* by stimulating signaling pathways that also maintain human ES cells pluripotent suggests a conserved role for these signaling pathways in the maintenance of pluripotency in these cells [17, 18]. Also, human ICM epithelializes faster then mouse and this may in fact be accelerated in culture. Therefore, we have cultured both porcine ICM cells and porcine epiblast cells on MEF-feeders in basic culture medium supplemented with bFGF alone or in combination with ACTIVIN or the BMP inhibitor NOGGIN [29, 38, 39]. Also, porcine ICM and epiblast cells were cultured using the serum-free modified TeSR culture medium in combination with Matrigel coated dishes. Using these conditions, human ES cells have been derived without the need for feeders or animal-derived compounds [40]. None of the culture conditions sustained the undifferentiated self-renewal of pluripotent porcine cells. Although almost half of the primary colonies derived from ICM cells had an ES-like morphology and expressed the key transcription factors involved in pluripotency, these cells differentiated within 4 passages. Interestingly, the highest ratios of colonies with an ES-like morphology were observed in medium supplemented with bFGF. This suggests that bFGF-signalling is important in culturing pluripotent porcine cells, although other factors are needed. Porcine epiblast cells were more prone to differentiation *in vitro* compared to cells from the ICM, as analyzed by the number of primary colonies with an ES-like morphology. While porcine epiblast cells from E9-E10 embryos still exhibited uniform *NANOG* and *OCT4* mRNA expression, these cells were derived from embryos just prior to gastrulation and this could be the reason for their rapid differentiation in culture.

In mouse and human ES cells high concentrations of ACTIVIN direct differentiation towards the mesoderm and definitive endoderm lineages [50, 51], and inhibition of BMP signaling induces mouse ES cells to differentiate into the neural lineage while maintaining human ES cells pluripotent [29, 52]. Presence of these various growth factors in the culture medium did not consistently influence lineage commitment of differentiating porcine cells; endogenous signals secreted by differentiating cells may have overruled signaling from the exogenous growth factors added. A relatively large percentage of the differentiated cells in culture exhibited an endoderm-like phenotype and expressed GATA4 mRNA. Possibly the isolated ICM and epiblast cells were contaminated with primitive endoderm cells from the embryo. GATA4 positive cells differentiate from the outer cells of the ICM and primitive

endoderm differentiation has thus started *in vivo* before *in vitro* culture. In conclusion, signaling pathways that maintain pluripotency and self-renewal in human ES cells and mouse EpiSCs do not seem to be conserved in porcine ICM and epiblast cells in culture.

Both mouse and rat ES cells have been derived and cultured *in vitro* using a serum free medium supplemented with three synthetic inhibitors (3i) of the ERK cascade, FGF receptor tyrosine kinases; and of glycogen synthase kinase-3 GSK3 [5, 53]. It is suggested that inhibition of these signaling pathways protect the cells from endogenous and exogenous stimuli that drive their developmental differentiation and keep the cells in a ground state of self- renewal. Although human ES cells have not been reported to maintain pluripotency and self-renewal in 3i culture medium, it would be of interest to investigate whether porcine ICM or epiblast cells cultured in 3i give rise to pluripotent cell lines. Preliminary results show that inhibition of GSK3 does not have a positive effect on the culture of porcine pluripotent cells. Finally, porcine somatic cells have been reprogrammed to induced pluripotent stem cells and these cells form an excellent tool for testing culture conditions on their ability to maintain pluripotency and self-renewal [54-56].

Acknowledgements

This work was supported by a SenterNovem grant from the Ministry of Economic Affairs. The authors would like to thank Anko M. de Graaff and Richard W. Wubbolts of the Center for Cell Imaging at the Faculty of Veterinary Medicine in Utrecht for assistance in confocal laser scanning microscopy. We are grateful to Arie van Nes, Louis van der Boom, Jan Vernooij and the animal caretakers from the Tolakker for their assistance in the porcine animal experiments.

References

1. Evans MJ, Kaufman MH. Establishment in culture of pluripotential cells from mouse embryos. Nature. 1981;292:154-156.
2. Martin GR. Isolation of a pluripotent cell line from early mouse embryos cultured in medium conditioned by teratocarcinoma stem cells. Proc Natl Acad Sci U S A. 1981;78:7634-7638.
3. Thomson JA, Itskovitz-Eldor J, Shapiro SS, et al. Embryonic stem cell lines derived from human blastocysts. Science. 1998;282:1145-1147.
4. Thomson JA, Kalishman J, Golos TG, et al. Isolation of a primate embryonic stem cell line. Proc Natl Acad Sci U S A. 1995;92:7844-7848.
5. Buehr M, Meek S, Blair K, et al. Capture of authentic embryonic stem cells from rat blastocysts. Cell. 2008;135:1287-1298.

6. Li P, Tong C, Mehrian-Shai R, et al. Germline competent embryonic stem cells derived from rat blastocysts. Cell. 2008;135:1299-1310.
7. Ibrahim Z, Busch J, Awwad M, et al. Selected physiologic compatibilities and incompatibilities between human and porcine organ systems. Xenotransplantation. 2006;13:488-499.
8. Li M, Ma W, Hou Y, et al. Improved isolation and culture of embryonic stem cells from Chinese miniature pig. J Reprod Dev. 2004;50:237-244.
9. Strojek RM, Reed MA, Hoover JL, et al. A method for cultivating morphologically undifferentiated embryonic stem cells from porcine blastocysts. Theriogenology. 1990;33:901-913.
10. Piedrahita JA, Anderson GB, BonDurant RH. Influence of feeder layer type on the efficiency of isolation of porcine embryo-derived cell lines. Theriogenology. 1990;34:865-877.
11. Evans MJ, Notarianni E, Laurie S, et al. derivation and preliminary characterization of pluripotent cell lines from porcine and bovine blastocysts. Theriogenology. 1990;33:125-128.
12. Gerfen RW, Wheeler MB. isolation of embryonic cell-lines from porcine blastocysts. animal biotechnology. 1995;6:1-14.
13. Wianny F, Perreau C, Hochereau de Reviers MT. Proliferation and differentiation of porcine inner cell mass and epiblast in vitro. Biol Reprod. 1997;57:756-764.
14. Chen LR, Shiue YL, Bertolini L, et al. Establishment of pluripotent cell lines from porcine preimplantation embryos. Theriogenology. 1999;52:195-212.
15. Talbot NC, Powell AM, Garrett WM. Spontaneous differentiation of porcine and bovine embryonic stem cells (epiblast) into astrocytes or neurons. In Vitro Cell Dev Biol Anim. 2002;38:191-197.
16. Hochereau-de Reviers MT, Perreau C. In vitro culture of embryonic disc cells from porcine blastocysts. Reprod Nutr Dev. 1993;33:475-483.
17. Brons IG, Smithers LE, Trotter MW, et al. Derivation of pluripotent epiblast stem cells from mammalian embryos. Nature. 2007;448:191-195.
18. Tesar PJ, Chenoweth JG, Brook FA, et al. New cell lines from mouse epiblast share defining features with human embryonic stem cells. Nature. 2007;448:196-199.
19. Chen AE, Egli D, Niakan K, et al. Optimal timing of inner cell mass isolation increases the efficiency of human embryonic stem cell derivation and allows generation of sibling cell lines. Cell Stem Cell. 2009;4:103-106.
20. Flechon JE, Degrouard J, Flechon B. Gastrulation events in the prestreak pig embryo: ultrastructure and cell markers. Genesis. 2004;38:13-25.
21. Geisert RD, Brookbank JW, Roberts RM, et al. Establishment of pregnancy in the pig: II. Cellular remodeling of the porcine blastocyst during elongation on day 12 of pregnancy. Biol Reprod. 1982;27:941-955.
22. Guillomot M. Cellular interactions during implantation in domestic ruminants. J Reprod Fertil Suppl. 1995;49:39-51.
23. Hogan BB, R. Costantini, F. Lacy, E. Manipulating the mouse embryo, a laboratory manual. Second edition. Cold Spring Harbor Laboratory Press. 1994.
24. Prelle K, Holtz W, Osborn M. Immunocytochemical analysis of vimentin expression patterns in porcine embryos suggests mesodermal differentiation from day 9 after conception. Anat Histol Embryol. 2001;30:339-344.
25. Senger PL. Pathways to pregnancy and parturition. Second edition. Washington: Current Conceptions, Inc;. 1997.
26. Drews U. Color atlas of embryology. New York: Thieme Medical Publishers;. 1995:40-64.
27. Finley MF, Devata S, Huettner JE. BMP-4 inhibits neural differentiation of murine embryonic stem cells. J Neurobiol. 1999;40:271-287.

28. Williams RL, Hilton DJ, Pease S, et al. Myeloid leukaemia inhibitory factor maintains the developmental potential of embryonic stem cells. Nature. 1988;336:684-687.
29. Xu RH, Peck RM, Li DS, et al. Basic FGF and suppression of BMP signaling sustain undifferentiated proliferation of human ES cells. Nat Methods. 2005;2:185-190.
30. Li M, Zhang D, Hou Y, et al. Isolation and culture of embryonic stem cells from porcine blastocysts. Mol Reprod Dev. 2003;65:429-434.
31. Moore K, Piedrahita JA. Effects of heterologous hematopoietic cytokines on in vitro differentiation of cultured porcine inner cell masses. Mol Reprod Dev. 1996;45:139-144.
32. Boiani M, Scholer HR. Developmental cell biology: Regulatory networks in embryo-derived pluripotent stem cells. Nat Rev Mol Cell Biol. 2005.
33. Rozen S, Skaletsky H. Primer3 on the WWW for general users and for biologist programmers. Methods Mol Biol. 2000;132:365-386.
34. Kuijk EW, du Puy L, van Tol HT, et al. Validation of reference genes for quantitative RT-PCR studies in porcine oocytes and preimplantation embryos. BMC developmental biology. 2007;7:58.
35. Kuijk EW, Du Puy L, Van Tol HT, et al. Differences in early lineage segregation between mammals. Dev Dyn. 2008;237:918-927.
36. Magnani L, Cabot RA. In vitro and in vivo derived porcine embryos possess similar, but not identical, patterns of Oct4, Nanog, and Sox2 mRNA expression during cleavage development. Mol Reprod Dev. 2008;75:1726-1735.
37. Nieto MA, Bennett MF, Sargent MG, et al. Cloning and developmental expression of Sna, a murine homologue of the Drosophila snail gene. Development. 1992;116:227-237.
38. Wang G, Zhang H, Zhao Y, et al. Noggin and bFGF cooperate to maintain the pluripotency of human embryonic stem cells in the absence of feeder layers. Biochem Biophys Res Commun. 2005;330:934-942.
39. Vallier L, Alexander M, Pedersen RA. Activin/Nodal and FGF pathways cooperate to maintain pluripotency of human embryonic stem cells. J Cell Sci. 2005;118:4495-4509.
40. Ludwig TE, Levenstein ME, Jones JM, et al. Derivation of human embryonic stem cells in defined conditions. Nature biotechnology. 2006.
41. du Puy L, Chuva de Sousa Lopes S, Haagsman H, et al. Differentiation of porcine ICM cells into proliferating neural cells. Stem cells and development. 2009.
42. Plusa B, Piliszek A, Frankenberg S, et al. Distinct sequential cell behaviours direct primitive endoderm formation in the mouse blastocyst. Development (Cambridge, England). 2008;135:3081-3091.
43. Cauffman G, De Rycke M, Sermon K, et al. Markers that define stemness in ESC are unable to identify the totipotent cells in human preimplantation embryos. Human reproduction (Oxford, England). 2009;24:63-70.
44. Hart AH, Hartley L, Ibrahim M, et al. Identification, cloning and expression analysis of the pluripotency promoting Nanog genes in mouse and human. Dev Dyn. 2004;230:187-198.
45. Avilion AA, Nicolis SK, Pevny LH, et al. Multipotent cell lineages in early mouse development depend on SOX2 function. Genes & development. 2003;17:126-140.
46. Chazaud C, Yamanaka Y, Pawson T, et al. Early lineage segregation between epiblast and primitive endoderm in mouse blastocysts through the Grb2-MAPK pathway. Dev Cell. 2006;10:615-624.
47. Strumpf D, Mao CA, Yamanaka Y, et al. Cdx2 is required for correct cell fate specification and differentiation of trophectoderm in the mouse blastocyst. Development. 2005;132:2093-2102.
48. Kirchhof N, Carnwath JW, Lemme E, et al. Expression pattern of Oct-4 in preimplantation embryos of different species. Biol Reprod. 2000;63:1698-1705.

49. Xiao L, Yuan X, Sharkis SJ. Activin A maintains self-renewal and regulates fibroblast growth factor, Wnt, and bone morphogenic protein pathways in human embryonic stem cells. Stem Cells. 2006;24:1476-1486.
50. Kubo A, Shinozaki K, Shannon JM, et al. Development of definitive endoderm from embryonic stem cells in culture. Development. 2004;131:1651-1662.
51. Schuldiner M, Yanuka O, Itskovitz-Eldor J, et al. Effects of eight growth factors on the differentiation of cells derived from human embryonic stem cells. Proc Natl Acad Sci U S A. 2000;97:11307-11312.
52. Ying QL, Nichols J, Chambers I, et al. BMP induction of Id proteins suppresses differentiation and sustains embryonic stem cell self-renewal in collaboration with STAT3. Cell. 2003;115:281-292.
53. Ying QL, Wray J, Nichols J, et al. The ground state of embryonic stem cell self-renewal. Nature. 2008;453:519-523.
54. Ezashi T, Telugu BP, Alexenko AP, et al. Derivation of induced pluripotent stem cells from pig somatic cells. Proc Natl Acad Sci U S A. 2009;106:10993-10998.
55. Wu Z, Chen J, Ren J, et al. Generation of Pig-Induced Pluripotent Stem Cells with a Drug-Inducible System. J Mol Cell Biol. 2009.
56. Esteban MA, Xu J, Yang J, et al. Generation of induced pluripotent stem cell lines from Tibetan miniature pig. J Biol Chem. 2009;284:17634-17640.

Chapter 3

Differentiation of porcine ICM cells into proliferating neural progenitors.

Leonie du Puy [(1)], Susana M. Chuva de Sousa Lopes [(2)], Henk P. Haagsman [(3)], Bernard A.J. Roelen[(1)].

[1] Department of Farm Animal Health, Faculty of Veterinary Medicine, Utrecht University, Utrecht, The Netherlands ; [2] Department of Anatomy & Embryology, Leiden University Medical Center, Leiden, The Netherlands; [3] Department of Infectious Diseases and Immunology, Faculty of Veterinary Medicine, Utrecht University, Utrecht, The Netherlands.

Adapted from Stem cells and Development 2009

Abstract

Here we report the culture and differentiation of porcine neural cells derived from the inner cell masses (ICMs) of blastocyst-stage embryos. Manually dissected ICMs were cultured on feeder layers of inactivated mouse embryonic fibroblasts (MEFs). Neural rosette-like structures were selected and passaged mechanically. These structures were transient and disappeared after six passages. After transfer to Matrigel-coated dishes the cells proliferated for approximately two months. Expression of neural progenitor cell (NPC) specific genes *NESTIN*, *SOX1*, *SOX2* and *MUSASHI* as detected by RT-PCR suggest that the cell culture contains neural progenitor-like cells. To further confirm the culture of neural progenitor-like cells, we analyzed their differentiation potential *in vitro*. The porcine neural cells were able to differentiate into glial fibrillary acidic protein (GFAP) positive astrocytes and O4-positive oligodendrocytes, identified by quantitative RT-PCR and immunofluorescence. Differentiated cells expressed microtubule associated protein 2 (*MAP2*) RNA but were unable to differentiate into neurons. It is concluded that porcine blastocysts have the ability to provide an expandable source of neural cells that can develop into glial subtypes.

Introduction

Embryonic stem (ES) cell lines have been generated from mouse and human blastocyst-stage embryos. ES cells are capable of self-renewal, are pluripotent, and neurons and glia (astrocytes and oligodendrocytes) were among the first cell types identified that differentiated from ES cells [1-3]. Neural stem cells have also been isolated from the (embryonic) central and peripheral nervous system and cultured *in vitro* [4, 5]. Neural stem cells are defined by their ability to self-renew and generate both neurons and glia.

Methods to direct the differentiation of ES cells to neural lineages include exposure to retinoic acid (RA) [6], culture in serum replacement medium using N2 and B27 supplements [7], or co-culture with stromal cell lines [8]. ES cell differentiation to the neuronal lineage is characterized by the formation of neural rosettes, structures of radially-organized columnar epithelial cells. Cells in neural rosettes express the neuroectoderm markers paired box 6 (PAX6) and sry box 1 (SOX1) and can differentiate into subtypes of neurons and glia cells that are region specific, for example into spinal motor neurons and midbrain dopamine neurons [9]. Without the proper signals, differentiation of the neural rosette cells can continue into neural progenitor cells (NPCs) with a differentiation potential that is regionally limited. ES-cell derived NPCs have a long term proliferation capacity *in vitro* and form neurons

and glia upon differentiation [10-12]. Studies have reported that ES-cell derived NPCs have properties of embryonic radial glia cells [13-15]. Radial glia cells are a heterogeneous population of precursor cells, responsible for the majority of neurogenesis in the developing brain [16]. *In vitro* neural differentiation of ES cells therefore resembles neural differentiation that takes place during embryonic central nervous system development.

The *in vitro* differentiation of ES cells towards neural progeny can be used to study early neural development and neurodegenerative disorders. These cells can also be used in neuropharmacological screening studies to identify neuroprotective and neurotoxic reagents. In addition, ES cells are a potential source of neural cells for use in cell transplantation therapies to treat neurological disorders by replacement of lost or damaged tissue. For such clinical purposes, results gained in rodent models need to be extended to larger mammals to test the safety and feasibility of these therapies in human medicine. Pigs are more similar in anatomy, physiology, immunology and life span to humans than mice, and therefore the pig could serve as a more predictive animal model in cell replacement studies.

However, true ES cell lines from the pig have not been described and although reports have been made about neural differentiation from porcine inner cell masses (ICMs) [17, 18] the differentiation potential of these neural-like cells was not studied. Here we report the culture and differentiation of porcine neural cells derived from the ICM of blastocyst-stage embryos.

Materials and Methods

Derivation of in vivo embryos.

Normal cycling sows were examined for the onset of estrus and upon detection, were artificially inseminated with fresh boar semen of proven fertility. The day of artificial insemination was designated as gestational day (gd) 0. Pregnant sows were slaughtered between gd 6.5 and gd 7.5. The reproductive tract was removed and flushed with Dulbeco's phosphate-buffered saline (PBS, Sigma) containing 1% fetal bovine serum (Greiner), 50 U/ml penicillin, and 50 µg/ml streptomyocin (Gibco). All procedures performed were approved by the institutional animal experiments committee.

Culture of porcine ICM cells.

The ICM from these embryos was mechanically separated from the trophectoderm using tungsten needles. After isolation, the ICM cells were placed on irradiated Mouse Embryonic Fibroblasts (MEFs) in basic culture medium consisting of Knockout (KO) DMEM (Invitrogen), 10% KO serum replacement (Invitrogen), 10% human plasmanate (Sanquin/Talecris), 1x non essential amino acids (Gibco), 2 mM Glutamax

(Invitrogen), 0.1 mM beta-mercapthoethanol (Gibco), 50 U/ml penicillin, 50 µg/ml streptomyocin (Gibco) and 10-20 ng/ml basic fibroblast growth factor (bFGF) (Peprotech/Invitrogen). Cell culture was carried out at 37.5ºC and 5% CO_2.

Culture and differentiation of neural derivatives.
Emerging neuronal rosettes were sub-cultured manually on MEFs in basic culture medium containing 20 ng/ml bFGF (Invitrogen). After 6 passages, rosette-like structures disappeared and the colonies were trypsinized and placed on Matrigel (BD Biosciences) in culture medium in which the 10% plasmanate was substituted by 15% KO serum replacement. Subsequently, the cells were passaged using trypsin every other day, keeping the cells at 50-100% confluency. For neurosphere formation, cells were cultured in suspension in basic medium containing 20 ng/ml bFGF. For differentiation, two day-old neurospheres were plated on Matrigel-coated dishes containing differentiation medium based on DMEM-F12 (Gibco) supplemented with 1x N2 and 1x B27 (Invitrogen), 1x non essential amino acids and 50 U/ml penicillin, 50 µg/ml streptomyocin. Platelet derived growth factor (PDGF) (10 ng/ml, Bio-Connect) and bFGF (10 ng/ml, Invitrogen) were added to stimulate oligodendrocyte differentiation; and (sonic hedgehog) SHH (100 ng/ml, Invitrogen) and (fibroblast growth factor 8) FGF8 (100 ng/ml, Invitrogen) to stimulate neural differentiation. Differentiation was induced for nine more days, a comparable differentiation period to the ones used in neural differentiation protocols from hESCs, as we differentiate our cells from a NPC-like state instead of an ES-like state.

RNA isolation, normal and quantitative RT-PCR.
Total RNA was extracted using the RNeasy microkit (Qiagen) and on-column DNAse treatment (Qiagen) was performed. Total RNA was reverse transcribed into cDNA using Superscript II reverse transcription-polymerase (Invitrogen) and random primers (Invitrogen) according to the supplier's protocol. For reverse transcriptase-polymerase chain reaction (RT-PCR) primers were designed using Primer 3 software or based on literature (Table 1) [19-23]. PCR was carried out in a final volume of 25 µl containing 1x PCR buffer (Invitrogen), 0.5 mM $MgCl_2$, 0.5 mM forward primer, 0.5 mM reverse primer, 0.625 units Taq DNA polymerase (Invitrogen) and 1 µl of cDNA. Initial denaturation for 5 min at 95ºC was followed by 40 cycles of 15 sec at 95ºC, 30 sec at the corresponding annealing temperature (Table 1) and 30 sec at 72ºC. The final step consisted of 7 min extension at 72ºC. PCR products were separated on a 1% agarose gels and visualized with ethidium bromide against a 100 bp ladder. To verify the specificity, the PCR products were sequenced.

For quantitative real-time PCR, each reaction contained 10 µl SYBRGreen Mastermix (Bio-Rad), 0.5 mM forward primer, 0.5 mM reverse primer and 1 µl cDNA as a template in a final volume of 20 µl. The experiments were performed in biological

triplicates by differentiating the cells starting at three different cultural passage numbers and the samples were pipetted in duplo on the PCR plate to correct for any pipetting and or plate errors. Reactions were carried out in duplicate for each sample. Negative controls were reactions containing template synthesized without reverse transcriptase and reactions containing H_2O instead of cDNA. The reaction was amplified on a Bio-Rad MyIQ Real-Time PCR detection system using the following program: initial denaturation at 95ºC for 3 min, followed by 40 cycles of 30 sec at 95ºC, 30 sec at the corresponding annealing temperature (Table 1) and 30 sec at 72ºC.

Table 1. Primers used for RT-PCR and Q-PCR.

Gene [reference nr]	5' forward primer 5' reverse primer	Ta (°C)	amplicon size (bp)
GAPDH **[18]**	TCGGAGTGAACGGATTTG CCTGGAAGATGGTGATGG	51.1	219
18S **[18]**	GGCTACCACATCCAAGGAAG TCCAATGGATCCTCGCGGAA	58.7	149
PGK1 **[18]**	AGATAACGAACAACCAGAGG TGTCAGGCATAGGGATACC	56.4	126
NANOG **[19]**	CCTCCATGGATCTGCTTATTC CATCTGCTGGAGGCTGAGGT	63.0	210
OCT4 **[19]**	GTTCTCTTTGGGAAGGTGTT ACACGCGGACCACATCCTTC	55.4	313
SOX2 **[21]**	CTGCGAGCGCTGCAGATGAA CCTCCGGGCAGTGTGTACTTATCCT	60.0	101
NESTIN **[17]**	GGCTTCTCTCAGCATCTTGG AAGGCTGGCATAGGTGTGTC	63.0	150
SOX1 **[PRIMER 3]**	CACAACTCGGAGATCAGCAA GTCCTTCTTGAGCAGCGTCT	60.0	173
MAP2 **[20]**	AAAGACCAACCTGCAGCTCTG TCCACTGGGACCGTCTGTTC	60.0	101
MBP **[20]**	GAGGCAGAGCTCCTGACTACAAA GTCCCGTCCTCCCAGCTT	61.4	101
GFAP **[17]**	TTGACCTGCGACGTGGAGTC AGGTGGCGATCTCGATGTCC	61.4	225
NEUROFILAMENT **[20]**	CAGAGCTGGAGGCACTGAA CATCTCCCACTTGGTGTTCC	57.0	146
MUSHASHI **[PRIMER 3]**	CGAGCTCGACTCCAAAACAAT GGCTTTCTTGCATTCCACCA	56.0	304

A melting curve was produced to verify single PCR product amplification. Efficiency of the PCR reaction was tested using a standard curve synthesized from either a dilution series of cDNA or PCR product [21]. Data were analyzed with iQ5 software (Bio-Rad). Starting quantities of all genes were calculated based on their standard curves. qPCR data were normalized to glyceraldehyde 3-phosphate dehydrogenase (*GAPDH),* phosphoglycerate kinase 1 (*PGK1),* and ribosomal protein *S18*. Genomic DNA contamination was determined by minus RT levels. If minus RT levels were higher than 5% of the plus RT levels, samples were excluded from the analysis for that particular gene. Gene expression levels for *SOX2*, *NESTIN*, Glial Fibrillary Acidic Protein (*GFAP)* and Microtubule-Associated Protein 2 (*MAP2)* are reported relative to expression levels in proliferating cells. As MBP expression levels in proliferating cells was around the detection limit, expression levels were calculated relative to cells differentiated 5 days in N2B27 medium. Statistical differences between expression levels were tested using a nonparametric Kruskal-wallis H test and a probability value <0.05 was considered significant. A Scheffe correction was applied for multiple comparisons.

Immunofluorescence

Cells were cultured on Matrigel coated glass cover slips then fixed in 4% (para formaldehyde) PFA for 10 min at room temperature (RT). Cells were permeabilized (0.1% Triton in PBS; 8 min) then non-specific binding sites blocked (4% normal goat serum, 0.1% Tween; 1 hr RT). Thereafter, cells were incubated overnight at 4ºC with primary antibody, then incubated for 1 hr at RT with secondary antibody incubation. Coverslips were mounted in Fluosave mounting medium (Calbiochem) and analysed by normal fluorescence or confocal laser scanning microscopy. Primary antibodies used are listed in Table 2. Specificity of the antibodies was tested on frozen sections of porcine brain (Supplemental Fig 1). Sections were fixed in 4% PFA for 10 min at RT and non specific binding sites blocked (4% normal goat serum, 0.1% Tween; 1 hr RT). Subsequently the protocol was identical to the method used for the immunofluorescence staining of cells cultured on coverslips described above.

Table 2. Antibodies used for immunofluorescence.

Protein	Manufacturer (Product code)	Concentration/ dilution	Description
SOX2	R&D Systems (clone 245610) (MAB2018)	10 µg/ml	Monoclonal mouse
GFAP	DakoCytomation (Z0334)	5.8 µg/ml	Polyclonal rabbit
VIMENTIN	DakoCytomation (M0725)	1.0 µg/ml	Monoclonal mouse
O4	Chemicon (clone 81) (MAB345)	5.25 µg/ml	Monoclonal mouse
PAX6	Chemicon (AB5409)	1 to 100	Rabbit serum
TUJ1	Chemicon (clone TU-20) (MAB1637)	1 to 250	Monoclonal mouse
KI67	DakoCytomation (MIB-I)	1 to 100	Monoclonal mouse
PH3	Millipore (catalog number 06-570)	1 to 100	Rabbit serum

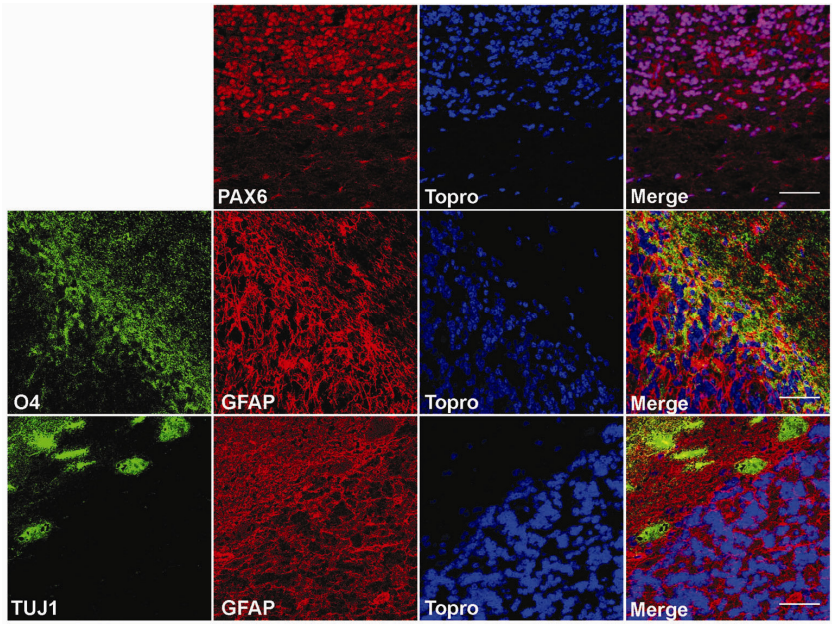

Supplemental Figure 1: Immunofluorescence staining on frozen sections of the porcine cerebellum.
Immunofluorescence stainings on frozen sections of the porcine cerebellum. PAX6: paired box 6, marker for NPCs. GFAP: glial fibrillary acidic protein, a marker for astrocytes and NPCs. O4: oligodendrocyte specific protein; TUJ1: Beta III Tubulin, marker for neurons. Topro: nuclear staining. Scale bars: 50 µm

Results

Porcine ICM cells can differentiate into the neural lineage in vitro.
The uteri of 6.5-7.5 gd pregnant sows were flushed to collect blastocyst-stage embryos. The embryos were no longer surrounded by the zona pellucida and contained an ICM that was not yet epithelialized (Fig 1A). At this stage a cell-layer of primitive endoderm could not be distinguished. Each ICM was mechanically isolated from the conceptuses using tungsten needles and plated on irradiated MEFs in KO DMEM containing 10% KO serum replacement and 10% human plasmanate supplemented with bFGF. Primary colony formation was evaluated after 3-5 days in culture, and 13 of the 15 ICMs formed primary colonies. Most primary colonies (10/13) were morphologically similar to undifferentiated mouse ES cells: small cells with large nuclei, unclear cell-cell boundaries and a well-defined colony border (Fig 1B). Other colonies contained cells with a more differentiated morphology (Fig 1C). The cells were subsequently passaged mechanically every 4-7 days. After three passages, rosette-like structures formed in 7 of the 13 cell-cultures (Fig 1D). Gene expression analysis of cells during this initial culture period showed progressive loss of expression of the pluripotency genes *NANOG* and *OCT4*, while expression of *SOX2*, a gene also expressed in neuroectoderm, was up-regulated (Fig 2).

Colonies containing rosette-like structures were mechanically separated from cells with different morphologies and plated in medium containing 20 ng/ml bFGF. Between passages 4-6, rosette-like structures gradually disappeared. At this time, cells were transferred to Matrigel-coated dishes, passaged using trypsin in medium containing 20 ng/ml bFGF and 15% KO serum.

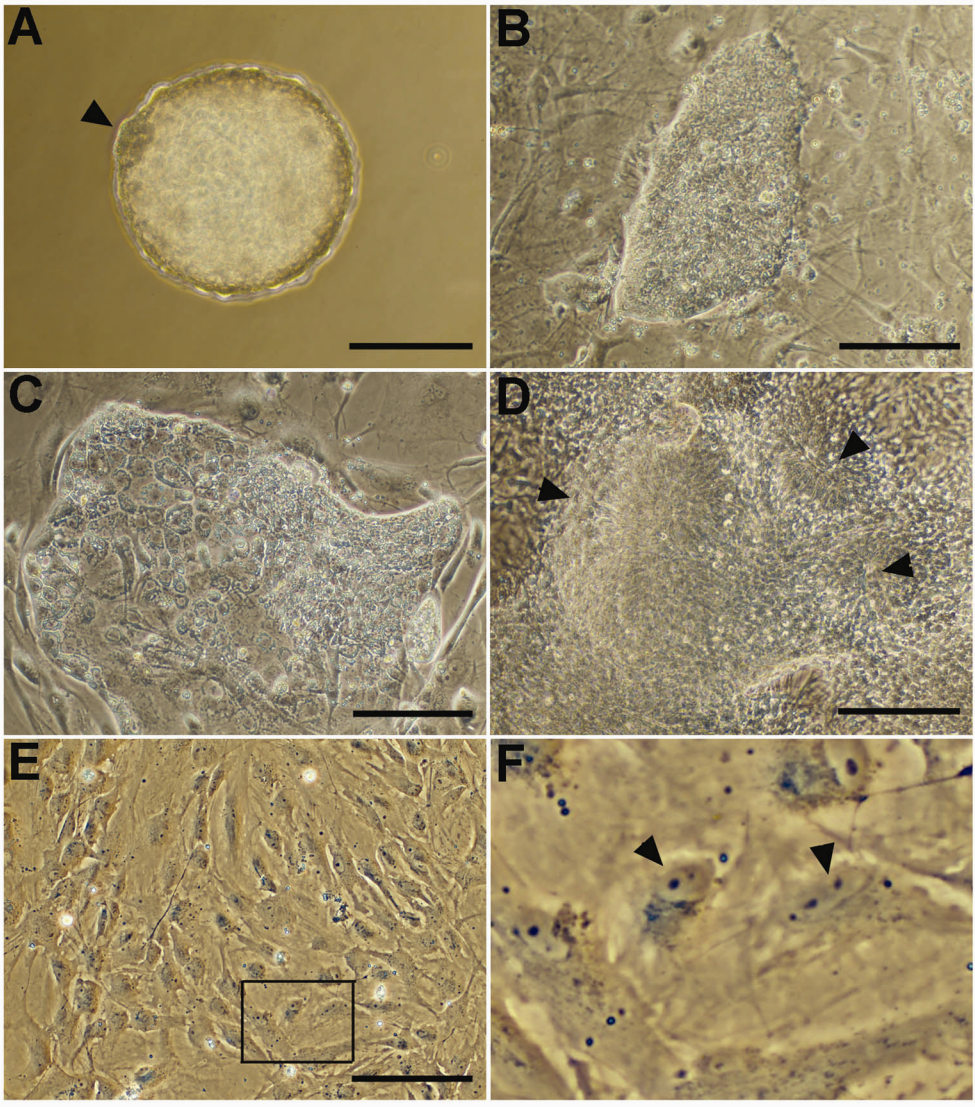

Figure 1: Morphology of porcine blastocysts and ICM-derived cells in culture.
(A) Blastocyst-stage embryo used for ICM isolation; arrow head points to the ICM; **(B)** Primary colony of porcine ICM derived cells morphologically similar to undifferentiated mouse ES cells, on MEFs; **(C)** Primary colony of porcine ICM derived cells with a differentiated morphology, on MEFs; **(D)** Differentiated cells at passage 3 containing rosette-like structures (arrow heads); **(E)** Morphology of porcine neural cells cultured on Matrigel-coated plastic derived from ICM cells; **(F)** Higher magnification of frame in (E): arrow heads indicate nuclei with nucleoli. Scale bars: 50 µm.

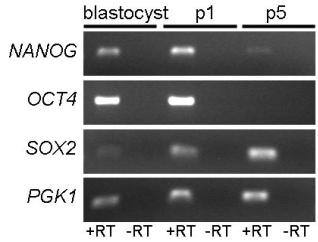

Figure 2: Differentiation of ICM derived cells characterized by RT-PCR.
RT-PCR analysis is shown of the expression of markers in porcine ICM derived cell cultures. All panels show 1% ethidium bromide stained 1% agarose gels. Reactions containing template synthesized without reverse transcriptase (-RT) served as a control for genomic DNA contamination. *P*1: ICM derived primary colonies; *P5*: ICM derived cells cultured to passage 5.

Due to the survival-promoting effect of cell-cell contact in NPC cultures, cells were passaged every other day, keeping cell density between 50-100% [24]. The cells could be cultured for approximately 24 passages (about two months) before proliferation stopped (Fig 3). Upon disappearance of the rosette-like structures, the cytoplasm of the cells was spread and an organized cytoskeletal network was clearly visible (Fig 1E). Nuclei of the cells were oval and speckled with one or two nucleoli (Fig 1F).

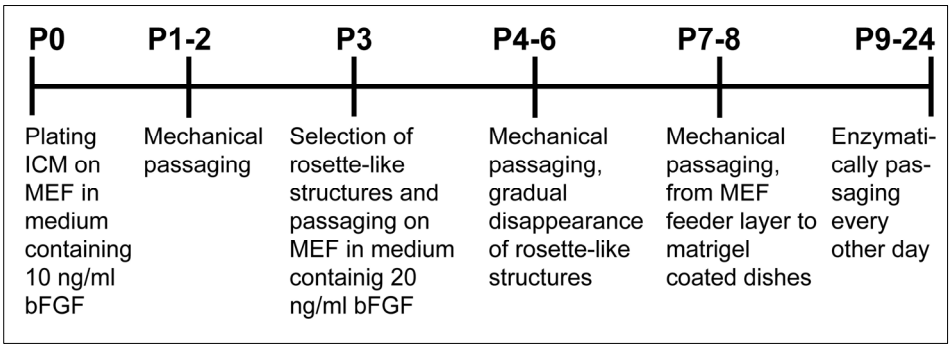

Figure 3: Schematic overview of the culture process.

ICM derived neural progeny express markers of NPCs.
For characterization of the cells, RT-PCR was used to examine the expression of genes suggested to be markers for NPCs in other mammalian species. PCR analysis detected expression of genes coding for the transcription factors *SOX1* and *SOX2*, both *Sry*-related HMG box-containing proteins highly expressed in the CNS and shown to have a function in the maintenance of NPC identity [25, 26]. Cells also expressed mRNA of the intermediate filament *NESTIN* and the RNA-binding protein *MUSASHI*, both proposed markers for NPCs [27, 28]. Cells at passages 11 and 18, but also brain tissue expressed *NANOG* and *OCT4* (Fig 4).

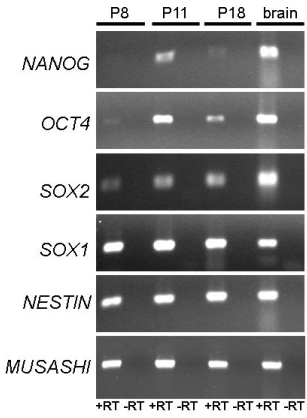

Figure 4: Characterization of neural cells by RT-PCR.
RT-PCR analysis is shown of the expression of proposed NPC markers in neural cell cultures derived from porcine ICM. All panels show 1% ethidium bromide stained 1% agarose gels. Reactions containing template synthesized without reverse transcriptase (-RT) served as a control for genomic DNA contamination. *P*8, *P*11, *P*18: ICM derived neural cells cultured to passage 8, 11 and 18 respectively.

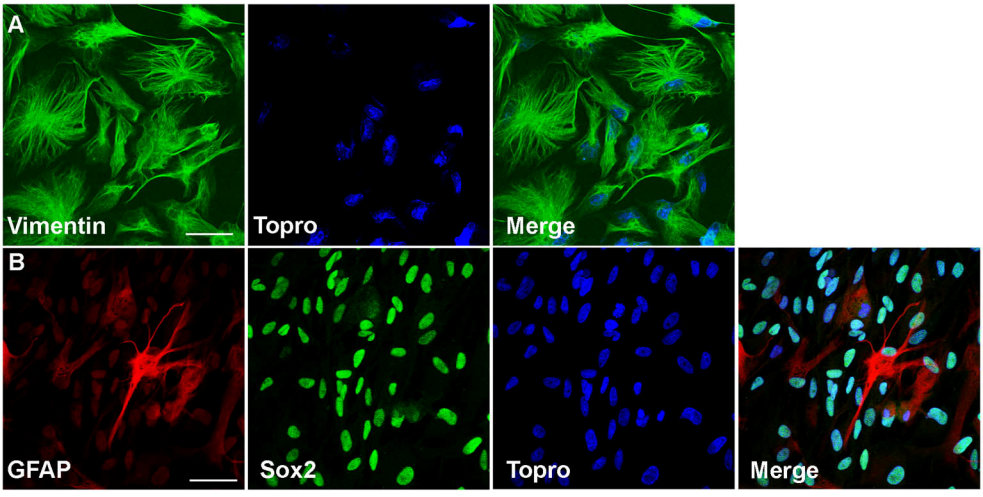

Figure 5: Characterization of neural cells by immunofluorescence staining.
Immunofluorescence staining of neural cells (passage 14) are shown. Vimentin: intermediate filament protein expressed in various tissues of the central nervous system. GFAP: glial fibrillary acidic protein, a marker for astrocytes and NPCs. Sox2: *Sry*-related HMG box-containing proteins highly expressed in the CNS. Topro: nuclear staining. Scale bars: 50 µm.

Further characterization of the cells was carried out by examining protein distribution using immunofluorescence. VIMENTIN, an intermediate filament protein expressed in various cell types of the CNS and in NPCs [29, 30], was widely expressed by the cells (Fig 5A). Virtually all cells (~97%) stained positive for SOX2 (Fig 5B),

confirming the results from RT-PCR. The expression pattern of GFAP, a marker for astrocytes and NPCs, was heterogeneous with 13% of the cells expressing high levels of GFAP (Fig 5B).
No expression was detected for PAX6 protein, a transcription factor involved in various developmental processes of the central nervous system and a suggested marker for neural stem cells (results not shown) [31]. The proliferative capacity of the cells as observed by the frequency of cell culture passaging was confirmed by immunofluoresence staining using Ki67 (stains all nuclei of cells in active phases of the cell-cycle) and PH3 (stains nuclei in the S-phase of the cell-cycle) antibodies. At passage 20, approximately 25% of the cells stained positive for PH3 and 50% stained positive for Ki67 (result not shown).

Differentiation of porcine neural cells into astrocytes and oligodendrocytes.
Neural cells can be cultured *in vitro* to form neurospheres: free floating cell aggregates that contain stem cells and some of their progeny. Suspension culture of the ICM-derived neural cells led to the formation of neurosphere-like structures (Fig 6A). As the cells expressed markers of NPCs, we next studied whether they could differentiate into cells with neuron and glial characteristics *in vitro*. Two day-old neurosphere-like structures were plated on Matrigel-coated dishes in N2B27 based differentiation medium lacking growth factors, or containing both PDGF (10 ng/ml) and bFGF (10 ng/ml) to induce differentiation towards oligodendrocytes, or containing SHH (200 ng/ml) together with FGF8 (100 ng/ml) to induce differentiation towards midbrain dopaminergic neurons. Differentiation was induced for 9 extra days. The neurospheres readily attached to the culture dish and extensive outgrowths were visible after 2 days (Fig 6).

During differentiation cells stopped proliferating (cells were Ki67 negative: results not shown). RNA expression levels of *SOX2* were significantly higher in neurospheres and differentiated cells compared to those of proliferating cells (Fig 7A). SOX2 protein expression was observed in almost all differentiated cells (~100%) (Fig 8B), but no differences were observed between the various differentiation media. *NESTIN* gene-expression levels of proliferating and differentiated cells were similar (Fig 7B).

Differentiation of the cells towards astrocytes was analyzed by studying gene and protein expression of GFAP. Gene expression levels of *GFAP* were significantly higher in differentiated cells compared to proliferating cells. *GFAP* RNA expression was maximal around day five of differentiation, with a subsequent down-regulation thereafter. No significant up-regulation of *GFAP* expression levels was found in cells differentiated in the presence of growth factors compared to cells differentiated without growth factors (Fig 7C).

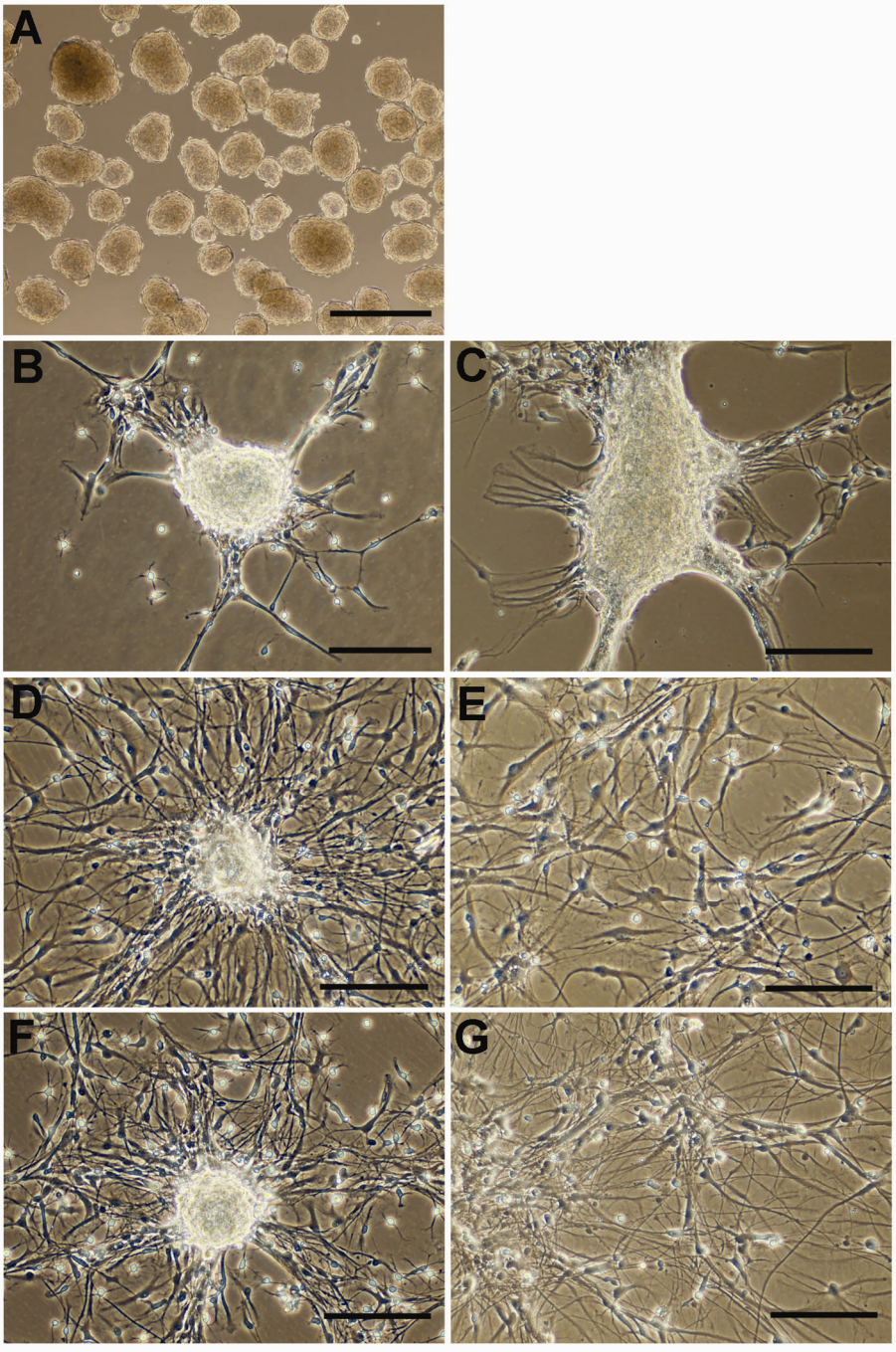
A
B
C
D
E
F
G

Figure 6: Morphology of the neural cells during differentiation.
(A) Neural cells cultured in suspension, forming neurosphere-like structures; **(B)** two day-old and **(C)** 6 day-old outgrowths of neurospheres plated on Matrigel coated dishes, in N2B27 based differentiation medium lacking growth factors; **(D)** two day-old and **(E)** 6 day-old outgrowths of neurospheres plated on Matrigel coated dishes in N2B27 based differentiation medium containing PDGF (10 ng/ml) and bFGF (10 ng/ml); **(F)** two day-old and **(G)** 6 day-old outgrowths of neurospheres plated on Matrigel coated dishes, in N2B27 based differentiation medium containing both or SHH (200 ng/ml) together with FGF8 (100 ng/ml). Scale bars: 50 µm.

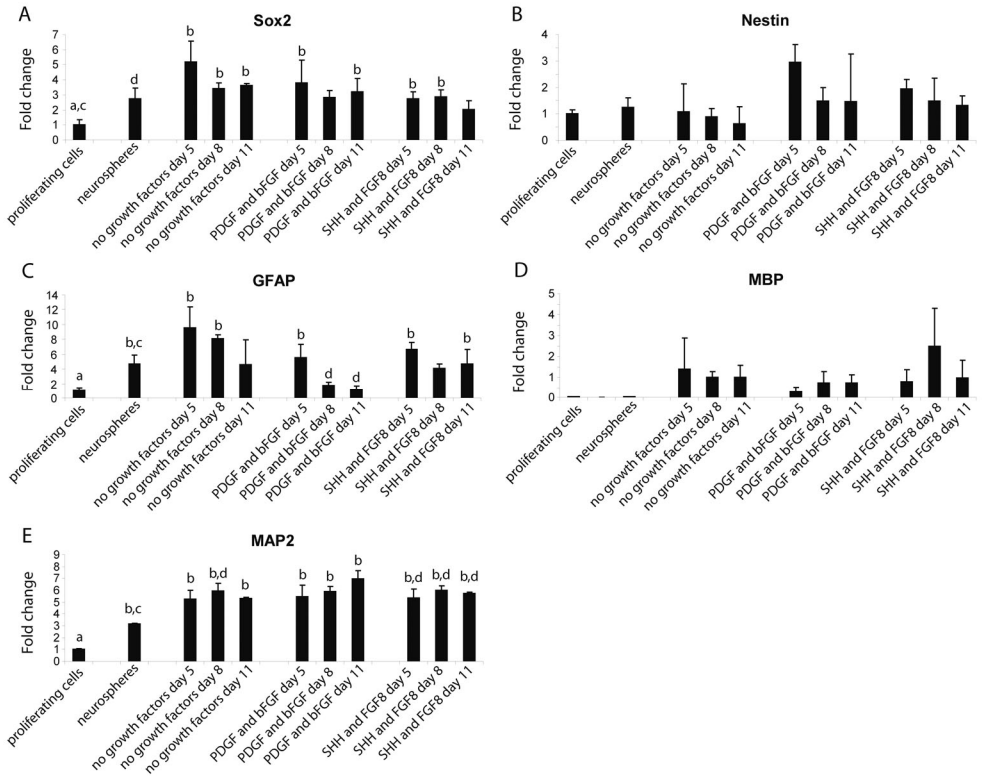

Figure 7: Relative mRNA expression levels of Sox2, Nestin, GFAP, MBP and MAP2 during neural cell differentiation.
Gene expression levels of the neural progenitor markers Sox2 and Nestin, neuron marker microtubule associated protein 2 (MAP2), astrocyte marker glial fibrillary acidic protein (GFAP) and oligodendrocyte marker myelin basic protein (MBP) as detected by quantitative RT-PCR. Values are normalized to the housekeeping genes GAPDH, PGK1 and 18S. The experiments were performed in biological triplicates by differentiating the cells starting at three different cultural passage numbers. Error bars represent standard error of the mean. a: $p<0.05$ versus b; c: $p<0.05$ versus d.

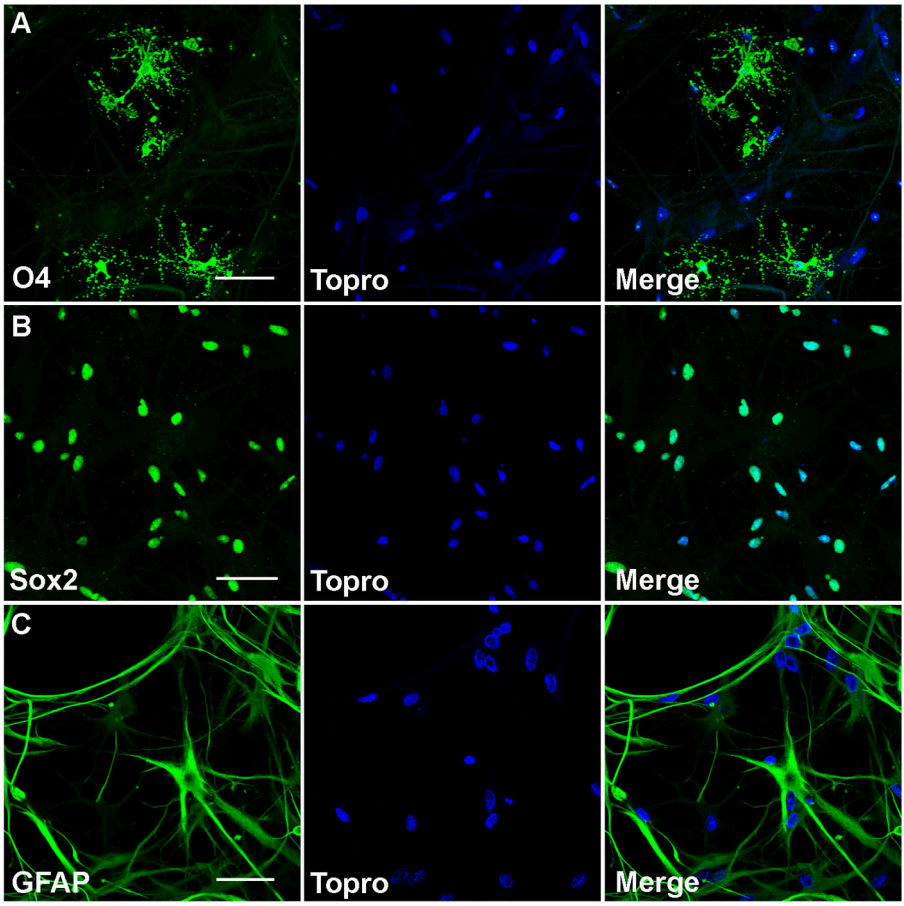

Figure 8: Characterization of neural cell differentiation by immunofluorescence staining. Immunofluorescence staining on differentiated neural cells in N2B27 based differentiation medium containing PDGF (10 ng/ml) and bFGF (10 ng/ml). O4: oligodendrocyte specific protein; Sox2: *Sry*-related HMG box-containing proteins highly expressed in the CNS. GFAP: glial fibrillary acidic protein, a marker for astrocytes and NPCs. Topro: nuclear staining. Scale bars: 50 µm

Immunofluorescent staining of GFAP showed that most differentiated cells (>90%) expressed high levels of GFAP (Fig 8C) and no difference was observed between the differentiation protocols (results not shown).

Differentiation of the cells towards oligodendrocytes was analyzed by studying gene expression levels of the oligodendrocyte specific Myelin Basic Protein (*MPB*) and O4 protein expression. *MBP* expression in proliferating cells was around the detection

limit but could be readily detected in differentiated cells (Fig 7D). Few cells (<10%) within the differentiated culture stained positive for O4 (Fig 8A), and exhibited the characteristic morphology of oligodendrocytes. O4 protein was not expressed in proliferating cells, and stimulation with different growth factors yielded comparable results (results not shown).

To test whether the cells differentiated into neurons, *MAP2* and *NEUROFILAMENT* RNA expression levels were measured. While the differentiated cells had up to six times higher expression levels of *MAP2* (Fig 7E) compared to proliferating cells, *NEUROFILAMENT* expression levels were around the detection limit (results not shown). Immunofluorescence staining on differentiated cells using an antibody against Beta III Tubulin (TUJ1) was negative (results not shown) indicating that the cells were unable to differentiate to neurons and therefore more specific markers for midbrain dopaminergic neurons were not tested.

In summary, the cells differentiated towards both GFAP-positive astrocytes and O4-positive oligodendrocytes, with GFAP-positive cells being the most abundant. No obvious differentiation towards neurons was detected. The various growth factors added to the differentiation medium did not have an effect on the timing or direction of differentiation.

Discussion

In this paper, we describe the derivation of neural cells from the culture of ICM from porcine blastocysts. These neural cells could be cultured *in vitro* while the expression of neuroectoderm markers was maintained. Differentiation of the neural cells was tested during culture and the cells differentiated into astrocytes and oligodendrocytes, while neuronal derivatives were not detected.

Initial differentiation of porcine ICM cells towards the neural lineage was inefficient. In addition to the formation of neural rosettes, a vast majority of the ICM cells differentiated into cells with both endodermal and mesodermal characteristics (results not shown). While presence of bFGF in the culture medium is required for the propagation of neural cells, the initial induction of neural fate is probably not affected by bFGF [32]. Possible methods to increase the efficiency of neural differentiation are to culture porcine ICM cells in the presence of RA or BMP-inhibitors, as it has been described that the differentiation of ES cells to neural cells is significantly increased by these culture conditions [33, 34].

Expression analysis of the cell population described here demonstrates that virtually all cells (~97%) were positive for SOX2, suggesting a homogenous population of cells with neural characteristics. At passages 11 and 18, RT-PCR analysis detected expression of both *OCT4* and *NANOG* mRNA in the cultured cells as well as

in brain tissue. Expression of *NANOG* mRNA in the porcine adult brain has been previously observed but its role in this tissue remains unknown [17]. OCT4 was found to be expressed in neural cells isolated from the fetal mouse brain and down-regulation of OCT4 in these cells promoted differentiation [35]. OCT4, NANOG and SOX2 are key regulators of pluripotency in the ICM of blastocysts and in ES cells. It is possible that the cultured cells described in this paper contained residual undifferentiated cells. *OCT4* and *NANOG* mRNA was not detected at passages 5 and 8 of cell-culture and re-appeared at passages 11 and 18. Perhaps the variation in *OCT4* and *NANOG* mRNA expression over passage is the result of differences in the self-renewal capacity of the cells. Human and mouse somatic cells can be reprogrammed into pluripotent stem cells by the ectopic expression of the transcription factors OCT4, SOX2, c-MYC and KLF4 [36, 37]. Inducing pluripotency in NPCs needs less genetic manipulation because of the endogenous expression of SOX2 and c-MYC [38-40]. ICM derived NPCs could therefore potentially serve as a source to generate porcine induced pluripotent stem cells.

Expression of *NESTIN*, *MUSASHI*, *SOX1*, and *SOX2* mRNA was detected by RT-PCR. These genes were detected over multiple passages, showing a constant expression during the culture period. All cells were positive for VIMENTIN and some were positive for GFAP. GFAP expression by some cells could indicate that the cell population contained neural cells differentiated into the astrocyte lineage.

Porcine NPCs have been derived from the fetal pig brain, cultured *in vitro* and shown to differentiate *in vivo* [41, 42]. In addition, spontaneous differentiation of *in vitro* cultured porcine and bovine ICM into the neural lineage has been previously reported [17, 18, 43, 44], but optimal culture conditions, to maintain undifferentiated growth of ICM cells or to direct differentiation into the neural lineage, were not reported. Neural cells differentiated from porcine ICM cells (from blastocyst stage embryos, g.d. 8) derived by Talbot and colleagues tested positive for VIMENTIN and GFAP and were cultured for multiple passages. However, there are no studies to test the differentiation potential of these cells into more specific neural cell types [17, 18, 43]. Neural crest cells derived from bovine ICM have been described by Lazzari and colleagues [44]. These cells had a high proliferation capacity and were capable of differentiating *in vitro* and *in vivo* into both neural and ectomesenchymal derivatives, with the latter becoming more dominant with every passage. In the cell culture described in this paper, no differentiation towards mesenchymal derivatives from porcine neural rosettes was observed. This could be due to differences in the culture methods used.

To further characterize the neural cells from porcine ICMs, differentiation was induced by plating neurospheres in N2B27 medium with or without supplement growth factors. The cells differentiated towards astrocytes (GFAP) and oligodendrocytes (O4, *MBP*), but were unable to differentiate towards the neuronal lineage *in vitro*. Astrocytes and oligodendrocytes are the non-neuronal cells of the nervous system belonging to a group collectively called glial cells which do not conduct nerve

impulses. Astrocytes regulate the external environment of neurons by removing excess ions and taking up neurotransmitters released during synaptic transmission. Oligodendrocytes produce myelin to insulate the nerve cell axons and thereby allow electrical signals to propagate more efficiently. These functions make glial cells important partners of neurons in the central nervous system [45]. Remarkably, cells cultured in conditions that promoted their differentiation still expressed SOX2 (Figs 7A, 8B). SOX2 expression in the nervous system has been shown to maintain the proliferative capacity of neural cells and inhibit their differentiation into the neuronal lineage while permitting astroglia differentiation [25, 46]. This suggests that continued SOX2 expression may have prevented the cells from differentiating into neurons.

In human and mouse ES cell derived NPCs, the combined use of SHH and FGF8 induced differentiation towards midbrain dopaminergic neurons [47, 48]. Differentiation of NPCs towards oligodendrocytes has been stimulated by supplementation of PDGF and bFGF [49, 50]. The neural cells derived from porcine ICMs did not respond to the supplementation of these growth factors to the differentiation medium. In the developing brain the frequency of stem cells with a broad differentiation potential declines while more restricted progenitors take their place [51], and this same process has been observed during the neural differentiation of ES cells *in vitro*. While neural rosette cells can still respond to the inductive signals described above, NPCs derived from these cells can not [9].

The results suggest that the cells described in this paper consisted of a more developmentally restricted neural cell population that either contained a single progenitor that could form both astrocytes and oligodendrocytes or consisted of a mixture of astrocytic and oligodendritic precursor cells.

The formation of donor-derived brain tumors has been described in a human patient after therapeutic fetal neural stem cell transplantation [52]. This finding stresses the importance of testing the safety of stem cell therapies in large animal models with physiology more similar to humans. The results reported in this paper describe both the generation of an expandable population of neural cells directly isolated from porcine ICM cells and the tools to characterize these cells. This work provides a starting point that may eventually lead to the generation of porcine neural cells with a broad differentiation capacity and may facilitate the use of pigs in studying the safety of NPC-based cell replacement therapies in human medicine.

Acknowledgements

This work was supported by a SenterNovem grant from the Ministry of Economic Affairs. The authors would like to thank Anko M. de Graaff and Richard W. Wubbolts of the Center for Cell Imaging at the Faculty of Veterinary Medicine in Utrecht for

assistance in confocal laser scanning microscopy. We are grateful to Arie van Nes, Louis van der Boom, Jan Vernooij and the animal caretakers from the Tolakker for their assistance in the porcine animal experiments.

References

1. Evans MJ, Kaufman MH. Establishment in culture of pluripotential cells from mouse embryos. Nature. 1981;292:154-156.
2. Martin GR. Isolation of a pluripotent cell line from early mouse embryos cultured in medium conditioned by teratocarcinoma stem cells. Proc Natl Acad Sci U S A. 1981;78:7634-7638.
3. Thomson JA, Itskovitz-Eldor J, Shapiro SS, et al. Embryonic stem cell lines derived from human blastocysts. Science. 1998;282:1145-1147.
4. Kilpatrick TJ, Bartlett PF. Cloning and growth of multipotential neural precursors: requirements for proliferation and differentiation. Neuron. 1993;10:255-265.
5. Temple S. Division and differentiation of isolated CNS blast cells in microculture. Nature. 1989;340:471-473.
6. Bain G, Kitchens D, Yao M, et al. Embryonic stem cells express neuronal properties in vitro. Dev Biol. 1995;168:342-357.
7. Ying QL, Stavridis M, Griffiths D, et al. Conversion of embryonic stem cells into neuroectodermal precursors in adherent monoculture. Nat Biotechnol. 2003;21:183-186.
8. Kawasaki H, Mizuseki K, Nishikawa S, et al. Induction of midbrain dopaminergic neurons from ES cells by stromal cell-derived inducing activity. Neuron. 2000;28:31-40.
9. Elkabetz Y, Panagiotakos G, Al Shamy G, et al. Human ES cell-derived neural rosettes reveal a functionally distinct early neural stem cell stage. Genes Dev. 2008;22:152-165.
10. Hong S, Kang UJ, Isacson O, et al. Neural precursors derived from human embryonic stem cells maintain long-term proliferation without losing the potential to differentiate into all three neural lineages, including dopaminergic neurons. J Neurochem. 2008;104:316-324.
11. Okabe S, Forsberg-Nilsson K, Spiro AC, et al. Development of neuronal precursor cells and functional postmitotic neurons from embryonic stem cells in vitro. Mech Dev. 1996;59:89-102.
12. Reubinoff BE, Itsykson P, Turetsky T, et al. Neural progenitors from human embryonic stem cells. Nat Biotechnol. 2001;19:1134-1140.
13. Nat R, Nilbratt M, Narkilahti S, et al. Neurogenic neuroepithelial and radial glial cells generated from six human embryonic stem cell lines in serum-free suspension and adherent cultures. Glia. 2007;55:385-399.
14. Liour SS, Yu RK. Differentiation of radial glia-like cells from embryonic stem cells. Glia. 2003;42:109-117.
15. Bibel M, Richter J, Schrenk K, et al. Differentiation of mouse embryonic stem cells into a defined neuronal lineage. Nat Neurosci. 2004;7:1003-1009.
16. Mori T, Buffo A, Gotz M. The novel roles of glial cells revisited: the contribution of radial glia and astrocytes to neurogenesis. Curr Top Dev Biol. 2005;69:67-99.
17. Blomberg le A, Schreier LL, Talbot NC. Expression analysis of pluripotency factors in the undifferentiated porcine inner cell mass and epiblast during in vitro culture. Mol Reprod Dev. 2008;75:450-463.
18. Talbot NC, Powell AM, Garrett WM. Spontaneous differentiation of porcine and bovine embryonic stem cells (epiblast) into astrocytes or neurons. In Vitro Cell Dev Biol Anim. 2002;38:191-197.

19. Dyce PW, Zhu H, Craig J, et al. Stem cells with multilineage potential derived from porcine skin. Biochem Biophys Res Commun. 2004;316:651-658.
20. Kuijk EW, du Puy L, van Tol HT, et al. Validation of reference genes for quantitative RT-PCR studies in porcine oocytes and preimplantation embryos. BMC Dev Biol. 2007;7:58.
21. Kuijk EW, Du Puy L, Van Tol HT, et al. Differences in early lineage segregation between mammals. Dev Dyn. 2008;237:918-927.
22. Zeng L, Rahrmann E, Hu Q, et al. Multipotent adult progenitor cells from swine bone marrow. Stem Cells. 2006;24:2355-2366.
23. Magnani L, Cabot RA. In vitro and in vivo derived porcine embryos possess similar, but not identical, patterns of Oct4, Nanog, and Sox2 mRNA expression during cleavage development. Mol Reprod Dev. 2008;75:1726-1735.
24. Oishi K, Kamakura S, Isazawa Y, et al. Notch promotes survival of neural precursor cells via mechanisms distinct from those regulating neurogenesis. Dev Biol. 2004;276:172-184.
25. Graham V, Khudyakov J, Ellis P, et al. SOX2 functions to maintain neural progenitor identity. Neuron. 2003;39:749-765.
26. Collignon J, Sockanathan S, Hacker A, et al. A comparison of the properties of Sox-3 with Sry and two related genes, Sox-1 and Sox-2. Development. 1996;122:509-520.
27. Mignone JL, Kukekov V, Chiang AS, et al. Neural stem and progenitor cells in nestin-GFP transgenic mice. J Comp Neurol. 2004;469:311-324.
28. Kaneko Y, Sakakibara S, Imai T, et al. Musashi1: an evolutionally conserved marker for CNS progenitor cells including neural stem cells. Dev Neurosci. 2000;22:139-153.
29. Schnitzer J, Franke WW, Schachner M. Immunocytochemical demonstration of vimentin in astrocytes and ependymal cells of developing and adult mouse nervous system. J Cell Biol. 1981;90:435-447.
30. Gotz M, Barde YA. Radial glial cells defined and major intermediates between embryonic stem cells and CNS neurons. Neuron. 2005;46:369-372.
31. Osumi N, Shinohara H, Numayama-Tsuruta K, et al. Concise review: Pax6 transcription factor contributes to both embryonic and adult neurogenesis as a multifunctional regulator. Stem Cells. 2008;26:1663-1672.
32. Di-Gregorio A, Sancho M, Stuckey DW, et al. BMP signalling inhibits premature neural differentiation in the mouse embryo. Development. 2007;134:3359-3369.
33. Strubing C, Ahnert-Hilger G, Shan J, et al. Differentiation of pluripotent embryonic stem cells into the neuronal lineage in vitro gives rise to mature inhibitory and excitatory neurons. Mech Dev. 1995;53:275-287.
34. Tropepe V, Hitoshi S, Sirard C, et al. Direct neural fate specification from embryonic stem cells: a primitive mammalian neural stem cell stage acquired through a default mechanism. Neuron. 2001;30:65-78.
35. Okuda T, Tagawa K, Qi ML, et al. Oct-3/4 repression accelerates differentiation of neural progenitor cells in vitro and in vivo. Brain Res Mol Brain Res. 2004;132:18-30.
36. Okita K, Ichisaka T, Yamanaka S. Generation of germline-competent induced pluripotent stem cells. Nature. 2007;448:313-317.
37. Takahashi K, Tanabe K, Ohnuki M, et al. Induction of pluripotent stem cells from adult human fibroblasts by defined factors. Cell. 2007;131:861-872.
38. Kim JB, Zaehres H, Wu G, et al. Pluripotent stem cells induced from adult neural stem cells by reprogramming with two factors. Nature. 2008;454:646-650.
39. Eminli S, Utikal JS, Arnold K, et al. Reprogramming of Neural Progenitor Cells into iPS Cells in the Absence of Exogenous Sox2 Expression. Stem Cells. 2008.
40. Di Stefano B, Prigione A, Broccoli V. Efficient genetic reprogramming of unmodified somatic neural progenitors uncovers the essential requirement of Oct4 and Klf4. Stem Cells Dev. 2008.

41. Schwartz PH, Nethercott H, Kirov, II, et al. Expression of neurodevelopmental markers by cultured porcine neural precursor cells. Stem Cells. 2005;23:1286-1294.
42. Smith PM, Blakemore WF. Porcine neural progenitors require commitment to the oligodendrocyte lineage prior to transplantation in order to achieve significant remyelination of demyelinated lesions in the adult CNS. Eur J Neurosci. 2000;12:2414-2424.
43. Talbot NC, Rexroad CE, Jr., Pursel VG, et al. Culturing the epiblast cells of the pig blastocyst. In Vitro Cell Dev Biol Anim. 1993;29A:543-554.
44. Lazzari G, Colleoni S, Giannelli SG, et al. Direct derivation of neural rosettes from cloned bovine blastocysts: a model of early neurulation events and neural crest specification in vitro. Stem Cells. 2006;24:2514-2521.
45. Kandel ER, Schwartz JH, Jessell TM. Principles of neural science. 2000.
46. Bani-Yaghoub M, Tremblay RG, Lei JX, et al. Role of Sox2 in the development of the mouse neocortex. Dev Biol. 2006;295:52-66.
47. Lee SH, Lumelsky N, Studer L, et al. Efficient generation of midbrain and hindbrain neurons from mouse embryonic stem cells. Nat Biotechnol. 2000;18:675-679.
48. Yan Y, Yang D, Zarnowska ED, et al. Directed differentiation of dopaminergic neuronal subtypes from human embryonic stem cells. Stem Cells. 2005;23:781-790.
49. Hu JG, Fu SL, Wang YX, et al. Platelet-derived growth factor-AA mediates oligodendrocyte lineage differentiation through activation of extracellular signal-regulated kinase signaling pathway. Neuroscience. 2008;151:138-147.
50. Brustle O, Jones KN, Learish RD, et al. Embryonic stem cell-derived glial precursors: a source of myelinating transplants. Science. 1999;285:754-756.
51. Temple S. The development of neural stem cells. Nature. 2001;414:112-117.
52. Amariglio N, Hirshberg A, Scheithauer BW, et al. Donor-Derived Brain Tumor Following Neural Stem Cell Transplantation in an Ataxia Telangiectasia Patient. PLoS Med. 2009;6:e29.

Chapter 4

Cazip, a novel protein expressed in the developing heart and nervous system

Leonie du Puy [(1)], Abdelazziz Beqalli [(2)], Jantine Monshouwer-Kloots[(2)], Henk P. Haagsman [(3)], Bernard A.J. Roelen[(1)], Robert Passier [(2)]

[1] Department of Farm Animal Health, Faculty of Veterinary Medicine, Utrecht University, Utrecht, The Netherlands ; [2] Department of Anatomy & Embryology, Leiden University Medical Center, Leiden, The Netherlands; [3] Department of Infectious Diseases and Immunology, Faculty of Veterinary Medicine, Utrecht University, Utrecht, The Netherlands.

Adapted from Developmental Dynamics 2009

Abstract

Recently we have performed a whole genome micro-array analysis on human embryonic stem cells (hESC) differentiating towards cardiomyocytes, which resulted in the identification of novel genes that were highly upregulated during differentiation. Here, we describe one of these novel candidate genes annotated as KIAA0774. The predicted protein contains a leucine-zipper domain at the C-terminus and has at least two isoforms (358 and 1354 amino acids) which are regulated in a temporal-spatial manner. Whole mount *in situ* hybridization confirmed that the mRNA of both the mouse and chicken orthologs of KIAA0774 is expressed during early cardiac development. Hence, we named this protein CAZIP (cardiac zipper protein). Later during embryonic development *Cazip* was also expressed in parts of the nervous system. Northern blot and real-time PCR analysis showed that *Cazip* is expressed in heart and brain in adult mice, but not in any other adult tissue examined. These results suggest a role for CAZIP in development and function of the heart and nervous system in vertebrates.

Introduction

The heart is the first organ to form and function during embryogenesis. Proper development from early cardiac progenitors, present at the "cardiac crescent" stage, to a fully functional four-chambered heart are under tight spatial and temporal control of gene activity. The identification and characterization of genes expressed in the embryonic heart are essential for a better understanding of the molecular program underlying cardiac development and function. Many genes involved in cardiovascular development have been identified through methods as (virtual) subtractive screening [1, 2], genetic screening [3], identification of orthologs of invertebrate genes [4] and in recent years by whole genome microarray analysis. Besides microarray analysis on different stages and regions of the heart, pluripotent stem cells, which were differentiated towards the cardiac lineage have also been used for the identification of genes that may be associated with cardiac differentiation. Recently, we have performed a whole genome micro-array analysis on human embryonic stem cells (hESC) differentiating towards cardiomyocytes [5]. This study has revealed several new genes, that are potentially involved in vertebrate cardiac development. Here, we describe one of these genes, annotated as KIAA0774, encoding a previously unidentified protein with a C-terminal leucine zipper domain. Whole mount *in situ* hybridization (ISH) and quantitative real-time PCR studies showed that the mouse and chicken orthologs of KIAA0774 were expressed during early cardiac development. We therefore named this protein: Cardiac zipper protein (CAZIP). At later stages and even in adult mice *Cazip,*

expression was maintained in the heart, but expression could now also be detected in regions of the brain and nervous system and in limb and wing buds, suggesting a role in heart and brain development and/or function.

Results and discussion

Identification of Cazip

Previously, we have differentiated pluripotent hESC to cardiomyocytes by co-culture with a mouse endodermal cell-line, END-2. Beating hESC-derived cardiomyocytes can be observed from 6 days onwards with an optimal cardiac differentiation at 12 days after the start of these hESC-END-2 co-cultures [6, 7]. Whole genome microarray analysis was recently performed on different times (0, 1, 3, 6, 9 and 12 days) during differentiation and compared to expression in human fetal heart [5]. An unknown gene, annotated as KIAA0774 (from now onwards referred to as CAZIP), was identified in a cluster of genes which were upregulated during differentiation (Fig 1A). Quantitative real-time PCR for *CAZIP* was performed on hESC differentiating towards cardiomyocytes (Fig 1B). Confirming microarray data, *CAZIP* mRNA levels increased between day 8 and 12 of differentiation. In this time period, genes responsible for cardiomyocyte differentiation and function are expected to be upregulated [5].

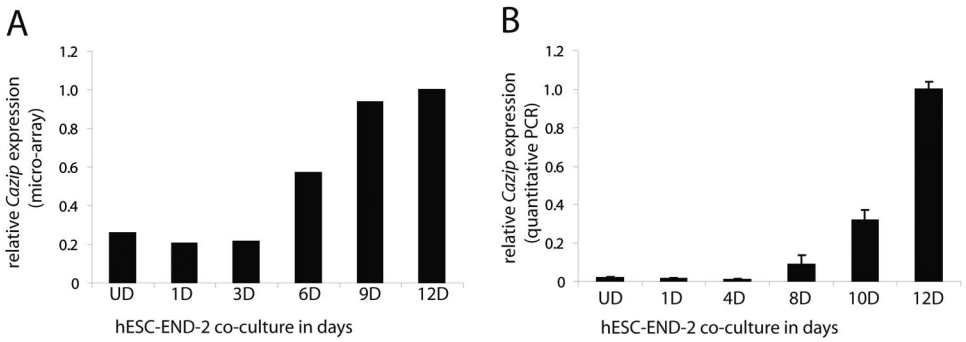

Fig 1. *CAZIP* mRNA expression levels in hESC differentiating towards cardiomyocytes. Expression levels of CAZIP mRNA in hESCs differentiating to cardiomyocytes as detected by microarray-analysis (A) and quantitative real time PCR (B). Microarray data can be obtained from online supplemental Figures 1a-j (http://stemcells.alphamedpress.org /cgi/content/full/24/1956/DC1) in our previous publication [5]. Expression levels were normalized to *ARP*; *CAZIP* mRNA expression levels in hESC differentiated to cardiomyocytes for 12 days (12D) is set to 1. UD: undifferentiated hESCs; 1D, 4D, 8D etc.: differentiation day 1, 4, 8 respectively.

After BLAST search with human CAZIP (Genbank accession number: KIAA0774) as entry, we identified orthologs in different species (Table 1), which revealed that CAZIP protein is conserved among vertebrates. Alignment of human and mouse CAZIP amino acid sequences revealed a 69% identity, whereas comparison of human and chicken sequences revealed a 48% identity (Fig 2A). By further database analysis we identified two transcript isoforms of mouse *Cazip* transcripts. The longest isoform *CazipA* is composed of 15 exons, and encodes a 1354 amino acid protein. In isoform *CazipB,* exons 1 to 6 are lacking, producing a unique 5'-untranslated region and causing a translation initiation at a different start codon. The encoded protein of CAZIPb is 358 amino acids in length (Fig 2B, C). The presence of both isoforms was confirmed by RT-PCR (result not shown), followed by sequencing. Proteins of both isoforms contain a predicted C-terminal leucine-zipper domain, a common protein dimerization domain found in a specific group of transcription factors. However, the basic region that is essential for DNA binding in transcription factors containing a leucine-zipper motif is absent in CAZIP.

Table 1. CAZIP orthologues identified from the NCBI database

Protein accesion nr	Gene	Organism
NP_001028774.2	KIAA0774	*Homo sapiens*
NP_084196.4	C130038G02Rik	*Mus musculus*
XP_509608.2	LOC452515	*Pan troglodytes*
XP_543149.2	LOC486024	*Canis lupus familiaris*
XP_615675.3	LOC535569	*Bos taurus*
XP_417117.2	LOC418923	*Gallus gallus*
XP_684038.3	LOC556195	*Danio rerio*

Based on CAZIPa sequence comparisons using BLASTp, significant homology to coiled-coil domain-containing protein 69 (UNC-69) (39%) and to Angiotensin II receptor type 2 interacting protein 1 (ATIP1) (36%) was shown. UNC-69 is a protein involved in axonal outgrowth and presynaptic organization in C. elegans [8]. ATIP defines a family of four members of which ATIP1 has been most extensively studied. ATIP1 interacts with the C-terminal tail of the AT2 receptor and cooperates with the receptor to mediate growth-inhibitory signaling cascades [9]. The angiotensin II receptor type 2 (AT2-receptor) has been shown to be involved in different biological processes, including cardiac hypertrophy and brain development [10, 11]. ATIP1 (also known as ATBP, AT2 receptor binding protein) is also reported to be a Golgi

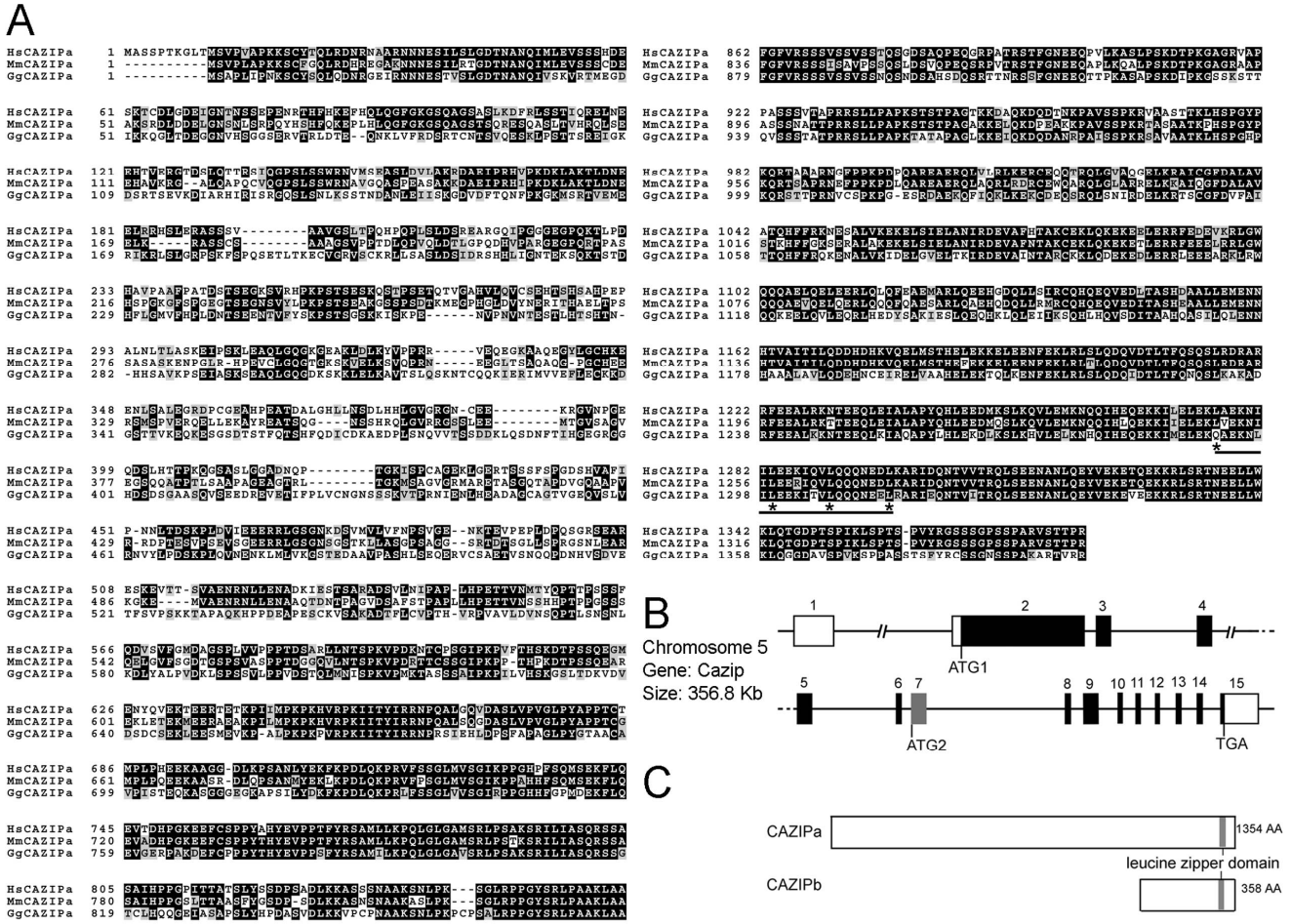
A
HsCAZIPa
MmCAZIPa
GgCAZIPa
B
Chromosome 5
Gene: Cazip
Size: 356.8 Kb
1
2
3
4
ATG1
5
6
7
8
9
10
11
12
13
14
15
ATG2
TGA
C
CAZIPa
1354 AA
leucine zipper domain
CAZIPb
358 AA

Fig 2. Sequence and genomic organization of CAZIP.
(A) Alignment and amino acid sequence comparison of different vertebrates. Identical amino acids are shaded in black and similar residues are shaded in gray. Gaps are represented by a dash and positions in the amino acid sequence are given by the numbers. Leucine zipper domain is underlined and Leucine residues are marked with an asterisk. Mm: *Mus musculus*, Hs: *Homo sapiens*, Gg: *Gallus gallus*. (B) Genomic organization of the mouse *Cazip* gene. ATG1: represents the startcodon of *CazipA*, ATG2: represents the startcodon of *CazipB*. Numbers represent the different exons. Non coding sequences are represented by the white boxes, coding sequences by the black boxes. (C) Schematic representation of the CAZIPa and CAZIPb proteins showing the C-terminal Leucine zipper domain

apparatus-associated protein that manages AT2-receptor trafficking to the cell surface [12]. ATIP1 has also been annotated as MTUS1 (mitochondrial tumor suppressor 1), which has been described as a tumor suppressor gene [13, 14].

Expression pattern during mouse and chick embryonic development
Whole mount ISH on staged mouse embryos showed *Cazip* expression in the heart during early development. The probe used for hybridization recognized both isoforms of *Cazip*. No expression was detected at embryonic day (E) 7.5 and E8.5 (data not shown). Expression was first detected from E9.5 onwards. At E9.5 and E10.5 *Cazip* expression was observed throughout the heart in both atria and ventricles and in the limb bud region (Fig 3A-F). Sectioning of the otic vesicles demonstrated that probe was trapped in this cavity during the experiment causing nonspecific staining. Whole mount ISH on isolated E14.5 heart-fragments showed clear expression in both atria and ventricles (Fig 3G-H). Hybridization with a sense probe did not reveal any expression (Fig 3 I). In sections of E9.5 and E10.5 embryos highest expression levels were observed at the outer curvatures of both the ventricles and the atria of the embryonic heart (Fig 3J, K). However, this expression pattern was not observed by section ISH (see results below) and therefore probably resulted from insufficient penetration of the probe into the heart during hybridization. Furthermore, *Cazip* expression was visible in the brain in the neuroepithelium lining the telencephalic vesicles (Fig 3L), in the second branchial arch (Fig 3M), the limb bud region (Fig 3N) and the dorsal root ganglia (Fig 3O). Expression in the heart and nervous system was confirmed by ISH on sections from E11.5 and E12.5 mouse embryos (Fig 4). Highest expression levels were observed in the ventricles of the heart, but *Cazip* was also expressed in the atria. *Cazip* expression was not observed in endocardial cushions, the atrial valves (Fig 4 A-C, G-I) or epicard (data not shown). In the nervous system, strong *Cazip* expression was observed in the mantle layer of the epithelium lining the fourth ventricle and in the epithelium lining the neural tube (Fig 4D, E, J, K). *Cazip* expression was also observed in the trigeminal ganglion (Fig 4F) and in the dorsal root ganglia (Fig 4K). Finally, *Cazip* mRNA was visible in the epithelium lining the bronchia of the lung (Fig 4L).

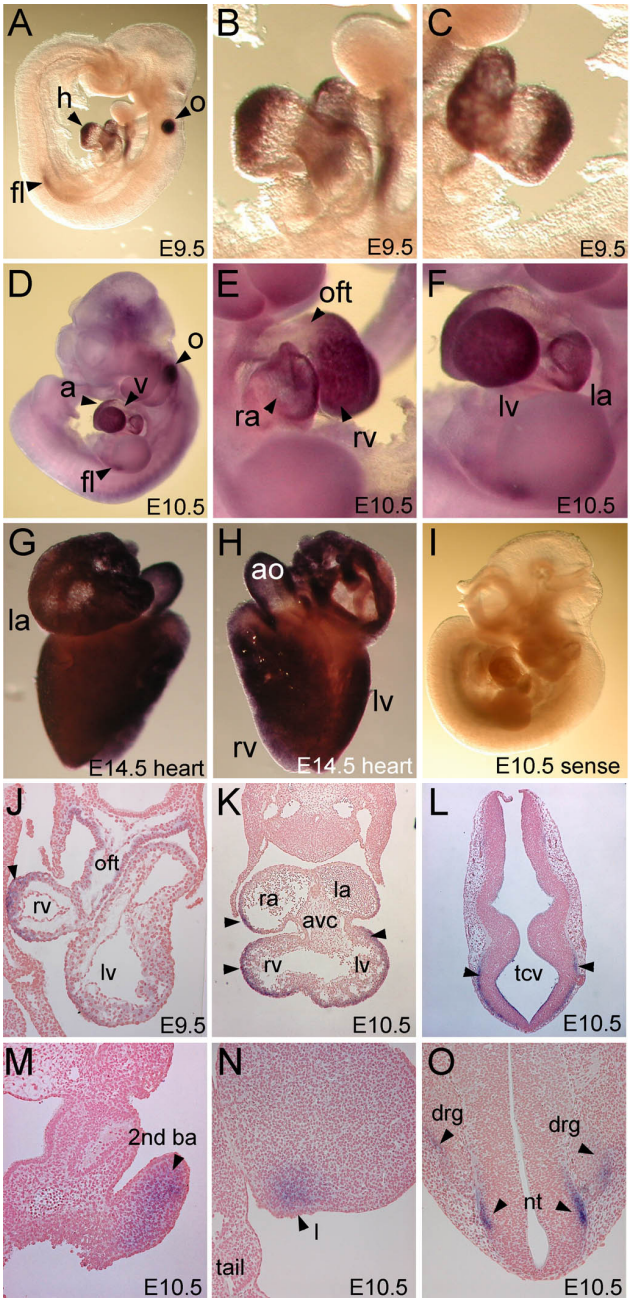

Fig 3: *In situ* hybridization of *Cazip* during early mouse development.
Whole mount *in situ* hybridization with digoxigenin-UTP labelled *Cazip* riboprobe was performed on mouse embryos at embryonic day 9.5 (E9.5) (A-C), E10.5 (D-F), and on dissected and fragmented E14.5 hearts (G-H). Hybridization with the sense probe revealed no signal (I). Expression is detected in the forelimb region (fl); in the atria (a) and ventricles (v) of the heart (h). Probe trapping caused nonspecific staining in the otic vesicle (o). (A, D) Higher magnification pictures of the heart are shown in B-C (E9.5) and E-F (E10.5). *Cazip* mRNA is expressed in the left atrium (la) and ventricle (lv) and the right atrium (ra) and ventricle (rv), *Cazip* is also expressed in the aorta (ao) (G-H, E14.5 heart). E9.5 and E10.5 embryos were subjected to whole mount *in situ* hybridization using *Cazip* labeled riboprobe and subsequently sectioned in the transverse plane (10 µm thick). High *Cazip* expression levels are visible in the atria and ventricles of the embryonic heart (arrow heads) (E9.5 heart: J oft: outflow tract, E10.5 heart: K: avc: atrioventrical canal). Higher expression levels in the outer-curvatures of the heart were the result of insufficient probe penetration. *Cazip* mRNA expression is seen in the neuroepithelium lining the telencephalic vesicles (tcv) (L), in the second branchial arch (ba) (M), the limb (l) region (N) and the dorsal root ganglia (drg: dorsal root ganglia), and lining the neural tube (nt) (O). Nuclear staining in red, hybridized *Cazip* antisense probe seen in blue. Arrow heads point to *Cazip* expression.

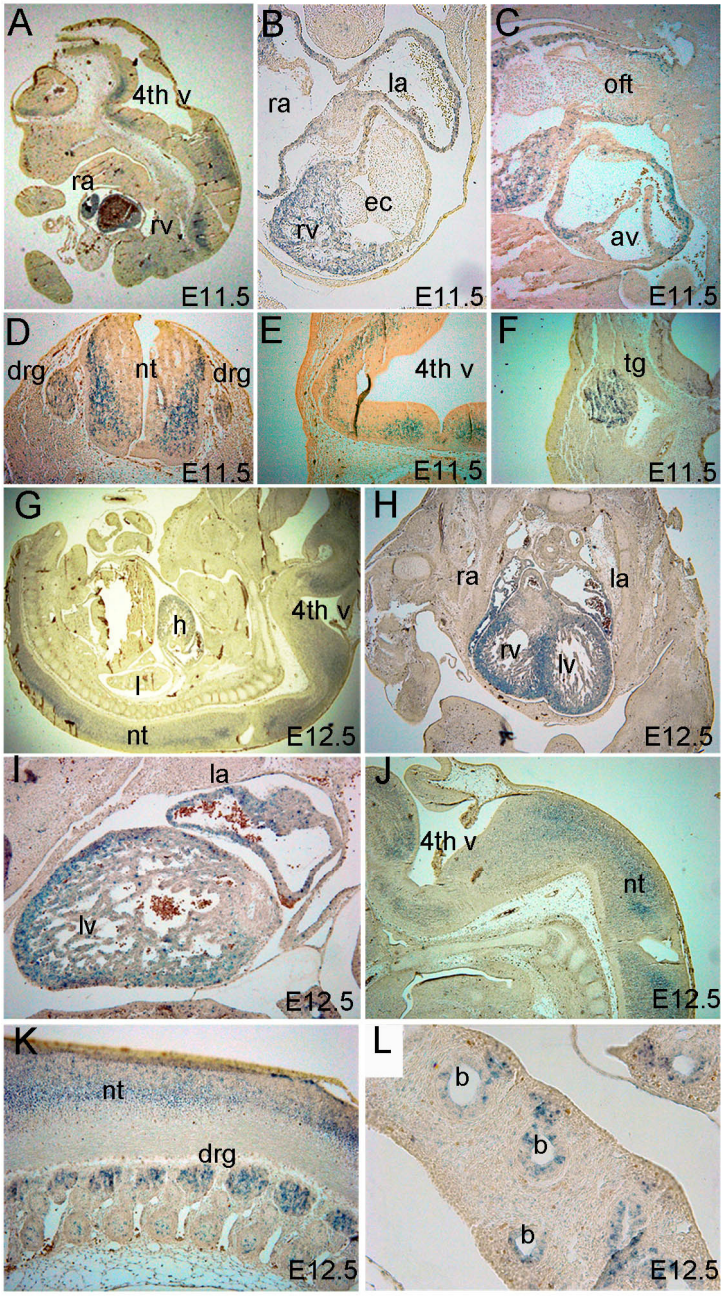

Figure 4: Section *in situ* hybridization of *Cazip* during early mouse development. *In situ* hybridization was performed on tissue sections of E11.5 (A-F) and E12.5 (G-L) mouse embryos. In transverse sections of a E11.5 hearts (B) *Cazip* mRNA expression is detected in the right and left atrium (ra, la) and in the right ventricle (rv). *Cazip* is not expressed in the endocardial cushions (ec). Sagittal sectioning of the E11.5 heart (C) show that *Cazip* mRNA is not expressed in the atrial valves (av) nor in the outflow tract (oft). In the nervous system, expression is visible in dorsal root ganglia (drg), and lining the neural tube (nt) (D, transverse section), in the mantle layer of the fourth ventricle (4th v) (E, transverse section) and in the trigeminal ganglion (tg) (F, transverse section). Section in situ hybridization on E12.5 embryos again confirmed *Cazip* expression in the heart (H, transverse section; I, sagittal section) in the mantle layer of the fourth ventricle (J, sagittal section), and in the neural tube and dorsal root ganglia (K, sagittal section). Cazip is also expressed in the epithelium lining the bronchia (b) of the lung (L, sagittal section). Nuclear staining is visualized in red, hybridized Cazip antisense probe is seen in blue.

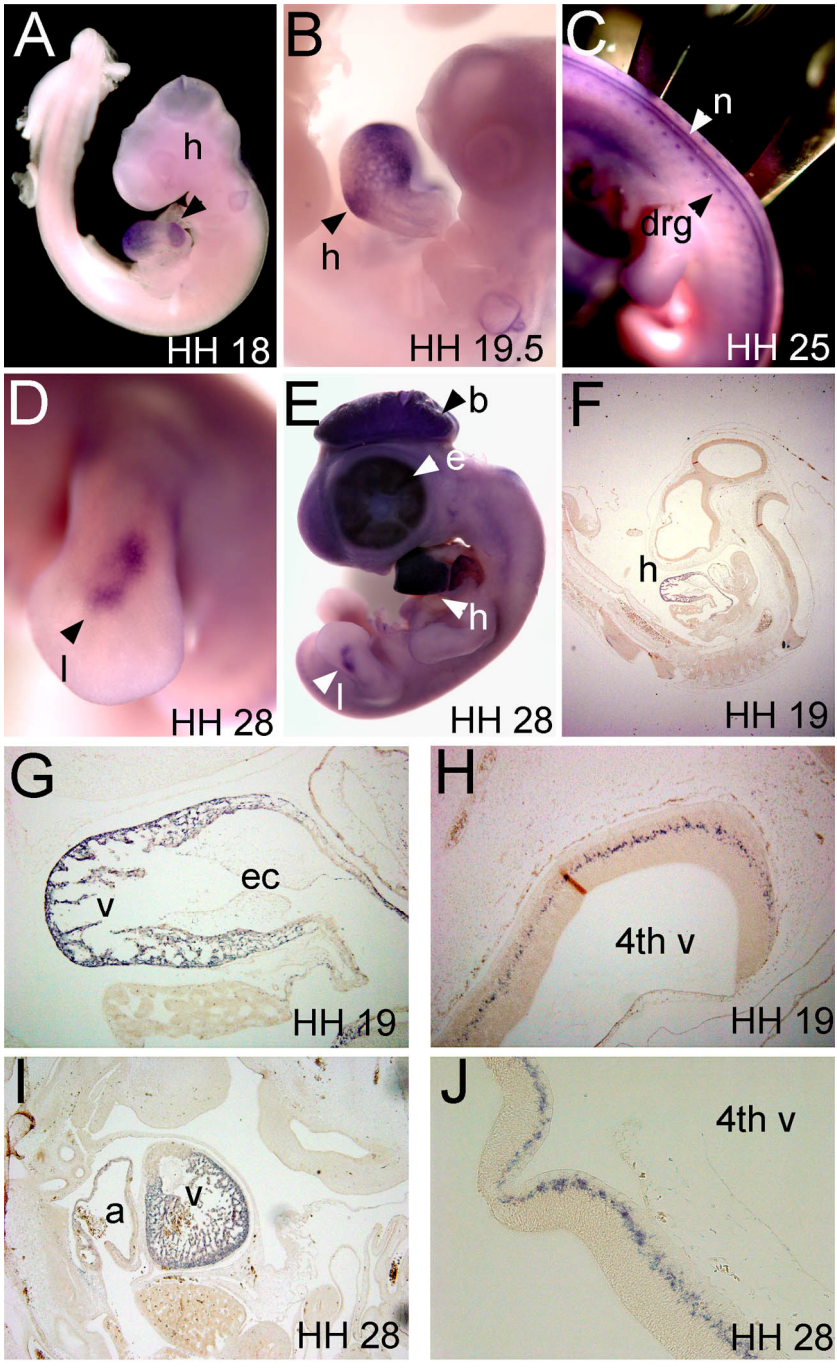
A
h
HH 18
B
h
HH 19.5
C
n
drg
HH 25
D
l
HH 28
E
b
e
h
l
HH 28
F
h
HH 19
G
ec
v
HH 19
H
4th v
HH 19
I
a
v
HH 28
J
4th v
HH 28

Fig 5: Whole mount *in situ* hybridization of *Cazip* during chick development.
In situ hybridization with digoxigenin-UTP labeled *Cazip* riboprobe was performed on whole mount chick embryos at Hamilton Hamburger stage (HH) 18 (A), HH 19.5 (B), HH 25 (C), and HH 28 (D, E). Expression is detected in the heart (h); lining the neural tube (n), in the ganglia (g), limb bud (l) Sectioning revealed that staining in the eye was caused by pigmented epithelium and not by *Cazip* expression (data not shown). In addition, staining on the outer surface of the brain (b) also did not appear to be specific (E). ISH on tissue sections of chick embryos confirmed *Cazip* expression in the heart and in the nervous system (F, sagittal section overview). Higher magnification of F shows *Cazip* expression is clearly visible in the trabeculated wall of the ventricle, but not in the endocardial cushions (ec) (G). In the nervous system, *Cazip* mRNA is observed in the mantle layer of the future fourth ventricle (H, sagittal section). At HH28, *Cazip* mRNA is expressed in the atria (a) and ventricle (v) of the heart (I, transverse section), and in the mantle layer of the future fourth ventricle (J, sagittal section).

In the chick, whole mount ISH studies revealed a similar pattern of *Cazip* expression. *Cazip* mRNA was visible in the heart from Hamburger-Hamilton stage (HH) 18 onwards (Fig 5A, B). At HH 25 *Cazip* expression lines the neural tube and was expressed in the dorsal root ganglia (Fig 5C). Expression in the limb bud was clearly visible at HH 28 (Fig 5D, E). Sectioning revealed that staining in the eye was caused by pigmented epithelium and not by *Cazip* expression (data not shown). In addition, staining in the outer parts of the brain ((b), Fig 5E) was probably as a result of probe trapping. No *Cazip* expression was observed in somites during both chick and mouse embryonic development, suggesting a specific role for CAZIP in cardiac muscle but not in skeletal muscle. By ISH on tissue sections from chick embryos we confirmed expression in the developing heart and neural system. At stage HH19 *Cazip* expression could be detected in the heart (Fig 5F), with highest levels in the ventricle (Fig 5G). Cazip expression was not observed in the endocardial cushions. In the nervous system, strong expression was oberved in the mantle layer of the myelocele (future fourth ventricle) (Fig 5H), but also in ependymal cells throughout the brain. High expression in heart and myeolocele can also be observed in sections of HH28 (Fig 5I and J).

An expression pattern as observed for *Cazip* in both the heart and limb region during embryonic development is not uncommon. Gene products that are involved in both cardiac and limb formation are for example the Limb-bud and heart gene (LBH) [15, 16], the basic helix loop helix transcription factors dHAND and eHAND ([17] for review and references therein), and the T-box transcription factors [18] TBX3 [19], TBX4 [20] and TBX5 [21]. Signals involved in controlling both heart and limb development are sonic hedgehog (SHH) [22, 23], fibroblast growth factor 8 (FGF8)[24, 25] and bone morphogenic proteins (BMPs) [26]. Cardiac abnormalities are frequently accompanied by limb defects [27], suggesting that the developmental signalling pathways of these different tissues share similar downstream elements, including CAZIP.

Expression in adult mouse tissues

Northern hybridization analysis confirmed the existence of two different *Cazip* mRNA products in adult mouse brain tissue at approximately 7 kb (*CazipA*) and 4.5 kb (*CazipB*). In the adult heart only the smaller isoform was detected. This shorter *Cazip* isoform was expressed at a far higher level in the heart compared to the brain. *Cazip* mRNA expression was not observed in any other adult tissue examined (Fig 6A).

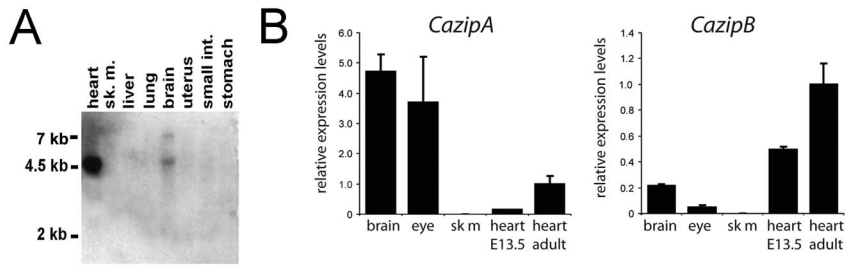

Figure 6: *Cazip* mRNA expression in adult mouse tissues.
Northern blot analysis of *Cazip* mRNA expression in mouse adult tissues (A). Quantitative real-time RT-PCR of *CazipA* mRNA and *CazipB* mRNA (B). QPCR data was normalized to *Gapdh, Pgk11, ß-Actin.* Gene expression levels are reported relative to expression levels in heart tissue. Error bars represent standard error of the mean. Skm: skeletal muscle, small int: small intestine.

Expression of *Cazip* mRNA in mouse tissues was also analyzed by qualitative reverse transcriptase and quantitative real-time PCR. Expression was undetectable by reverse transcriptase PCR in skeletal muscle, stomach, liver, kidney, spleen, uterus, intestines and lung (result not shown). As expected, expression was detected in heart, brain and eye tissue and further examined by quantitative real-time PCR (Fig 6B). *Cazip* expression levels differed between the tissues examined for the two transcript variants and expression levels were higher in adult heart tissue compared to the embryonic heart. The longer isoform *CazipA* was highly expressed in brain and eye tissue and at lower levels in the adult and embryonic heart, while mRNA levels of *CazipB* were much higher in the heart when compared to brain and eye tissue, confirming the results obtained by Northern hybridization analysis.

Overexpression of CAZIP in COS cells.

To study the intracellular localization of CAZIP protein, CAZIPb was ectopically expressed in COS-1 cells (Fig 7). CAZIPb protein was expressed in the cytoplasm,

peri-nuclear and in unidentified cytosolic structures. Although it is clear that CAZIPb is localized in the cytoplasm, sub-cellular localization in the cytosolic "vesicle-like" structure may represent an artifact of overexpression in these cells. Besides cytoplasmic localization, CAZIPb was found in the nucleus in sub-nuclear bodies, which may be associated with RNA processing and regulating transcription [28, 29], the peri-nuclear localization is indicative of ER expression. The sub-cellular localization of CAZIPa was not examined, and we can therefore not exclude that the localization of CAZIPa differs from that of CAZIPb.

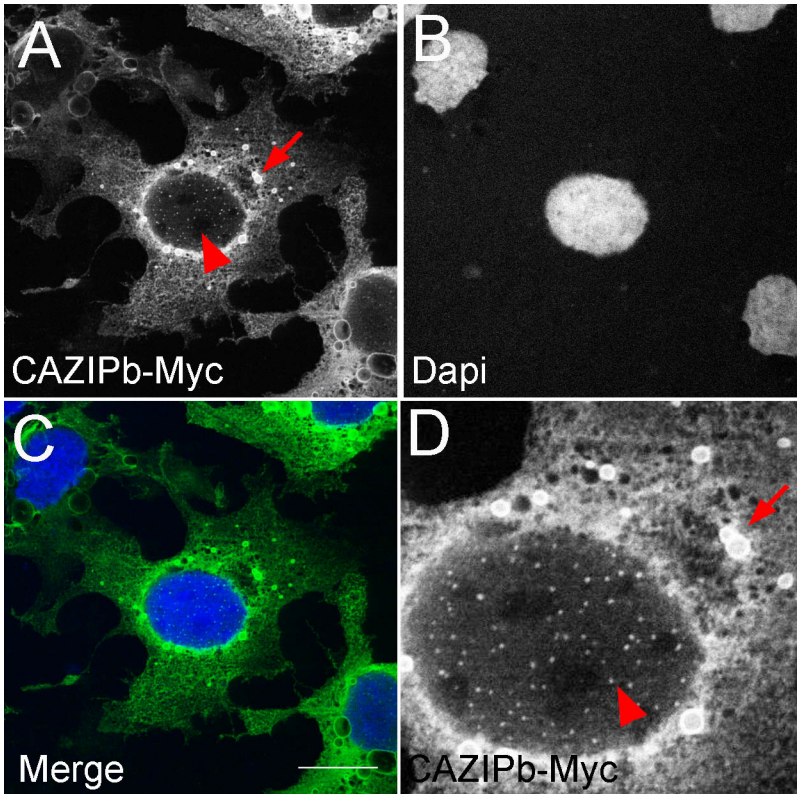

Figure 7: CAZIPb overexpression in COS-1 cells
Multifoton images of exogenous CAZPb-Myc expression (A), nuclear stain (B) and the merge (C; CAZIP-Myc in green, nuclear stain in blue) in COS-1 cells. A larger magnification of A is presented in D. Red arrow head points to nucleus with CAZIPb expression in sub-nuclear structures. Red arrow points to exogenous CAZIPb expression in 'vesicle-like' structures in the cytosol. Scale bar: 20 μm

Conclusion

The present study reports the identification, genomic structural organization, evolutionary conservation and tissue and sub-cellular expression patterns of a novel gene, which we name *CAZIP*. *CAZIP* expression was found to be upregulated in a whole genome microarray study during the differentiation of hESC to cardiomyocytes. CAZIP protein has highest identity to UCN-69 (39%), a protein involved in axon guidance and ATIP1 (36%), a protein involved in cardiac hypertrophy and neural differentiation. *Cazip* expression was detected in the limb and in the heart and nervous system tissues of both mouse and chicken during embryonic development. Exogenous CAZIP overexpressed in COS-1 cells localized in the cytoplasm and in sub-nuclear structures. Further research into the intracellular location of endogenous CAZIP protein, gain-and loss-of-function studies and identification of possible interaction partners of CAZIP will help to elucidate its function and role in heart and brain development.

Experimental procedures

Animals

C57Bl/6 mice were intercrossed, and females sacrificed for collection of embryos at various time points (E7.5, E8.5, E9.5, E10.5 and E14.5). Detection of vaginal plugs in the morning were considered to be day E0.5. Fertilized eggs of White Leghorn chicken (*Gallus domesticus*) were incubated at 37^{o}C and 80% humidity. Embryos were staged according to the criteria of Hamburger and Hamilton [30]. Mouse and chick embryos were fixed in 4% (w/v) paraformaldehyde in PBS at 4 °C overnight and stored in 100% methanol at -20 ºC.

Whole mount and tissue sections in situ hybridization

Whole mount *in situ* hybridization was performed as described previously [31] For *Cazip* probe preparation, purified PCR product was generated to use as a template, with mouse *Cazip* specific primers (forward: CCAGGTGGACACGCTAACTT, reverse: GGCTCTGCATGTCTTCTTCC) or chicken *Cazip* specific primers (forward: CGCTCCAGGACCAGATAGAC, reverse AGATTGGCGTTCTCCTCTGA) with the T3 promoter sequence (ATACAATTAACCCTCACTAAAGGG) at the 5'end of the forward primer and the T7 promoter sequence (ATAGGTAATACGACTCACTATAGGGC) at the 3'end of the reverse primer. RNA probes were synthesized using either T3 (sense) or T7 (antisense) polymerase, or after subcloning in the pCRII-TOPO (Invitrogen), containing a Sp6 and a T7 promoter. Probes were DIG labeled according to the manufacturer's protocol (Roche Applied Sciences, Almere, The Netherlands). Embryos were imaged using a Zeiss Axioplan

SZX9 coupled to a Leica DFC480 digital camera. ISH on 10 µm sagittal sections from HH19 and HH28 chick embryo's and from E11.5 and E12.5 mouse embryos was performed as described previously [32].

Northern hybridization analysis

Total RNA was isolated from adult mouse heart, skeletal muscle, brain, liver, lung, uterus, stomach and intestine using Trizol reagent (Gibco). Briefly, tissues were homogenized in Trizol, extracted by chloroform and precipitated by isopropyl alcohol. The RNA concentration was measured by spectrophotometry at 260 nm. RNA integrity was verified by gel electrophoresis. Poly(A)$^+$ mRNA was purified using a mRNA purification kit (Pharmacia). For all tissues, 3 µg of mRNA was separated on a 1.5 % formaldehyde/MOPS-agarose gel. After the RNA was blotted overnight on a nitrocellulose filter and UV cross-linked, hybridization was performed with a ^{32}P-labeled, randomly primed, 400 bp PCR fragment at the C-terminus of *Cazip*, which recognizes both *CazipA* and *–B* isoforms. Hybridization was performed in Rapid-hyb (Pharmacia) at 65°C for 3 h. Following hybridization, the filter was washed in 2× saline sodium citrate buffer (SSC; 0.3 M NaCl, 0.03 M Sodium citrate) at room temperature (2×5 min), 0.2×SSC/0.1% SDS at 65°C (2×30 min) and 2×SSC at room temperature. The filters were exposed to Kodak autoradiography film for 18 h and developed afterwards.

RNA isolation, cDNA synthesis and RT-PCR

Total RNA was isolated from adult mouse heart, brain, eye, skeletal muscle, stomach, liver, kidney, spleen, uterus, intestines, lung and hESCs differentiating towards cardiomyocytes using Trizol reagent (Invitrogen, Carlsbad, CA). Total RNA was reverse transcribed into cDNA using Superscript II reverse transcription-polymerase (Invitrogen) and random primers (Invitrogen) according to the supplier's protocol. For reverse transcriptase-polymerase chain reaction (RT-PCR) primers were designed using Primer 3 software. For quantitative real time RT-PCR, each reaction contained 10 µl SybrGreen Mastermix (Bio-Rad, Hercules, CA), 0.5 mM forward primer, 0.5 mM reverse primer and 1 µl cDNA as a template in a final volume of 20 µl. Mouse specific primers for *CazipA*: forward 5'AAAATGTCAGCCGGTGTAGG3', reverse 5'CTCAAGAGCCCAGAGGTGTC3' and *CazipB*: forward 5'CATCACTGCTGCAAGCCTTA3', reverse 5'AACTCTCTCAGCTCCTCCTC3'. Human specific primers for *CAZIPa+b*: forward 5' ACAGCTGTCGGAGGAAAATG', reverse 5' AGCAGCTCTTCATTGGTTCG'. PCR products were electrophoresed on 1% agarose gels and visualized with ethidium bromide against a 100 basepair ladder. To verify the specificity, the PCR products were sequenced. Biological triplicates were used and reactions were carried out in duplicate for each sample. Negative controls were reactions containing template synthesized

without reverse transcriptase and reactions containing H_2O instead of cDNA. PCR was run on a Bio-Rad ICycler using the following program: initial denaturation at 95ºC for 3 min, followed by 40 cycles of 30 sec at 95ºC, 30 sec at 58 ºC and 30 sec at 72ºC. A melting curve was produced to verify single PCR product amplification. Efficiency of the PCR reaction was tested using a standard curve synthesized from either a dilution series of cDNA or PCR product [33]. Data were analyzed with IQ5 software (Bio-Rad). Starting quantities of all genes were calculated based on their standard curves. Mouse QPCR data was normalized to *Gapdh* (forward: 5'CGTGCCGCCTGGAGAAAC 3', reverse: 5'TGGGAGTTGCTGTTGAAGTCG 3') , *Pgk1* (forward: 5'CTCCGCTTTCATGTAGAGGAAG 3', reverse: 5'GACATCTCCTAGTTTGGACAGTG 3'), *ß-Actin* (forward: 5'GACATCCGTAAAGACCTCTAT, reverse: 5'ACTCCTGCTTGCTGATCC 3'). Gene expression levels are reported relative to expression levels in mouse heart tissue. Human QPCR data was normalized to *ARP* (forward 5' CACCATTGAAATCCTGAGTGATGT' reverse 5' TGACCAGCCCAAAGGAGAAG') and expression levels are reported relative to expression levels in hESCs differentiated for 12 days. Genomic DNA contributions were determined by minus RT levels

Plasmid construct, cell culture and transient transfection

Full-length Mouse CazipB PCR product was amplified from mouse E17.5 heart cDNA and cloned into the pCRII-TOPO or pcDNA6.2/C-EmGFP/TOPO mammalian expression vector (Invitrogen). The cDNA encoding mCAZIPb with a N-terminal Myc epitope were subcloned into the EcoRI site of pcDNA3.1 (Invitrogen).

COS-1 cells were cultured in Dulbecco's modified Eagle's medium (DMEM) (Invitrogen) containing 10% fetal calf serum (FCS) (Gibco-BRL). Cells grown on 0.1% gelatin-coated glass coverslips were transiently transfected using Lipofectamin 2000 (Invitrogen) following the manufacturer's protocol and fixed in 4% paraformaldehyde 48 hours after transfection.

Immunofluorescence

Fixed cells were permeabilized (0.1% Triton-X100 in PBS; 8 min) then non-specific binding sites blocked (4% normal goat serum, 0.1% Tween-20; 1 hr RT). Thereafter, cells were incubated overnight at 4ºC with 1 to 200 dilution of mouse anti-myc antibody (clone 9E10, SantaCruz), then incubated for 1 hr at RT with secondary antibody. Coverslips were mounted in vectashield mounting medium containing DAPI (Vector Laboratories, Burlingame, CA.) and analyzed by multi-photon laser scanning microscopy.

Acknowledgements

We would like to thank Richard Wubbolts (Center for Cell Imaging at the Faculty of Veterinary Medicine in Utrecht) for assistance in multi-photon laser scanning microscopy. This research was partly supported by a grant of the European Community's Sixth Framework Programme contract ("HeartRepair") LSHM-CT-2005-018630 and by SenterNovem grant from the ministry of Economic Affairs.

References

1. Passier R, Richardson JA, Olson EN. Oracle, a novel PDZ-LIM domain protein expressed in heart and skeletal muscle. Mech Dev. 2000;92:277-284.
2. Wang D, Chang PS, Wang Z, et al. Activation of cardiac gene expression by myocardin, a transcriptional cofactor for serum response factor. Cell. 2001;105:851-862.
3. Osio A, Tan L, Chen SN, et al. Myozenin 2 is a novel gene for human hypertrophic cardiomyopathy. Circ Res. 2007;100:766-768.
4. Komuro I, Izumo S. Csx: a murine homeobox-containing gene specifically expressed in the developing heart. Proc Natl Acad Sci U S A. 1993;90:8145-8149.
5. Beqqali A, Kloots J, Ward-van Oostwaard D, et al. Genome-wide transcriptional profiling of human embryonic stem cells differentiating to cardiomyocytes. Stem Cells. 2006;24:1956-1967.
6. Mummery C, Ward-van Oostwaard D, Doevendans P, et al. Differentiation of human embryonic stem cells to cardiomyocytes: role of coculture with visceral endoderm-like cells. Circulation. 2003;107:2733-2740.
7. Passier R, Oostwaard DW, Snapper J, et al. Increased cardiomyocyte differentiation from human embryonic stem cells in serum-free cultures. Stem Cells. 2005;23:772-780.
8. Su CW, Tharin S, Jin Y, et al. The short coiled-coil domain-containing protein UNC-69 cooperates with UNC-76 to regulate axonal outgrowth and normal presynaptic organization in Caenorhabditis elegans. J Biol. 2006;5:9.
9. Nouet S, Amzallag N, Li JM, et al. Trans-inactivation of receptor tyrosine kinases by novel angiotensin II AT2 receptor-interacting protein, ATIP. J Biol Chem. 2004;279:28989-28997.
10. Li JM, Mogi M, Tsukuda K, et al. Angiotensin II-induced neural differentiation via angiotensin II type 2 (AT2) receptor-MMS2 cascade involving interaction between AT2 receptor-interacting protein and Src homology 2 domain-containing protein-tyrosine phosphatase 1. Mol Endocrinol. 2007;21:499-511.
11. D'Amore A, Black MJ, Thomas WG. The angiotensin II type 2 receptor causes constitutive growth of cardiomyocytes and does not antagonize angiotensin II type 1 receptor-mediated hypertrophy. Hypertension. 2005;46:1347-1354.
12. Wruck CJ, Funke-Kaiser H, Pufe T, et al. Regulation of transport of the angiotensin AT2 receptor by a novel membrane-associated Golgi protein. Arterioscler Thromb Vasc Biol. 2005;25:57-64.
13. Di Benedetto M, Bieche I, Deshayes F, et al. Structural organization and expression of human MTUS1, a candidate 8p22 tumor suppressor gene encoding a family of angiotensin II AT2 receptor-interacting proteins, ATIP. Gene. 2006;380:127-136.
14. Seibold S, Rudroff C, Weber M, et al. Identification of a new tumor suppressor gene located at chromosome 8p21.3-22. Faseb J. 2003;17:1180-1182.

15. Briegel KJ, Joyner AL. Identification and characterization of Lbh, a novel conserved nuclear protein expressed during early limb and heart development. Dev Biol. 2001;233:291-304.
16. Briegel KJ, Baldwin HS, Epstein JA, et al. Congenital heart disease reminiscent of partial trisomy 2p syndrome in mice transgenic for the transcription factor Lbh. Development. 2005;132:3305-3316.
17. Firulli AB. A HANDful of questions: the molecular biology of the heart and neural crest derivatives (HAND)-subclass of basic helix-loop-helix transcription factors. Gene. 2003;312:27-40.
18. Gibson-Brown JJ, Agulnik SI, Silver LM, et al. Involvement of T-box genes Tbx2-Tbx5 in vertebrate limb specification and development. Development. 1998;125:2499-2509.
19. Mesbah K, Harrelson Z, Theveniau-Ruissy M, et al. Tbx3 is required for outflow tract development. Circ Res. 2008;103:743-750.
20. Krause A, Zacharias W, Camarata T, et al. Tbx5 and Tbx4 transcription factors interact with a new chicken PDZ-LIM protein in limb and heart development. Dev Biol. 2004;273:106-120.
21. Koshiba-Takeuchi K, Takeuchi JK, Arruda EP, et al. Cooperative and antagonistic interactions between Sall4 and Tbx5 pattern the mouse limb and heart. Nat Genet. 2006;38:175-183.
22. Zhu J, Nakamura E, Nguyen MT, et al. Uncoupling Sonic hedgehog control of pattern and expansion of the developing limb bud. Dev Cell. 2008;14:624-632.
23. Washington Smoak I, Byrd NA, Abu-Issa R, et al. Sonic hedgehog is required for cardiac outflow tract and neural crest cell development. Dev Biol. 2005;283:357-372.
24. Abu-Issa R, Smyth G, Smoak I, et al. Fgf8 is required for pharyngeal arch and cardiovascular development in the mouse. Development. 2002;129:4613-4625.
25. Crossley PH, Minowada G, MacArthur CA, et al. Roles for FGF8 in the induction, initiation, and maintenance of chick limb development. Cell. 1996;84:127-136.
26. Yang L, Cai CL, Lin L, et al. Isl1Cre reveals a common Bmp pathway in heart and limb development. Development. 2006;133:1575-1585.
27. Wilson GN. Correlated heart/limb anomalies in Mendelian syndromes provide evidence for a cardiomelic developmental field. Am J Med Genet. 1998;76:297-305.
28. Cioce M, Lamond AI. Cajal bodies: a long history of discovery. Annu Rev Cell Dev Biol. 2005;21:105-131.
29. Dundr M, Misteli T. Functional architecture in the cell nucleus. Biochem J. 2001;356:297-310.
30. Hamburger V, Hamilton HL. A series of normal stages in the development of the chick embryo. J Morphol. 1951;88:49-92.
31. Nieto MA, Bennett MF, Sargent MG, et al. Cloning and developmental expression of Sna, a murine homologue of the Drosophila snail gene. Development. 1992;116:227-237.
32. Moorman AF, Houweling AC, de Boer PA, et al. Sensitive nonradioactive detection of mRNA in tissue sections: novel application of the whole-mount in situ hybridization protocol. J Histochem Cytochem. 2001;49:1-8.
33. Kuijk EW, du Puy L, van Tol HT, et al. Validation of reference genes for quantitative RT-PCR studies in porcine oocytes and preimplantation embryos. BMC Dev Biol. 2007;7:58.

Chapter 5

Early embryonic expression pattern of Sarcosin in mice and its localization and knock-down in differentiating C2C12 myoblasts

Leonie du Puy [(1)], Abdelazziz Beqalli [(2)], Jantine Monshouwer-Kloots[(2)], Robert Passier [(2)], Henk P. Haagsman [(3)], Bernard A.J. Roelen[(1)],

[1] Department of Farm Animal Health, Faculty of Veterinary Medicine, Utrecht University, Utrecht, The Netherlands ; [2] Department of Anatomy & Embryology, Leiden University Medical Center, Leiden, The Netherlands; [3] Department of Infectious Diseases and Immunology, Faculty of Veterinary Medicine, Utrecht University, Utrecht, The Netherlands.

Submitted for publication

Abstract

Sarcosin, also named Krp1, was previously identified as a protein exclusively expressed in striated muscle tissue. Here we report on the role of Sarcosin in skeletal muscle development and differentiation. We demonstrate, by means of whole-mount *in situ* hybridization, that *Sarcosin* mRNA was expressed in the myotome part of the mature somites in mouse embryos from embryonic day 9.5 onwards. *Sarcosin* was not expressed in the developing heart at these embryonic stages and in adult tissues the mRNA expression levels were five times lower in heart compared to skeletal muscle. SARCOSIN protein partially co-localized with the M-band protein myomesin and between and below laterally fusing myofibrils in adult skeletal muscle tissue. RNA interference mediated knock-down of SARCOSIN in the C2C12 myoblast cell line did not affect myoblast fusion and myotube formation, and no obvious effect on myofibrillogenesis was observed. However, SARCOSIN knock-down accelerated differentiation as analyzed by quantitative real-time PCR and immunoblotting.

Introduction

SARCOSIN, also named Kelch related protein 1 (Krp1) is originally identified and described to be exclusively expressed in striated muscle [1]. Little is known about the expression and role of SARCOSIN during embryogenesis. In cultures of primary cardiomyocytes, SARCOSIN is described to be involved in late myofibril assembly [2]. However, important processes that take place in skeletal muscle differentiation such as withdrawal from the cell cycle, fusion, de novo myofibrillogenesis and myotube formation do not occur in primary cardiomyocyte cultures and the function of SARCOSIN in these processes is unknown.

The amino-acid sequence of SARCOSIN encodes five Kelch repeats at its carboxyl terminus and a BTB/POZ domain at the amino terminus [1, 3]. Kelch repeats form a tertiary structure named a ß-propeller which is important for interactions with proteins of the cytoskeleton. Proteins containing Kelch repeats are reported to have diverse functions in cell morphology and organization [4]. The BTB domain, standing for Broad-Complex, Tramtrack and Bric a brac also known as a Poxvirus and Zinc-finger (POZ) domain, mediates homomeric and heteromeric protein dimerizations.

SARCOSIN was demonstrated to be a binding partner of nebulin-related anchoring protein (N-RAP), an actin-binding LIM-protein expressed in skeletal and cardiac muscle tissues [5]. N-RAP is expressed in the regions where actin-bundles link myofibrils to the cell membrane, these regions are called myotendinous junctions in skeletal muscle and intercalated disks in cardiac muscle [6, 7]. In embryonic cardiac

cells N-RAP is associated with premyofibril structures and newly formed mature myofibrils [8]. NEBULIN, another binding partner of SARCOSIN [9], is an actin-binding protein thought to function as a 'ruler' to regulate the precise lengths of the actin (thin) filaments in skeletal muscle [10]. Also, NEBULIN can interact with the intermediate filament DESMIN, possibly laterally linking Z-lines and integrating myofibrils with the cell membrane [11]. Immunofluorescence staining in cultured chick cardiomyocytes showed localization of SARCOSIN between narrow myofibrils that appear to be fusing laterally [5]. Identification of SARCOSIN as a binding partner of N-RAP and NEBULIN and its localization in myofibrils suggest a role for SARCOSIN in myofibril function. SARCOSIN knock-down by RNAi in cultured mouse embryonic cardiomyocytes resulted in an α-ACTININ staining pattern that is characteristic of newly forming myofibrils suggesting that SARCOSIN affects the assembly and or maintenance of myofibril structure [2].

Besides its expression in striated muscle, SARCOSIN was also up-regulated in oncogenic transformed rat fibroblasts which upon transformation with v-fos became invasive and underwent extensive cytoskeletal reorganizations forming long pseudopodia. SARCOSIN localized at the tip of these pseudopodia, and while over-expression of SARCOSIN resulted in elongated pseudopodia, siRNA-mediated down-regulation caused shortening of these structures. This effect of SARCOSIN expression is dependent on the binding of SARCOSIN to LIM and SH3-containing protein 1 (LASP-1) [3, 9]. LASP-1 is expressed in almost all adult mouse tissues and over-expressed in human breast cancers [12, 13]. In addition to an N-terminal LIM domain and C-terminal SH3 domain, LASP-1 also contains two nebulin repeats, binds to non-muscle F-actin *in vitro* and is localized to focal adhesions and pseudopodia [14-16]. A specific role for LASP-1 in muscle has not been described.

Finally, a subset of BTB proteins functions as substrate adaptor proteins for the Cul3-Rbx1 E3 ubiquitin ligase complex [17, 18]. SARCOSIN was demonstrated to be a substrate protein for this complex. It was suggested that SARCOSIN, as does another Kelch and BTB domain containing protein named KEAP1, could function both as substrate and as a substrate adaptor protein for the Cul3-Rbx E3 ubiquitin ligase complex [19].

In this study the expression of *Sarcosin* mRNA during mouse embryonic development was visualized by whole-mount *in situ* hybridization (ISH) and SARCOSIN protein expression in adult skeletal muscle by immunofluorescence. SARCOSIN role in myoblast differentiation and fusion into myotubes was studied by RNA interference (RNAi)-mediated down-regulation of SARCOSIN in the C2C12 myoblast cell line.

Material and Methods

Animals

C57Bl/6 mice were intercrossed, and females sacrificed for collection of embryos at various time points: Embryonic day (E)8, E9.5, and E10.5. The following morning detection of vaginal plugs was considered day E0.5. Embryos were fixed in 4% (w/v) paraformaldehyde (Electron Microscopy Science, Hatfield, PA) in phosphate buffered saline (PBS, Braun, Melsungen, Germany) at 4°C overnight and stored in 100% methanol at -20 ºC. All animal handling procedures were approved by the institutional animal experiments committee.

Whole- mount in situ hybridization

Whole-mount in situ hybridization (ISH) was performed as described previously [20]. For probe preparation, purified PCR product was generated to use as a template, with *Sarcosin*-specific primers (forward: CCTTACCCAGGTTCCTCACA, reverse: CCAATCTTAGGATGGCCAGA) with the T3 promoter sequence (ATACAATTAACCCTCACTAAAGGG) at the 5'end of the forward primer and the T7 promoter sequence (ATAGGTAATACGACTCACTATAGGGC) at the 3'end of the reverse primer. RNA probes were synthesized using T7 (antisense) polymerase and DIG labelled nucleotides according to the manufacturer's protocol (Roche Applied Sciences, Almere, The Netherlands). Embryos were imaged using a Zeiss Axioplan SZX9 coupled to a Leica DFC480 digital camera.

Cell culture and transfection

The murine myoblast cell line C2C12 (ATCC CRL-1772) was cultured at 37ºC, 5% CO_2 in Dulbecco's Modified Eagle's Medium (DMEM-HG, Invitrogen, Carlsbad, CA) based proliferation medium supplemented with 10% fetal bovine serum (FBS, Invitrogen), 1x non-essential amino acids (Invitrogen) and 50 U/ml penicillin and 50 µg/ml streptomyocin (Invitrogen). Myotube formation was induced by replacing FBS in the culture medium with 2% horse serum (Differentiation medium, Vector Laboratories, Burlingame, CA). To reduce endogenous SARCOSIN expression, cells were transfected with stealth siRNA duplex oligoribonucleotides against *Sarcosin* (5'-CCACTGAAGTCAATGACATATGGAA- 3') (Invitrogen) using Lipofectamine 2000 according to the manufacturer's protocol (Invitrogen). Universal control siRNAs (Invitrogen) with GC percentage similar to the *Sarcosin* stealth siRNA were used as a negative control. Briefly, one day before transfection cells were plated at a density of 4000 cells/cm^2 on gelatin-coated dishes in proliferation medium. Cells were transfected with 40 pmol/ml *Sarcosin* siRNA and medium was changed 8 hrs after transfection. Differentiation was induced 48 hrs after transfection. Cells were collected for either RNA isolation or protein isolation at days zero to five of differentiation.

Table 1. Primers used for RT-PCR and Q-PCR.

Gene [reference nr]	5' forward primer 5' reverse primer	Ta (°C)	amplicon size (bp)
Gapdh **[beacon designer]**	CGTGCCGCCTGGAGAAAC TGGGAGTTGCTGTTGAAGTCG	56	136
Oaz1 **[22]**	GGATCCTCAATAGCCACTGC TACAGCAGTGGAGGGAGACC	58	150
Rpl22 **[22]**	CTGGGCTGCTGCTCCTTTG AATCACCTGTCTGCTTCTGAGG	58	250
Pgk1 **[26]**	CTCCGCTTTCATGTAGAGGAAG GACATCTCCTAGTTTGGACAGTG	58	117
B-actin **[beacon designer]**	GACATCCGTAAAGACCTCTATG ACTCCTGCTTGCTGATCC	58	223
Sarcosin **[PRIMER 3]**	CCTAGCAACGCGCTTAAATC GAAACTGCGTGAATCCCTGT	62	161
Nebulin **[23]**	ACTGTCCTCTATCCCATCAC GCCATACATCCAGCCTTCAT	60	151
N-rap **[23]**	AAACCAACGCAGCCAACCTG CGTGCCTGTAGAGAAAGTCA	60	150
α-actinin(2+3) **[23]**	ATCATCCTCCGCTTCGCCATTC TCTTCAGCATCCAACATCTTAGG	58	290
Lasp1 **[PRIMER 3]**	GCCTGCAGTGAAGGGTAGAG GACACGACGACAGAAAAGCA	58	249
MHC-embryonic **[24]**	GCCAGGATGGGAAAGTCACTGTGG GGGCTCGTTCAGGTGGGTCAGC	62	137
MHC2B **[25]**	ACAGACTAAAGTGAAAGCC CTCTCAACAGAAAGATGGAT	54	215
NM-MHC2B **[23]**	TGTCATCTACAACCCTGCCACTC GCTTTCTTCCCATTCTCTGCCAG	58	150
Atrogin **[27]**	CTCTGTACCATGCCGTTCCT GGCTGCTGAACAGATTCTCC	55	172

RNA isolation and quantitative real- time PCR

Total RNA of C2C12 cells was extracted using the RNeasy minikit (Qiagen, Valencia, CA) and on-column DNAse treatment (Qiagen) was performed. Total RNA from adult mouse heart and skeletal muscle was isolated using Trizol reagent (Invitrogen). Total RNA was reverse transcribed into cDNA using Superscript II reverse-transcription polymerase (Invitrogen) and random primers (Invitrogen) according to the supplier's protocol.

For quantitative real-time PCR, each reaction contained 10 µl SYBRGreen Mastermix (BIO-RAD, Hercules, CA), 0.5 mM forward primer, 0.5 mM reverse primer and 1 µl cDNA as a template in a final volume of 20 µl. Primers were designed using Primer 3 software [21] or based on literature (Table 1) [22-27]. Reactions were carried out in duplicate for each sample. Negative controls were reactions containing template synthesized without reverse transcriptase and reactions containing H_2O instead of cDNA. The reactions were amplified on a MyIQ Real-Time PCR detection system (BIO-RAD) using the following program: initial denaturation at 95ºC for 3 min, followed by 40 cycles of 30 sec at 95ºC, 30 sec at the corresponding annealing temperature (Table 1) and 30 sec at 72ºC. A melting curve was produced to verify single PCR product amplification. Efficiency of the PCR reaction was tested using a standard curve synthesized from either a dilution series of cDNA or PCR product. PCR products were separated on 1% agarose gels against a 100 bp ladder and visualized with ethidium bromide. To verify the specificity, the PCR products were sequenced. Data were analyzed with iQ5 software (BIO-RAD). Starting quantities of all genes were calculated based on their standard curves. Using GeNorm, gene expression normalization factors for each sample were calculated based on the expression levels of the reference genes glyceraldehyde-3-phosphate dehydrogenase (*Gapdh*), phosphoglycerate kinase 1 (*Pgk1*), and beta-ctin (*B-actin*) for data in figure 1, and to the expression levels of Ornithine decarboxylase antizyme 1 (*Oaz1*), ribosomal protein l22 (*Rpl22*) and *Gapdh* for data in figures 3-5. The underlying principles and calculations used are described in [28]. Statistical differences between expression levels were tested using a nonparametric Mann-Whitney test.

Protein isolation and immunoblotting.

To prepare protein cell extracts C2C12 cells were washed with ice cold PBS and lysed in buffer containing 140 mM NaCl, 50 mM Tris-HCL pH7.5, 1 mM EDTA, 0.1% Triton X-100, 10% Glycerol and protease inhibitor cocktail (1 tablet per 50 ml lysis buffer) (Roche Applied Sciences). Cell lysates were clarified by centrifugation at 10,000 rpm at 4ºC for 15 min and the supernatants protein contents were measured using a DC-protein assay (BIO-RAD). Because of incomplete protein lysis due to the lysis buffer used and the subsequent centrifugation step, protein levels of cytoskeletal elements and myofibrils in the reported immunoblot analysis do not reflect the total levels of these proteins in the cells. Equal concentrations of protein were suspended in Laemmli's sodium dodecylsulfate-(SDS) sample buffer. Protein samples were separated by SDS-polyacrylamide gel electrophoresis and transferred to Trans-Blot nitrocellulose transfer membrane (BIO-RAD). Membranes were blocked using 5% Blotting Grade Blocker non-fat dry milk (BIO-RAD) in 1x Tris Buffered Saline-0.1% Tween (TBST) for 1 hr at room temperature (RT) and subsequently probed with primary antibody (Table 2) overnight at 4ºC. Next the membranes were incubated with

1 to 10,000 dilution of either horseradish peroxidase-conjugated goat anti-rabbit IgG or goat anti-mouse IgG (Santa Cruz Biotechnology, Santa Cruz, CA) for 1 hr at RT, signals were visualized on film using SuperSignal West Dura Extended Duration Substrate (Pierce, ThermoScientific, Erembodegem, Belgium).

Immunofluorescence staining and microscopy
C2C12 cells cultured on gelatine-coated glass cover slips and frozen tissue sections of mouse skeletal muscle and heart tissue were fixed in 4% PFA for 10 min at RT. C2C12 cells were permeabilized after fixation for 8 min using 0.1% Triton X100 in PBS. Slides were blocked in PBS-0.1% Tween 20 containing 4% normal goat serum for 1 hr at RT. For staining cells were incubated overnight at 4ºC with primary antibody (Table 2), and subsequently incubated for 1 hr at RT with secondary antibodies: goat anti-mouse Alexa488-conjugated and goat anti-rabbit Alexa568-conjugated (1:200, Invitrogen). Slides were mounted in Fluosave mounting medium (Calbiochem, Merck Chemicals Ltd, Nothingham, UK) and analyzed by normal fluorescence or confocal laser scanning microscopy.

Results

Sarcosin mRNA is expressed in the somites during early mouse embryonic development.
In order to investigate the expression of Sarcosin during early development we performed whole-mount ISH on mouse embryos. *Sarcosin* mRNA was first observed in E9.5 embryos, and expression was exclusively observed in the oldest somites (Fig 1A, B). At E10.5 *Sarcosin* mRNA was expressed in all somites (Fig 1C). During the period examined (E8-E10.5) *Sarcosin* mRNA was not expressed in the embryonic heart. Sections of whole-mount ISH of E9.5 embryos demonstrated *Sarcosin* expression in the myotome part of the somite (Fig 1D). Quantitative real-time PCR analysis demonstrated expression in mouse adult heart and skeletal muscle, with expression levels of *Sarcosin* mRNA in the heart being five times lower compared to skeletal muscle expression (Fig 1E).

Table 2. Antibodies

Protein	Manufacturer (Product code)	Immuno blot (IB) /Immunofluorescence (IF)	Description
SARCOSIN	aviva systems biology (ARP38732)	1 to 1600 (IB)	rabbit polyclonal
SARCOSIN	generous gift of Prof. Bradford Ozanne	1 to 500 (IF)	rabbit polyclonal
GAPDH	SIGMA (G8795)	1 to 20000 (IB)	mouse monoclonal
ACTIN	Chemicon (MAB1501, clone C4)	1 to 1000 (IB)	mouse monoclonal
α-ACTININ	SIGMA (A7811)	1 to 2500 (IB) / 1 to 500 (IF)	mouse monoclonal
MYOGENIN	BD Pharmingen (556358)	1 to 200 (IF)	mouse monoclonal
MYOSIN (all sarcomeric)	Development studies hybridoma bank (MF20)	1 to 1000 (IB)	mouse monoclonal
NON MUSCLE MYOSIN	Development studies hybridoma bank (CMII23)	1 to 500 (IB)	mouse monoclonal
DESMIN	DakoCytomation (M0760)	1 to 200 (IB)	mouse monoclonal
MYOMESIN	generous gift of Dr Elisabeth Ehler	1 to 10 (IF)	mouse monoclonal

SARCOSIN is localized between laterally fusing myofibrils in adult skeletal muscle.
SARCOSIN protein localization was studied in adult skeletal muscle using immunofluorescence, Z-discs were visualized by α-ACTININ staining (Fig 2A-D), M-bands by MYOMESIN staining (Fig 2E-H). In adult skeletal muscle tissue an overall staining of SARCOSIN was observed, and SARCOSIN protein partially co-localized with the M-band protein MYOMESIN but was also present expressed underneath the M-bands. Confocal imaging at planes above and below the laterally fusing myofibrils revealed that SARCOSIN was not only concentrated between fusing myofibrils but also underneath these structures. SARCOSIN did not co-localize with α-ACTININ.

Sarcosin is highly up-regulated in C2C12 myoblast differentiation into myotubes.
To investigate the role of SARCOSIN in skeletal muscle cells we used the C2C12 cell line as a model system. This cell line is derived from muscle precursor cells obtained from dystrophic mouse muscle, and when cultured in differentiation medium containing 2% horse serum C2C12 myoblasts readily fuse into multinucleated myotubes. *Sarcosin* mRNA levels were measured by real-time qPCR in C2C12 myoblasts differentiating to myotubes (Fig 3A). *Sarcosin* mRNA levels were readily detectable in undifferentiated myoblasts (day 0), and expression levels were highly up-regulated (approximately 60 fold) in day 6 differentiated myotubes compared to proliferating myoblasts. Immunoblot analysis of SARCOSIN protein expression during

myoblast differentiation (Fig 3B) confirmed the results observed with quantitative real-time PCR. SARCOSIN protein was present in proliferating myoblasts and expression was up-regulated during differentiation of the myoblasts to myotubes. At the beginning of myoblast differentiaton a down-regulation of SARCOSIN protein was observed compared to proliferating myoblasts; this was not observed at the mRNA level.

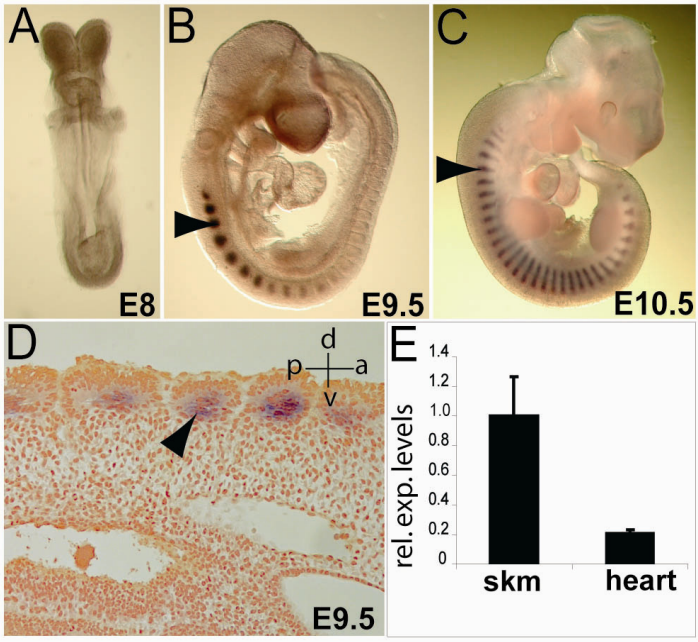

Fig 1: Sarcosin mRNA expression during mouse embryonic development and in adult heart and skeletal muscle tissue.
In situ hybridization with digoxigenin-UTP labelled specific riboprobe performed on whole-mount mouse embryos at (A) embryonic day (E)8, (B) E9.5, and (C) E10.5. Sarcosin expression is visible in the somites (arrowheads) from E9.5 onwards. (D) E9.5 embryos subjected to whole-mount in situ hybridization sectioned in the sagital plane (10 µm thick). Sarcosin specific mRNA expression is visible in the myotome part of the somite (arrowhead). D: dorsal, v: ventral, a: anterior, p: posterior. (E) Sarcosin mRNA transcript levels measured using quantitative RT-PCR in mouse adult skeletal muscle (skm) and heart. Expression levels in skm are set to 1. Values are normalized to the house keeping genes Gapdh, Pgk1 and B-actin. Error bars represent standard error of the mean.

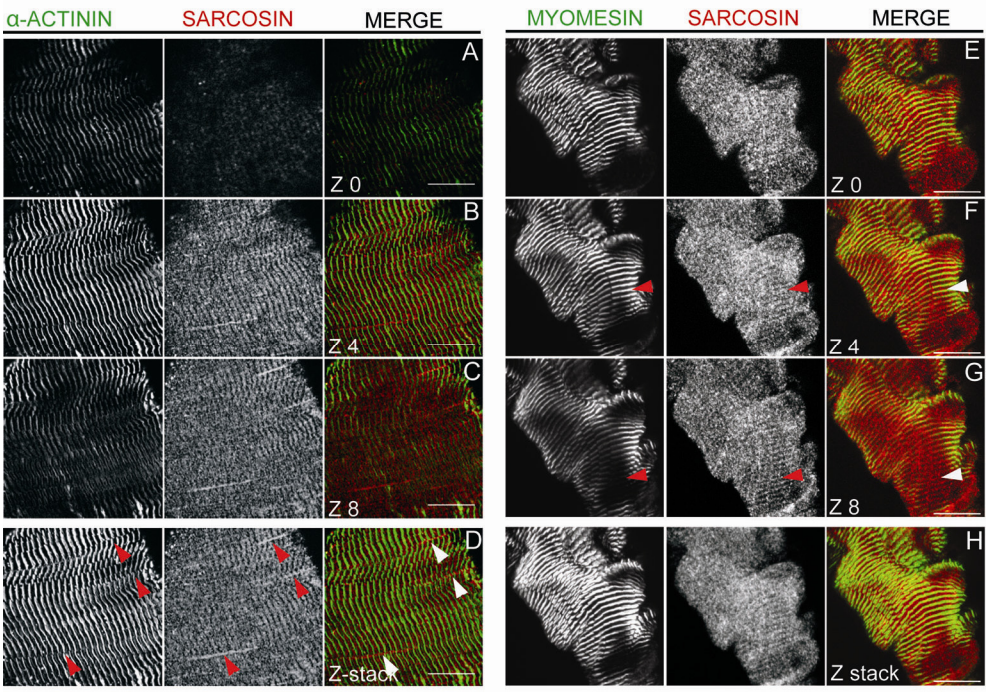

Fig 2: SARCOSIN protein expression in adult skeletal muscle.
Immunofluorescence staining in adult skeletal muscle tissue. Panel A to D: α-ACTININ (green) and SARCOSIN (red); arrowheads point to concentrated SARCOSIN staining between laterally fusing myofibrils. Z0-Z8: focal planes, with a stepsize of 0.122 µm between the individual Z-planes. Panel E to H: MYOMESIN (green) and SARCOSIN (red). Arrowhead points to concentrated SARCOSIN staining at the M-band. Z0-Z8: focal planes with a stepsize of 0.163 µm between the individual Z-planes, Scale bars 10 µm.

In proliferating C2C12 cells an overall expression of SARCOSIN was observed using immunofluorescence, with a higher SARCOSIN concentration in the nucleus compared to the cytoplasm in α-ACTININ-negative cells (Fig 3C, panel 1). After 24 hrs of differentiation, more α-ACTININ positive cells were present compared with cultures of proliferating cells, and occasionally fused cells were observed (Fig 3C, panel 2). At day three of differentiation, Z-bodies were visible and a co-localization of α-ACTININ and SARCOSIN was observed in these Z-bodies (Fig 3C, panel 3). In fused myotubes on day five of differentiation, immature myofibrils were identified by α-ACTININ staining. SARCOSIN was equally distributed in these myotubes but no concentration of SARCOSIN between the Z-discs was observed (Fig 3C, panel 4).

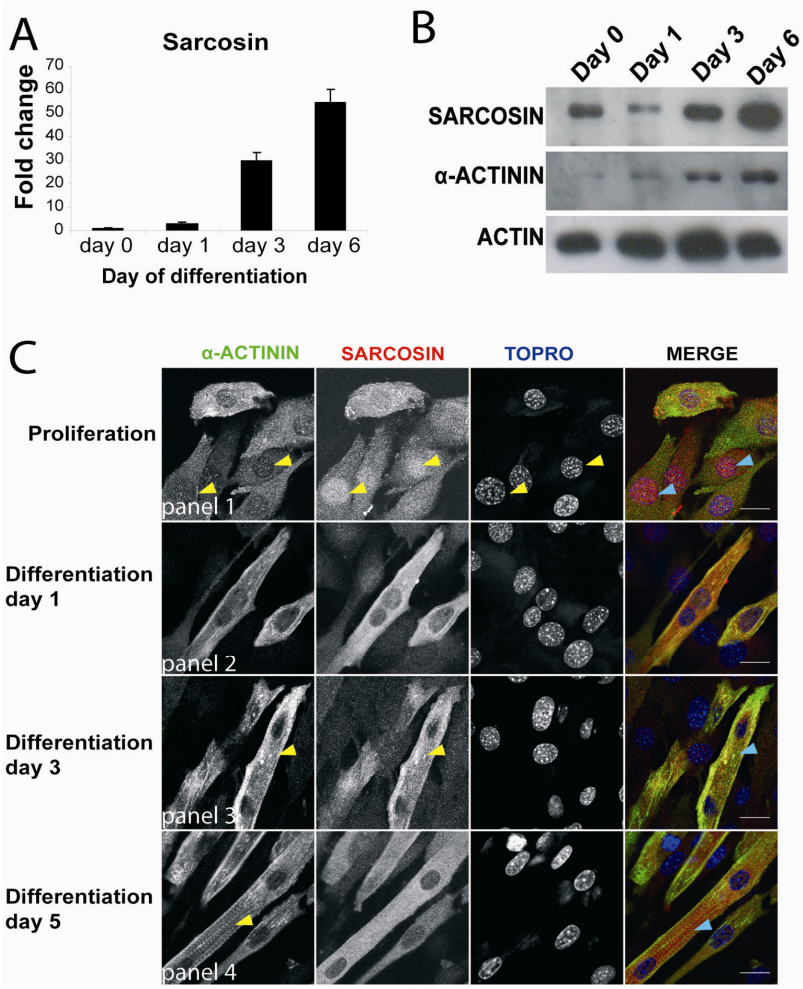

Fig 3: SARCOSIN RNA and protein expression in C2C12 myoblasts differentiating to myotubes.
(A) *Sarcosin* mRNA transcript levels measured using quantitative RT-PCR in C2C12 myoblast differentiating into myotubes. Values are normalized to the house keeping genes *Gapdh*, *Oaz1* and *Rpl22*. Error bars represent standard error of the mean. (B) Immunoblot analysis of SARCOSIN, α-ACTININ and the house keeping protein ACTIN in C2C12 myoblast differentiating to myotubes, samples collected at days 0, 1, 3 and 6 of differentiation. Because of incomplete protein lysis, protein levels in this immunoblot analysis do not reflect the total levels of α-ACTININ and SARCOSIN in the cells. (C) Immunofluorescence staining of α-ACTININ (green), SARCOSIN (red) and nuclei (blue) in differentiating C2C12 cells, scale bars 20 µm. Arrowheads in panel 1 point to nuclei of α-ACTININ negative cells with a higher SARCOSIN staining in the nucleus compared to the cytoplasm. Arrowheads in panel 3 point to Z-bodies, arrowheads in panel 4 point to Z-disc staining.

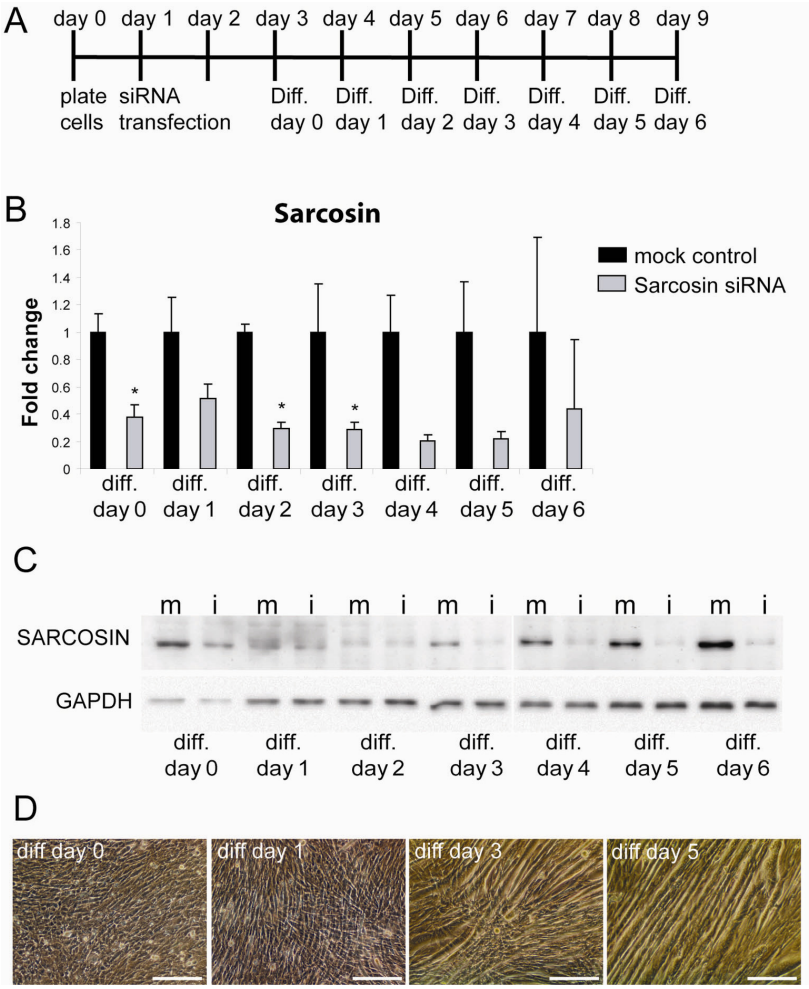

Fig 4 RNAi mediated knock-down of SARCOSIN expression in C2C12 myoblasts and their differentiation to myotubes. (A) Schematic presentation of the experimental procedure. (B) Sarcosin mRNA transcript levels measured using quantitative real time PCR in C2C12 myoblast, transfected with Sarcosin siRNA or with mock negative control, differentiating into myotubes. Values are normalized to the housekeeping genes Gapdh, Oaz1 and Rpl22. Expression levels of mock control are set to 1. Error bars represent standard error of the mean, $*$ $p<0.05$ indicates statistical differences between mock control and sarcosin siRNA on the same day of differentiation. (C) Immunoblot analysis of SARCOSIN expression in C2C12 myoblast differentiating to myotubes, transfected with siRNA against Sarcosin (i) or with mock negative control (m). Samples collected at day 0 to 6 of differentiation. GAPDH expression was analyzed as loading control. Because of incomplete protein lysis, protein levels in this immunoblot analysis do not reflect the total levels of SARCOSIN in the cells. (D) Morphology of myoblasts at different days of differentiation into myotubes, transfected with Sarcosin siRNA. Scale bars 20 µm

RNAi mediated knock-down of SARCOSIN expression in C2C12 myoblasts.
In order to establish the function of SARCOSIN in skeletal muscle cells, SARCOSIN expression was down-regulated in C2C12. Proliferating C2C12 myoblasts were transfected with stealth siRNA to *Sarcosin* or with a mock-control, and 48 hrs after transfection differentiation was induced by replacing the culture medium with differentiation medium containing 2% horse serum (Fig 4A). *Sarcosin* knock-down was evaluated using quantitative real time PCR and immunoblot analysis. Two days after transfection *Sarcosin* mRNA levels were decreased to approximately 30% compared to the mock-control transfected cells and this decrease persisted during the differentiation experiment (Fig 4B). As expected, a decrease of SARCOSIN protein levels was somewhat delayed when compared to mRNA expression levels. Starting at day 3 of myoblast differentiation and thus 5 days after transfection, SARCOSIN protein levels were substantially decreased in siRNA transfected cells compared to their mock-controls (Fig 4C). No difference was observed between the timing of myotube formation and morphology of the myotubes in cells transfected with siRNA (Fig 4D) compared to their mock-control. In fact, both in siRNA transfected myoblasts and in the mock-controls spontaneously contracting myotubes were observed.

Knock-down of SARCOSIN in C2C12 myoblasts leads to accelerated differentiation.
To assess the effects of SARCOSIN knock-down on C2C12 myoblast differentiation, the expression of genes involved in myofibril function was analyzed by quantitative RT-PCR. Expression levels of *Lasp-1* (Fig 5A), coding for a binding partner of SARCOSIN that is involved in cell-migration [9], decreased during differentiation of C2C12 cells to myotubes. On days 4 and 6 of differentiation, *Lasp-1* transcript levels were significantly increased in cells treated with *Sarcosin* siRNA when compared to the mock-controls, although differences were minor.

N-RAP is involved in myofibril assembly and was identified as a binding partner of SARCOSIN [5, 23]. Transcript levels of *N-rap* increased considerably (up to 16 times) during myoblast differentiation (Fig 5B). Between days 2 and 4 of myoblast differentiation *N-rap* transcript levels in siRNA transfected cells were up-regulated compared to their mock-controls and this up-regulation was significant on day 2 of differentiation. *α-Actinin* and *Nebulin* code for two building blocks of the sarcomeric structures [29] and the expression was highly up-regulated during myoblast differentiation (Fig 5C, D). *α-Actinin* transcript levels were readily detectable in proliferating myoblasts, and transcript levels were up-regulated in *Sarcosin* siRNA transfected cells compared to their mock-controls between days 2 and 4 of myoblast differentiation, this up-regulation was significant on day 3 of differentiation (Fig 5C).

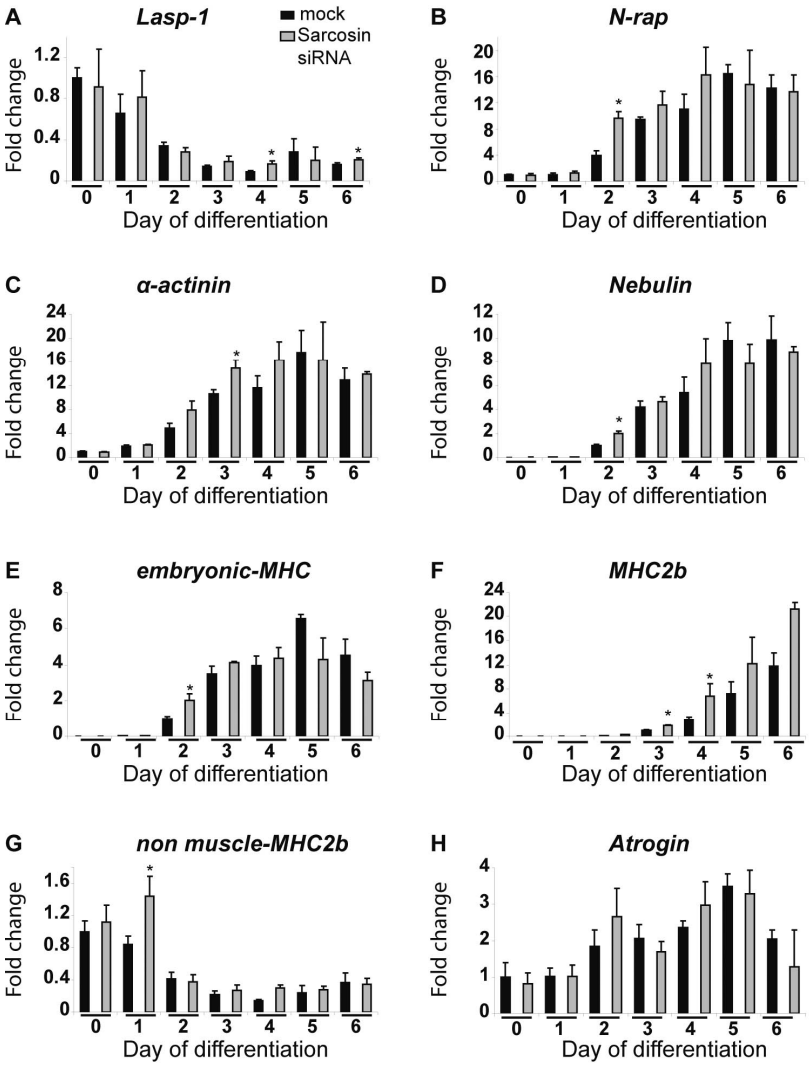

Fig 5 Effect of SARCOSIN knock-down on mRNA transcript levels of genes involved in C2C12 myoblast differentiation. Messenger RNA transcript levels of (A) *Lasp-1*; (B) *N-rap*; (C) *α-actinin*; (D) *Nebulin*; (E) *embryonic myosin heavy chain-embyronic* (*embryonic MHC*); (F) *MHC2B*; (G) *Non muscle MHC2B* and (H) *Atrogin* measured using quantitative real time PCR in C2C12 myoblasts, transfected with stealth siRNA against Sarcosin or with mock negative control, differentiating into myotubes. Experiments were carried out in triplicate. Values are normalized to the housekeeping genes *Gapdh*, *Oaz1* and *Rpl22*. Error bars represent standard error of the mean, $*$ $p<0.05$ indicates statistical differences between mock control and *sarcosin* siRNA on the same day of differentiation.

Knock-down of SARCOSIN in C2C12 myoblasts leads to accelerated differentiation.
Nebulin mRNA levels could only be detected reliably as of day 2 of myoblast differentiation and *Nebulin* transcript levels were up-regulated in siRNA transfected myoblasts compared to their mock controls between day 2 and 4 of myoblast differentiation (Fig 5D).

To assess the effects of SARCOSIN knock-down on C2C12 myoblast differentiation, the expression of genes involved in myofibril function was analyzed by quantitative RT-PCR. Expression levels of *Lasp-1* (Fig 5A), coding for a binding partner of SARCOSIN that is involved in cell-migration [9], decreased during differentiation of C2C12 cells to myotubes. On days 4 and 6 of differentiation, *Lasp-1* transcript levels were significantly increased in cells treated with *Sarcosin* siRNA when compared to the mock-controls, although differences were minor.

N-RAP is involved in myofibril assembly and was identified as a binding partner of SARCOSIN [5, 23]. Transcript levels of *N-rap* increased considerably (up to 16 times) during myoblast differentiation (Fig 5B). Between days 2 and 4 of myoblast differentiation *N-rap* transcript levels in siRNA transfected cells were up-regulated compared to their mock-controls and this up-regulation was significant on day 2 of differentiation. *α-Actinin* and *Nebulin* code for two building blocks of the sarcomeric structures [29] and the expression was highly up-regulated during myoblast differentiation (Fig 5C, D). *α-Actinin* transcript levels were readily detectable in proliferating myoblasts, and transcript levels were up-regulated in *Sarcosin* siRNA transfected cells compared to their mock-controls between days 2 and 4 of myoblast differentiation, this up-regulation was significant on day 3 of differentiation (Fig 5C). *Nebulin* mRNA levels could only be detected reliably as of day 2 of myoblast differentiation and *Nebulin* transcript levels were up-regulated in siRNA transfected myoblasts compared to their mock controls between day 2 and 4 of myoblast differentiation (Fig 5D).

RNA expression levels were measured for 3 isoforms of myosin heavy chain (MHC). *Embryonic-MHC* is expressed in developing skeletal muscle and increased during C2C12 myoblast differentiation (Fig 5E). MHC2B is expressed in fast-twitching muscle and *MHC2B* transcript levels increased up to 12 times during myoblast differentiation (Fig 5F). Finally, *Non-muscle MHC2B*, coding for the myosin present in premyofibril structures before replacement with muscle myosin, decreased during myoblast differentiation (Fig 5G). Of these myosins, only *MHC2B* transcripts were consistently up-regulated in siRNA treated myoblasts compared to their mock controls.

To examine whether SARCOSIN is involved in muscle atrophy *Atrogin* RNA expression levels were measured. No difference in mRNA expression levels were observed between SARCOSIN down-regulated cells and their mock controls (Fig 5H).

Protein expression in differentiating myoblasts in which SARCOSIN was down-regulated by siRNA treatment was analyzed by immunoblotting (Fig 6A).

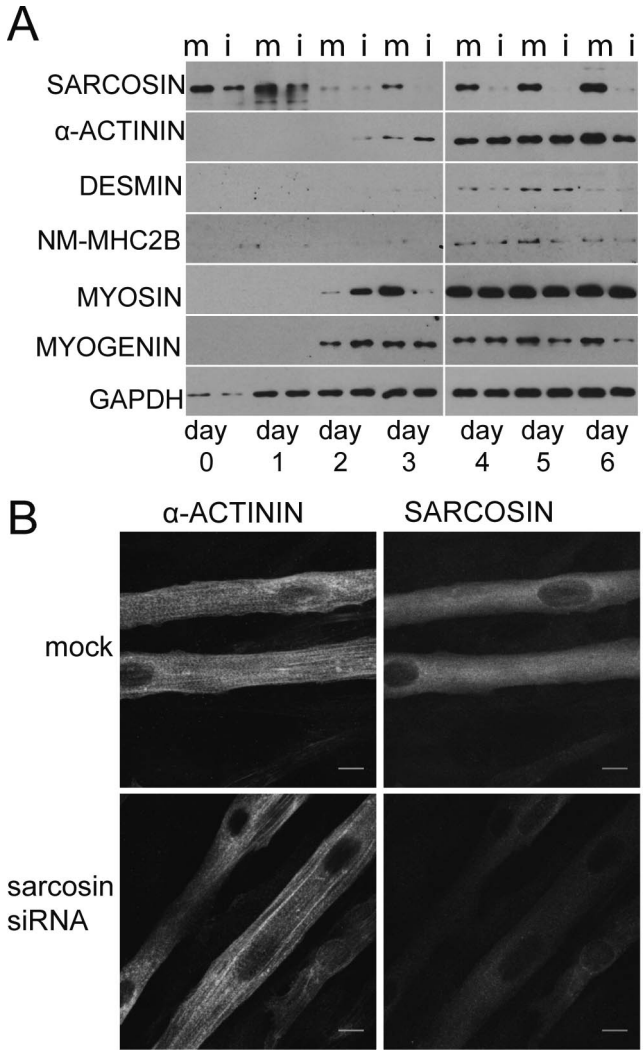

Fig 6 Effect of SARCOSIN knock-down on proteins involved in C2C12 myoblast differentiation. A: Immunoblot analysis of SARCOSIN, α-ACTININ, DESMIN, non muscle myosin heavy chain 2B (NM-MHC2B), all sarcomeric myosin (MYOSIN), MYOGENIN and GAPDH in C2C12 myoblasts, transfected with stealth siRNA against *Sarcosin* (i) or with mock negative control (m), differentiating into myotubes (day 0-6: differentiation day 0-6). Because of incomplete protein lysis, protein levels of cytoskeletal elements and myofibrils in this immunoblot analysis do not reflect the total levels of alfa-actinin and SARCOSIN in the cells. B: Immunofluorescence staining of α-ACTININ (left) and SARCOSIN (right) in myotubes, transfected with either mock control (top) or *Sarcosin* siRNA (bottom); scale bars 10 µm.

Equal amounts of total cellular protein were loaded for siRNA transfected samples and their respective mock-controls. GAPDH expression was used as a loading control. At day 2 of differentiation, α-ACTININ, MYOSIN and MYOGENIN expression was up-regulated in the siRNA treated cells compared to their mock controls. Expression of α-ACTININ was slightly less in siRNA transfected myotubes at day 6 of differentiation compared to the mock-control. Expression levels of DESMIN and Non-muscle MHC2B in the siRNA transfected cells did not appear to differ from their mock controls. At days 5 and 6, siRNA mediated down-regulation of SARCOSIN resulted in a down-regulation of MYOGENIN in these myotubes.

Immunofluorescence analysis of the myotubes in which SARCOSIN was down-regulated did not reveal any disruption or delay in myofibril assembly as studied by α-ACTININ staining (Fig 6B).

Discussion

SARCOSIN is a protein exclusively expressed in sarcomeric muscle and is described to play a role in late myofibril assembly in cultured cardiomyoctes. However, SARCOSIN's role in skeletal myoblast differentiation is unknown [1, 2].

To identify the role of SARCOSIN in skeletal muscle, expression of *Sarcosin* mRNA during early mouse embryonic development was studied. *Sarcosin* mRNA expression was first observed in the myotome part of mature somites in E9.5 embryos. This late expression during somite development implicates that *Sarcosin* expression is not necessary for initial somite formation from the paraxial mesoderm. Whether SARCOSIN plays a role in somite epithelialization and somite segmentation into the sclerotome and myotome remains to be determined (for review on somitogensis see [30] and references therein). Remarkably, *Sarcosin* mRNA was not expressed in the early embryonic heart (E8-E10.5) while at these embryonic stages the heart is contracting and thus functional sarcomeres are present. It is possible that the *Sarcosin* mRNA levels in the heart are below the detection limit for ISH at these embryonic stages. In adult tissues *Sarcosin* mRNA was expressed at a lower level in the heart compared to skeletal muscle as was previously demonstrated [1]. Knockout studies in mice will help reveal the role of SARCOSIN in somite maturation and in heart development.

SARCOSIN protein is expressed throughout the cytoplasm and is concentrated between laterally fusing Z-discs of nascent myofibrils in cultured cardiomyocytes [2, 5]. A similar protein localization pattern was observed by us in mouse adult skeletal muscle. SARCOSIN was also concentrated underneath laterally fusing myofibrils in adult skeletal muscle, and SARCOSIN partially co-localized with the M-band protein MYOMESIN. This expression pattern suggests that SARCOSIN has a function in the

lateral fusion of myofibrils in skeletal muscle. A similar function for SARCOSIN in cultured cardiomyocytes has recently been reported [2].

For studying the function of SARCOSIN in skeletal myoblast differentiation the C2C12 cell line was used. In proliferating C2C12 myoblasts SARCOSIN was already expressed at high levels, and during myoblast differentiation and fusion, SARCOSIN expression was highly up-regulated. An initial down-regulation of SARCOSIN protein levels upon differentiation suggests different roles for SARCOSIN in proliferating myoblasts and myotubes. This down-regulation at day 1 of differentiation was not observed in the mRNA expression, which indicates a direct degradation of SARCOSIN at the protein level. A role for SARCOSIN has been identified in the formation of pseudopodia [3]. However, no concentration of SARCOSIN protein was observed in cytoplasmic extensions of proliferating C2C12 cells. In proliferating myoblasts that exhibited low α-ACTININ expression, SARCOSIN was more concentrated in the nucleus compared to the cytoplasm. This nuclear localization of SARCOSIN suggests a possible role for SAROCOSIN in transcriptional regulation. At day three of differentiation α-ACTININ -containing Z-bodies (the initial structures formed during myofibril assembly [31]), were present in the differentiating myoblasts and SARCOSIN was expressed in these structures. Six days after the start of differentiation immature myofibrils were visible by α-ACTININ staining in myotubes, while SARCOSIN was equally distributed in these myotubes.

To test whether SARCOSIN functions in myoblast differentiation and fusion, SARCOSIN expression levels were down-regulated in C2C12 cells using siRNA. While mRNA levels of *Sarcosin* were significantly down-regulated at the start of differentiation, protein levels were not. Consequently the role of SARCOSIN in myoblast proliferation and their exit from the cell cycle could not be studied. From day 3 of differentiation and onwards, SARCOSIN protein levels were substantially decreased in siRNA treated cells compared to their mock controls. The delay in protein down-regulation compared to mRNA expression levels suggests a long half-life for SARCOSIN protein.

During differentiation, RNA expression levels of sarcomeric proteins and binding partners of SARCOSIN were measured using quantitative real-time PCR in siRNA treated cells and their mock controls. During skeletal muscle differentiation the mRNA levels of *N-rap*, *α-actinin*, *Nebulin*, *embryonic-MHC* and *MHC2B* were highly up-regulated. RNA expression levels from these sarcomeric proteins were higher in the siRNA treated cells compared to their mock controls starting from day 2 of differentiation, suggesting that knock-down of SARCOSIN accelerated differentiation. In agreement with this, α-ACTININ, MYOSIN and MYOGENIN protein levels were increased at day 2 of differentiation compared to their mock controls. SARCOSIN has been described to be associated with the Cul3-Rbx E3 ubiquitin ligase complex [19]. Possibly SARCOSIN plays a role in protein degradation and thereby delays the onset

of differentiation. However, knock-down of SARCOSIN did not influence *Atrogin* mRNA expression and the molecular mechanism by which SARCOSIN influences differentiation onset remains to be elucidated.

Our finding that SARCOSIN knock-down did not influence myofibril assembly is in contrast with the results described by Greenberg et al. that SARCOSIN promotes lateral fusion of adjacent myofibrils into mature myofibrils in cultured cardiomyocytes [2]. While α-ACTININ immunofluorescence staining did visualize Z-discs in C2C12 myotubes, these myofibrils were mostly thin and of an immature morphology making the C2C12 cell line a less suitable system to study myofibrillogenesis compared with cardiomyocytes. We therefore do not exclude the possibility that SARCOSIN plays a role in the lateral fusion of myofibrils in skeletal muscle, also taking into account SARCOSIN's association with Z-bodies in differentiating C2C12 myoblasts and its localization between laterally fusing myofibrils in adult skeletal muscle tissue.

In conclusion, our findings demonstrate that SARCOSIN is not involved in myoblast fusion and myotube formation, while a role for SARCOSIN in myofibrillogenesis can not be excluded. Further studies must provide insight into a possible role for SARCOSIN in somitogenesis.

Acknowledgements

This work was supported by a SenterNovem grant from the Ministry of Economic Affairs. The authors would like to thank Anko M. de Graaff and Richard W. Wubbolts of the Center for Cell Imaging at the Faculty of Veterinary Medicine in Utrecht for assistance in confocal laser scanning microscopy. We thank Prof Bradford W. Ozanne (Beatson Institute for Cancer research, Glasgow, UK) for the generous gift of the Sarcosin antibody and Dr Elisabeth Ehler (Kings College, London, UK) for the Myomesin antibody.

References

1. Taylor A, Obholz K, Linden G, et al. DNA sequence and muscle-specific expression of human sarcosin transcripts. Molecular and cellular biochemistry. 1998;183:105-112.
2. Greenberg CC, Connelly PS, Daniels MP, et al. Krp1 (Sarcosin) promotes lateral fusion of myofibril assembly intermediates in cultured mouse cardiomyocytes. Experimental cell research. 2008;314:1177-1191.
3. Spence HJ, Johnston I, Ewart K, et al. Krp1, a novel kelch related protein that is involved in pseudopod elongation in transformed cells. Oncogene. 2000;19:1266-1276.
4. Adams J, Kelso R, Cooley L. The kelch repeat superfamily of proteins: propellers of cell function. Trends Cell Biol. 2000;10:17-24.

5. Lu S, Carroll SL, Herrera AH, et al. New N-RAP-binding partners alpha-actinin, filamin and Krp1 detected by yeast two-hybrid screening: implications for myofibril assembly. Journal of cell science. 2003;116:2169-2178.
6. Herrera AH, Elzey B, Law DJ, et al. Terminal regions of mouse nebulin: sequence analysis and complementary localization with N-RAP. Cell Motil Cytoskeleton. 2000;45:211-222.
7. Zhang JQ, Elzey B, Williams G, et al. Ultrastructural and biochemical localization of N-RAP at the interface between myofibrils and intercalated disks in the mouse heart. Biochemistry. 2001;40:14898-14906.
8. Lu S, Borst DE, Horowits R. N-RAP expression during mouse heart development. Dev Dyn. 2005;233:201-212.
9. Spence HJ, McGarry L, Chew CS, et al. AP-1 differentially expressed proteins Krp1 and fibronectin cooperatively enhance Rho-ROCK-independent mesenchymal invasion by altering the function, localization, and activity of nondifferentially expressed proteins. Molecular and cellular biology. 2006;26:1480-1495.
10. Witt CC, Burkart C, Labeit D, et al. Nebulin regulates thin filament length, contractility, and Z-disk structure in vivo. Embo J. 2006;25:3843-3855.
11. Bang ML, Gregorio C, Labeit S. Molecular dissection of the interaction of desmin with the C-terminal region of nebulin. J Struct Biol. 2002;137:119-127.
12. Schreiber V, Masson R, Linares JL, et al. Chromosomal assignment and expression pattern of the murine Lasp-1 gene. Gene. 1998;207:171-175.
13. Tomasetto C, Moog-Lutz C, Regnier CH, et al. Lasp-1 (MLN 50) defines a new LIM protein subfamily characterized by the association of LIM and SH3 domains. FEBS Lett. 1995;373:245-249.
14. Chew CS, Chen X, Parente JA, Jr., et al. Lasp-1 binds to non-muscle F-actin in vitro and is localized within multiple sites of dynamic actin assembly in vivo. Journal of cell science. 2002;115:4787-4799.
15. Lin YH, Park ZY, Lin D, et al. Regulation of cell migration and survival by focal adhesion targeting of Lasp-1. J Cell Biol. 2004;165:421-432.
16. Schreiber V, Moog-Lutz C, Regnier CH, et al. Lasp-1, a novel type of actin-binding protein accumulating in cell membrane extensions. Mol Med. 1998;4:675-687.
17. Pintard L, Willis JH, Willems A, et al. The BTB protein MEL-26 is a substrate-specific adaptor of the CUL-3 ubiquitin-ligase. Nature. 2003;425:311-316.
18. Xu L, Wei Y, Reboul J, et al. BTB proteins are substrate-specific adaptors in an SCF-like modular ubiquitin ligase containing CUL-3. Nature. 2003;425:316-321.
19. Zhang DD, Lo SC, Sun Z, et al. Ubiquitination of Keap1, a BTB-Kelch substrate adaptor protein for Cul3, targets Keap1 for degradation by a proteasome-independent pathway. The Journal of biological chemistry. 2005;280:30091-30099.
20. Wilkinson DG. In situ hybridizations: A practical approach. Oxford University Press, USA. 1992.
21. Rozen S, Skaletsky H. Primer3 on the WWW for general users and for biologist programmers. Methods Mol Biol. 2000;132:365-386.
22. de Jonge HJ, Fehrmann RS, de Bont ES, et al. Evidence based selection of housekeeping genes. PLoS ONE. 2007;2:e898.
23. Dhume A, Lu S, Horowits R. Targeted disruption of N-RAP gene function by RNA interference: a role for N-RAP in myofibril organization. Cell Motil Cytoskeleton. 2006;63:493-511.
24. Martinez-Fernandez S, Hernandez-Torres F, Franco D, et al. Pitx2c overexpression promotes cell proliferation and arrests differentiation in myoblasts. Dev Dyn. 2006;235:2930-2939.
25. Sakiyama K, Abe S, Tamatsu Y, et al. Effects of stretching stress on the muscle contraction proteins of skeletal muscle myoblasts. Biomed Res. 2005;26:61-68.

26. Willems E, Mateizel I, Kemp C, et al. Selection of reference genes in mouse embryos and in differentiating human and mouse ES cells. Int J Dev Biol. 2006;50:627-635.
27. Sultan KR, Henkel B, Terlou M, et al. Quantification of hormone-induced atrophy of large myotubes from C2C12 and L6 cells: atrophy-inducible and atrophy-resistant C2C12 myotubes. Am J Physiol Cell Physiol. 2006;290:C650-659.
28. Vandesompele J, De Preter K, Pattyn F, et al. Accurate normalization of real-time quantitative RT-PCR data by geometric averaging of multiple internal control genes. Genome biology. 2002;3:RESEARCH0034.
29. Clark KA, McElhinny AS, Beckerle MC, et al. Striated muscle cytoarchitecture: an intricate web of form and function. Annu Rev Cell Dev Biol. 2002;18:637-706.
30. Kalcheim C, Ben-Yair R. Cell rearrangements during development of the somite and its derivatives. Curr Opin Genet Dev. 2005;15:371-380.
31. Ojima K, Lin ZX, Zhang ZQ, et al. Initiation and maturation of I-Z-I bodies in the growth tips of transfected myotubes. Journal of cell science. 1999;112:4101-4112.

Chapter 6

Summarizing discussion

Pluripotency - the potential to differentiate into derivatives of the three embryonic germ layers endoderm, ectoderm and mesoderm - is the main characteristic of embryonic stem (ES) cells. ES cells are derived from the inner cell mass (ICM) of a pre-implantation blastocyst and can self-renew indefinitely in culture. Because of their differentiation capabilities, ES cells can potentially be used in cell-based therapies in human medicine as well as for toxicology screening and drug testing. Moreover, ES cells can be used to study early differentiation events and developmental decisions [1]. As the pig is an important large-animal model in biomedical research [2] the first two studies presented in this thesis focused on the culture of pluripotent cells from pig blastocysts. As mentioned in the introduction, porcine stem cells can also be a potential source for *in vitro* meat, a possible alternative for conventional meat, produced from stem cells cultured and differentiated into muscle cells *in vitro*. Therefore, the subjects of the second part of this thesis address muscle development and differentiation.

Porcine early embryonic development

Remarkably, cell culture conditions that maintain ES cells in a pluripotent state differ between mouse and human [3-6], and pluripotent ES cell lines from species other than mice, rat, monkey and human have not been reported [7-12] Differences in early embryonic development between species are considered to underlie difficulties in deriving ES cell lines from different species [13]. In order to determine the optimal developmental stage for the generation of ES cell lines from porcine blastocysts, we have identified the expression pattern of key factors involved in pluripotency in porcine embryos between blastocyst formation and gastrulation (Chapter 2 of this thesis) We found that the expression pattern of important factors in pluripotency (OCT4, NANOG and SOX2) and in lineage segregation (CDX2, GATA4) in porcine blastocysts is to a certain extent similar to that of human and mouse embryos, but we also demonstrated some important species differences. We detected the expression of both NANOG and SOX2 restricted to the ICM and epiblast, while OCT4, as in human embryos, was also detected in the trophectoderm of early blastocysts. In mouse blastocysts, GATA6 and NANOG expression is complementary and heterogeneously distributed in the ICM cells and segregation of the primitive endoderm lineage is suggested to be dependent on expression of GATA factors and simultaneous NANOG down-regulation [14]. In mouse ES cells and ICMs from NANOG null embryos, loss of NANOG consistently results to a parietal endoderm-like fate of all cells [15]. In pigs however, NANOG is not expressed in early blastocysts (E5) while only some cells in the ICM express GATA6 [16]. This demonstrates that the start of primitive endoderm lineage segregation in pigs, in contrast to mice, is therefore not coupled to NANOG expression. At E8.5 all cells from the ICM expressed NANOG, and GATA4 staining revealed that primitive endoderm lineage segregation had taken place. Therefore although NANOG is not

critically important in initial primitive endoderm specification in pigs, NANOG expression does define the pluripotent cell population in late blastocyst-stage porcine embryos. In mice, trophectoderm lineage specification occurs through down-regulation of OCT4 with simultaneous up-regulation of CDX2. In pigs (as in man) OCT4 continues to be expressed in the trophectoderm after segregation of this lineage, although expression is less in the trophectoderm compared to the ICM. Consequently, down-regulation of OCT4, together with CDX2 expression, may be sufficient for trophectoderm lineage specification in this species. We have shown that in pigs, OCT4 protein expression is reduced in the trophectoderm around E9. In humans, restriction of OCT4 expression to the ICM coincides with a peak in efficiency of ES cell line derivation [17]. However, cultures of porcine ICM cells derived from embryos which still express OCT4 in the trophectoderm (E6.5-E8.5), resulted in a higher percentage of primary colonies with an ES-like morphology compared to primary epiblast cultures derived from embryos in which OCT4 expression in the trophectoderm was down-regulated. (E9.5-E10.5).
Although we were unable to maintain self-renewal of the cultured cells and therefore have not established porcine ES cell lines, the results do suggest that E6.5-8.5 would be the better source for derivation of such cell lines.

Culture of porcine pluripotent cells

In both human ES cells and mouse EpiSCs pluripotency and self-renewal are maintained by signalling through bFGF, ACTIVIN and NOGGIN-mediated inhibition of BMP-signalling while pluripotency in mouse ES cells is maintained by LIF-STAT3 and BMP-signalling. We have cultured porcine ICM and epiblast cells in medium supplemented with bFGF with or without ACTIVIN or NOGGIN and found that these conditions did not support undifferentiated self-renewal of porcine pluripotent cells (Chapter 2). This suggests that pluripotency and self-renewal of porcine pluripotent cells *in vitro* is maintained by signalling pathways that differ from those maintaining pluripotency in human ES and mouse EpiSCs. Regarding their response to bFGF, porcine ICM cells in culture resemble mouse ES cells as FGF signalling induces differentiation of mouse ES cells [18]. However, porcine ICM cells do not respond to LIF [19].
While methods to culture human and mouse ES cells have proven inefficient for obtaining porcine ES cells, new insights into pathways and factors involved in self-renewal of pluripotent cells provide prospects for the derivation of porcine ES cells. For example, in mouse and rat ES cells it was found that inhibition of autoinductive phospho-ERK signaling and GSK3 signaling using small-molecule inhibitors suppresses differentiation [11, 12, 20]. Therefore, it is argued that ES cells have an innate self-renewal program which is destabilized by autoinductive phospho-ERK signaling,

causing differentiation [21]. However, to this date there are no reports on the culture of human ES cells using similar conditions. Although preliminary results show that inhibition of GSK3 using the selective small molecule inhibitor AR-A014418 does not have a positive effect on the self-renewal of primary ICM cells in culture, it would be of interest to further examine whether targeting the ERK and GSK3 pathways of porcine ICM or epiblast cells can give rise to pluripotent cell lines.

Another possible route to the generation of porcine pluripotent stem cells lines is via *induced* pluripotency. Nuclei from differentiated cells can be reprogrammed to a pluripotent state by transfer of these nuclei into enucleated oocytes (somatic cell nuclear transfer) [22, 23]. Also, fusion of somatic cells with ES cells can reprogram the nuclei of these somatic cells to an embryonic-like state [24]. Via these methods patient-derived pluripotent cells with a potential use in cellular therapies can be obtained. However, derivation of human oocytes requires a medically invasive procedure that is rather aggravating for the patient, and both derivation and use of oocytes is subject to legal and ethical limitations. Fusion of somatic cells with already established ES cell lines is less controversial but results in tetraploid DNA content. A major breakthrough was achieved in 2006 when screening of candidate factors resulted in the identification of four transcription factors (SOX2, OCT4, C-MYC and KLF4) which, when over-expressed in mouse somatic cells and using ES cell culture conditions, can reprogram these cells into (induced) pluripotent stem (iPS) cells [25]. One year later, germline-competent mouse iPS cells were derived through selection for NANOG expression and the generation of human iPS cells was achieved [26, 27]. Several groups have reprogrammed porcine somatic cells to a pluripotent state. Importantly however, knock-down of the exogenous expressed transcription factors in porcine iPS cells leads to differentiation [28-30]. This demonstrates that the specific culture conditions used were unable to ensure the pluripotent status of porcine iPS. Nonetheless, porcine iPS cells, and especially those generated using drug-inducible factors, form an excellent tool for testing culture conditions on their ability to maintain pluripotency and self-renewal.

ICM cells as a source of progenitors.

Although porcine ICM cells loose their capacity to remain pluripotent while cultured *in vitro* under the conditions that we have used, progenitor cells can be isolated from this differentiated population of cultured ICM/epiblast cells. In chapter 3 of this thesis we report on the generation of proliferating neural cells from cultured porcine ICM cells and the differentiation of these neural cells into astrocytes and oligodendrocytes *in vitro*. Differentiated cells derived from human ES cells can potentially serve as a cell source for cell transplantation therapies in regenerative medicine. Using these therapies, functions lost by cell death or malfunction of a particular cell-type can possibly be restored. Although human ES cell lines have been derived more than a

decade ago, successful regeneration therapies using ES cells have not been performed in humans, partly due to a lack of proper animal model systems. A serious danger of the use of ES cells in cell replacement therapies is the risk of donor-derived tumor development from these cells. Therefore, it is important to test the safety of these therapies in large animal models such as the pig, which have a life span, physiology, immunology and organ size that is more comparable to humans than to mice. The results described in chapter 3 on the derivation of neural cells from porcine ICM cells may facilitate the use of pigs in studying the safety of neural precursor-based cell replacement therapies in human medicine.

Cazip, characterization of a novel gene possibly involved in muscle differentiation

The main subject of the second part of this thesis is cellular differentiation. For the generation of vitro meat, stem cells need to differentiate *in vitro* into the skeletal muscle lineage. Because gene products involved in the formation of a certain lineage *in vivo* are often also import in the differentiation of stem cells to this lineage *in vitro*, we focused on the identification and characterization of genes involved in muscle differentiation.

In chapter 4 we discuss the initial characterization of a novel gene possibly involved in muscle differentiation, which we named Cazip. Cazip was previously identified through whole genome micro-array analysis on human embryonic stem cells (hESC) differentiating towards cardiomyocytes [31]. Studying the predicted amino acid sequence revealed that CAZIP contains a leucine-zipper domain at the C-terminus, hence the name CAZIP (cardiac zipper protein). We identified two isoforms of mouse CAZIP by database analysis, which we named CAZIPa (358 amino acids) and CAZIPb (1354 amino acids). Using RT-PCR, we examined the expression of these isoforms in adult mouse tissues and demonstrated that these isoforms are differentially expressed in the heart and brain of mice. *CazipA* is highly expressed in brain and eye tissue and at a far lower level in the embryonic and adult heart, while the opposite expression pattern was found for *CazipB*. Whole mount *in situ* hybridization on staged mouse and chick embryos confirmed a possible role for CAZIP in cardiac and brain tissue as *Cazip* expression was detected in the developing heart and nervous system in both species. *Cazip* expression was not detected in the somites or in adult skeletal muscle tissue, suggesting a specific role for CAZIP in cardiac muscle but not in skeletal muscle. *Cazip* is also expressed in the developing limb; an expression pattern in both the developing heart and the developing limbs is not uncommon as the developmental pathways of heart and limb use some of the same signaling pathways and downstream elements [32-37]. However, these signaling pathways have diverse functions during development; it is therefore unlikely that expression in both heart and limb is merely the result from activation through common regulatory pathways. In this respect, it has

been suggested that cells migrating to the limb and heart field originate from a common pool of progenitor cells [38, 39].

Ectopically expressed CAZIPb protein in COS-1 cells localizes in the cytoplasm, in peri-nuclear and sub-nuclear bodies, and in unidentified cytosolic structures. CAZIPb expression in sub-nuclear bodies may be associated with RNA processing and regulation of transcription [40, 41]. Perhaps CAZIP interacts with transcription factors through the protein interaction leucine-zipper domain, and renders these transcription factors inactive by sequestering them to sub-nuclear sites. Studies on endogenous CAZIPa and CAZIPb expression in cardiomyocytes and neural cells will provide more information on the localization of CAZIP in these cells. Collectively, our findings suggest a role for CAZIP in development and function of the heart and nervous system in vertebrates. There are multiple options for future studies into the functional role of CAZIP. Over-expression and knock-down studies of CAZIP in cardiomyocytes and neural cells *in vitro* can provide information on the cellular role of CAZIP in these cells and identification of binding partners of CAZIP using immunoprecipitation and mass spectrometry can give insight into regulatory pathways in which CAZIP may be involved. To study the role of CAZIP during development, zebrafish can be used as a model system. The zebrafish ortolog of CAZIP is predicted by the NCBI database (XP_684038.3) and temporary knock-down of genes during zebrafish development can be achieved by morpholino-injection into the 1 cell stage embryo [42]. This knock-down can last up to 50 hours post-fertilization and this time period includes the fundamental vertebrate processes of organogenesis [43-45]. Finally, the generation of CAZIP knockout mice or transgenic over-expression will give insight into the *in vivo* role of CAZIP in the heart and nervous system.

SARCOSIN and its functional role in skeletal muscle differentiation

SARCOSIN was originally identified and described to be exclusively expressed in striated muscle tissue, and in cultures of primary cardiomyocytes SARCOSIN is reported to be involved in the late myofibril assembly of the sarcomeres [46, 47]. However, its function in skeletal muscle development and differentiation remains unknown. We investigated the functional role of SARCOSIN in skeletal muscle differentiation and its expression during embryonic development and in adult muscle tissue (chapter 5). Using whole-mount *in situ* hybridization, we demonstrated that *Sarcosin* mRNA was expressed in the myotome part of mature somites in mouse embryos from embryonic day 9.5 onwards. Surprisingly, *Sarcosin* expression was not detected in the embryonic heart, while at the embryonic stages examined the heart is contracting and thus contains functional sarcomeres. SARCOSIN protein was observed between and below laterally fusing myofibrils in adult skeletal muscle tissue suggesting a role for SARCOSIN in sarcomere assembly. In the skeletal myoblast cell

line C2C12, SARCOSIN was readily expressed in proliferating myoblasts and highly up-regulated during differentiation. By RNA interference mediated knock-down of SARCOSIN in the C2C12 myoblast cell line we were able to study the functional role of SARCOSIN in skeletal myoblast differentiation. SARCOSIN knock-down did not affect myoblast fusion and myotube formation, and no obvious effect on myofibrillogenesis was observed. However, SARCOSIN knock-down accelerated differentiation as α-ACTININ, MYOSIN and MYOGENIN protein levels were increased at day 2 of differentiation in C2C12 cells in which SARCOSIN expression was down-regulated. SARCOSIN has been described to be associated with the Cul3-Rbx E3 ubiquitin ligase complex [48]. Possibly SARCOSIN plays a role in targeting proteins for degradation and thereby delays the onset of differentiation. As mentioned for CAZIP, *in vivo* studies in zebrafish or mice in which SARCOSIN is either over-expressed or expression is downregulated will help to understand SARCOSINs role in skeletal muscle development and differentiation.

Concluding remarks and perspectives

It took over 17 years to generate ES cell lines from human blastocysts since the derivation of the first mouse ES cell line in 1981. While early embryology of mice and rats is highly similar mouse ES cell culture conditions do not yield ES cells from rat, and germline competent rat ES cells were just recently derived using small molecule inhibitors. It is therefore perhaps not surprising that we were unable to generate true ES cell lines from the pig using conventional procedures. However, by examining the temporal and spatial expression pattern in porcine embryos of factors important in mouse pluripotency, and through exclusion of culture conditions, the results reported in this thesis will benefit future research into the generation of ES cell lines from the pig. Although porcine ICM cells differentiate in culture, these differentiated cells may still be used to provide progenitor cells. The results on the generation of neural progenitor cells from cultured porcine ICM cells can be of use when testing the safety of neural progenitor-transplantation in human medicine.

Characterization of genes such as Cazip and investigating the functional role of proteins such as SARCOSIN, which are involved in muscle development and differentiation, is important for the development of therapeutics in muscle disease. Also for the production of in vitro meat, knowledge on muscle differentiation is essential. The generation of *in vitro* meat is not a new idea; in 1932 Winston Churchill argued that: ‘Fifty years hence we shall escape the absurdity of growing a whole chicken in order to eat the breast or wing by growing these parts separately under a suitable medium’ [49]. Suffice to say that this claim was somewhat overconfident and more fundamental research is necessary to achieve the production of cultured meat.

References

1. Wobus AM, Boheler KR. Embryonic stem cells: prospects for developmental biology and cell therapy. Physiol Rev. Apr 2005;85(2):635-678.

2. Matsunari H, Nagashima H. Application of genetically modified and cloned pigs in translational research. J Reprod Dev. Jun 2009;55(3):225-230.

3. Wang G, Zhang H, Zhao Y, et al. Noggin and bFGF cooperate to maintain the pluripotency of human embryonic stem cells in the absence of feeder layers. Biochem Biophys Res Commun. May 13 2005;330(3):934-942.

4. Williams RL, Hilton DJ, Pease S, et al. Myeloid leukaemia inhibitory factor maintains the developmental potential of embryonic stem cells. Nature. Dec 15 1988;336(6200):684-687.

5. Xiao L, Yuan X, Sharkis SJ. Activin A maintains self-renewal and regulates fibroblast growth factor, Wnt, and bone morphogenic protein pathways in human embryonic stem cells. Stem Cells. Jun 2006;24(6):1476-1486.

6. Xu RH, Peck RM, Li DS, Feng X, Ludwig T, Thomson JA. Basic FGF and suppression of BMP signaling sustain undifferentiated proliferation of human ES cells. Nat Methods. Mar 2005;2(3):185-190.

7. Evans MJ, Kaufman MH. Establishment in culture of pluripotential cells from mouse embryos. Nature. Jul 9 1981;292(5819):154-156.

8. Martin GR. Isolation of a pluripotent cell line from early mouse embryos cultured in medium conditioned by teratocarcinoma stem cells. Proc Natl Acad Sci U S A. Dec 1981;78(12):7634-7638.

9. Thomson JA, Itskovitz-Eldor J, Shapiro SS, et al. Embryonic stem cell lines derived from human blastocysts. Science. Nov 6 1998;282(5391):1145-1147.

10. Thomson JA, Kalishman J, Golos TG, et al. Isolation of a primate embryonic stem cell line. Proc Natl Acad Sci U S A. Aug 15 1995;92(17):7844-7848.

11. Buehr M, Meek S, Blair K, et al. Capture of authentic embryonic stem cells from rat blastocysts. Cell. Dec 26 2008;135(7):1287-1298.

12. Li P, Tong C, Mehrian-Shai R, et al. Germline competent embryonic stem cells derived from rat blastocysts. Cell. Dec 26 2008;135(7):1299-1310.

13. Keefer CL, Pant D, Blomberg L, Talbot NC. Challenges and prospects for the establishment of embryonic stem cell lines of domesticated ungulates. Anim Reprod Sci. Mar 2007;98(1-2):147-168.

14. Chazaud C, Yamanaka Y, Pawson T, Rossant J. Early lineage segregation between epiblast and primitive endoderm in mouse blastocysts through the Grb2-MAPK pathway. Dev Cell. May 2006;10(5):615-624.

15. Mitsui K, Tokuzawa Y, Itoh H, et al. The homeoprotein Nanog is required for maintenance of pluripotency in mouse epiblast and ES cells. Cell. May 30 2003;113(5):631-642.

16. Kuijk EW, Du Puy L, Van Tol HT, et al. Differences in early lineage segregation between mammals. Dev Dyn. Apr 2008;237(4):918-927.

17. Chen AE, Egli D, Niakan K, et al. Optimal timing of inner cell mass isolation increases the efficiency of human embryonic stem cell derivation and allows generation of sibling cell lines. Cell Stem Cell. Feb 6 2009;4(2):103-106.

18. Kunath T, Saba-El-Leil MK, Almousailleakh M, Wray J, Meloche S, Smith A. FGF stimulation of the Erk1/2 signalling cascade triggers transition of pluripotent embryonic stem cells from self-renewal to lineage commitment. Development. Aug 2007;134(16):2895-2902.

19. Wianny F, Perreau C, Hochereau de Reviers MT. Proliferation and differentiation of porcine inner cell mass and epiblast in vitro. Biol Reprod. Oct 1997;57(4):756-764.

20. Ying QL, Wray J, Nichols J, et al. The ground state of embryonic stem cell self-renewal. Nature. May 22 2008;453(7194):519-523.

21. Silva J, Smith A. Capturing pluripotency. Cell. Feb 22 2008;132(4):532-536.

22. Hochedlinger K, Jaenisch R. Monoclonal mice generated by nuclear transfer from mature B and T donor cells. Nature. Feb 28 2002;415(6875):1035-1038.

23. Wilmut I, Schnieke AE, McWhir J, Kind AJ, Campbell KH. Viable offspring derived from fetal and adult mammalian cells. Nature. Feb 27 1997;385(6619):810-813.

24. Cowan CA, Atienza J, Melton DA, Eggan K. Nuclear reprogramming of somatic cells after fusion with human embryonic stem cells. Science. Aug 26 2005;309(5739):1369-1373.

25. Takahashi K, Yamanaka S. Induction of pluripotent stem cells from mouse embryonic and adult fibroblast cultures by defined factors. Cell. Aug 25 2006;126(4):663-676.

26. Takahashi K, Tanabe K, Ohnuki M, et al. Induction of pluripotent stem cells from adult human fibroblasts by defined factors. Cell. Nov 30 2007;131(5):861-872.

27. Okita K, Ichisaka T, Yamanaka S. Generation of germline-competent induced pluripotent stem cells. Nature. Jul 19 2007;448(7151):313-317.

28. Esteban MA, Xu J, Yang J, et al. Generation of induced pluripotent stem cell lines from tibetan miniature pig. J Biol Chem. June 26 2009;284(26):17634-17640.

29. Ezashi T, Telugu BP, Alexenko AP, Sachdev S, Sinha S, Roberts RM. Derivation of induced pluripotent stem cells from pig somatic cells. Proc Natl Acad Sci U S A. Jul 7 2009;106(27):10993-10998.

30. Wu Z, Chen J, Ren J, et al. Generation of Pig-Induced Pluripotent Stem Cells with a Drug-Inducible System. J Mol Cell Biol. Jun 3 2009;Published ahead of print.

31. Beqqali A, Kloots J, Ward-van Oostwaard D, Mummery C, Passier R. Genome-wide transcriptional profiling of human embryonic stem cells differentiating to cardiomyocytes. Stem Cells. Aug 2006;24(8):1956-1967.

32. Abu-Issa R, Smyth G, Smoak I, Yamamura K, Meyers EN. Fgf8 is required for pharyngeal arch and cardiovascular development in the mouse. Development. Oct 2002;129(19):4613-4625.

33. Crossley PH, Minowada G, MacArthur CA, Martin GR. Roles for FGF8 in the induction, initiation, and maintenance of chick limb development. Cell. Jan 12 1996;84(1):127-136.

34. Zhu J, Nakamura E, Nguyen MT, Bao X, Akiyama H, Mackem S. Uncoupling Sonic hedgehog control of pattern and expansion of the developing limb bud. Dev Cell. Apr 2008;14(4):624-632.

35. Washington Smoak I, Byrd NA, Abu-Issa R, et al. Sonic hedgehog is required for cardiac outflow tract and neural crest cell development. Dev Biol. Jul 15 2005;283(2):357-372.

36. Mesbah K, Harrelson Z, Theveniau-Ruissy M, Papaioannou VE, Kelly RG. Tbx3 is required for outflow tract development. Circ Res. Sep 26 2008;103(7):743-750.

37. Gibson-Brown JJ, Agulnik SI, Silver LM, Niswander L, Papaioannou VE. Involvement of T-box genes Tbx2-Tbx5 in vertebrate limb specification and development. Development. Jul 1998;125(13):2499-2509.

38. Ahn DG, Kourakis MJ, Rohde LA, Silver LM, Ho RK. T-box gene tbx5 is essential for formation of the pectoral limb bud. Nature. Jun 13 2002;417(6890):754-758.

39. Wilson GN. Correlated heart/limb anomalies in Mendelian syndromes provide evidence for a cardiomelic developmental field. Am J Med Genet. Apr 1 1998;76(4):297-305.

40. Dundr M, Misteli T. Functional architecture in the cell nucleus. Biochem J. Jun 1 2001;356(Pt 2):297-310.

41. Cioce M, Lamond AI. Cajal bodies: a long history of discovery. Annu Rev Cell Dev Biol. 2005;21:105-131.

42. Bill BR, Petzold AM, Clark KJ, Schimmenti LA, Ekker SC. A primer for morpholino use in zebrafish. Zebrafish. Mar 2009;6(1):69-77.

43. Ekker SC. Morphants: a new systematic vertebrate functional genomics approach. Yeast. Dec 2000;17(4):302-306.
44. Lowery LA, Sive H. Initial formation of zebrafish brain ventricles occurs independently of circulation and requires the nagie oko and snakehead/atp1a1a.1 gene products. Development. May 2005;132(9):2057-2067.
45. Stainier DY. Zebrafish genetics and vertebrate heart formation. Nat Rev Genet. Jan 2001;2(1):39-48.
46. Taylor A, Obholz K, Linden G, Sadiev S, Klaus S, Carlson KD. DNA sequence and muscle-specific expression of human sarcosin transcripts. Mol Cell Biochem. Jun 1998;183(1-2):105-112.
47. Greenberg CC, Connelly PS, Daniels MP, Horowits R. Krp1 (Sarcosin) promotes lateral fusion of myofibril assembly intermediates in cultured mouse cardiomyocytes. Exp Cell Res. Mar 10 2008;314(5):1177-1191.
48. Zhang DD, Lo SC, Sun Z, Habib GM, Lieberman MW, Hannink M. Ubiquitination of Keap1, a BTB-Kelch substrate adaptor protein for Cul3, targets Keap1 for degradation by a proteasome-independent pathway. J Biol Chem. Aug 26 2005;280(34):30091-30099.
49. Churchill W. Fifty years hence. In thoughts and adventures. London: Thorton Butterworth. 1932:24-27.

Chapter 7

Summary in Dutch

Inleiding

Embryonale stamcellen (ES cellen) van zoogdieren zijn in staat om in elk celtype te specialiseren (differentiëren); ze zijn 'pluripotent'. ES cellen worden gegenereerd van een klompje cellen, de 'inner cell mass', welke geïsoleerd wordt uit preïmplantatie-embryo's. Deze cellen kunnen *in vitro* worden gekweekt en eenmaal in kweek genomen kunnen ze onder gecontroleerde omstandigheden onbeperkt blijven delen, ze vertonen self-renewal. ES zijn bijzonder nuttig voor biomedisch onderzoek en mogelijk kunnen deze cellen zelfs gebruikt worden voor therapeutische doeleinden in de humane en diergeneeskunde. Men hoopt humane ES cellen in de toekomst in te zetten om zieke of beschadigde weefsels te vervangen. Onderzoek naar ES cellen en de differentiatie van deze cellen kan ook licht werpen op vroeg embryonale ontwikkeling en de ontwikkeling van specifieke weefseltypes. Bovendien kunnen ES cellen gebruikt worden voor toxicologisch onderzoek en ontwikkeling van nieuwe medicijnen. Omdat het varken wat betreft fysiologie, orgaangrootte en levensduur overeenkomt met de mens, is het varken een belangrijk diermodel in de biomedische wetenschap. ES cellen van het varken zouden dus gebruikt kunnen worden om celtherapieën te testen. Maar hoewel verscheidene pogingen tot het genereren van ES cellen van het varken zijn gerapporteerd, zijn varkens-ES cellijnen welke onbeperkt blijven delen terwijl ze hun pluripotentie behouden nog niet beschreven. Het praktische werk beschreven in de **hoofdstukken 2 en 3** van dit proefschrift richt zich op de *in vivo* ontwikkeling en de *in vitro* kweek van pluripotente cellen van het varken. Varkens-stamcellen kunnen in theorie ook gebruikt worden als bron voor het produceren van in vitro vlees. *In vitro* gekweekte stamcellen die zijn gedifferentieerd naar spiercellen kunnen een alternatief zijn voor conventionele vleesproducten. Om meer inzichten te verkrijgen in de mechanismen verantwoordelijk voor differentiatie van spiercellen worden daarom in de **hoofdstukken 4 en 5** verschillende genen bestudeerd die van invloed kunnen zijn op spierontwikkeling en differentiatie.

Embryonale ontwikkeling van het varken

Pluripotente ES cellijnen van andere soorten dan muis, rat, rhesusaap en de mens zijn nog niet beschreven. Omdat de kweekcondities waaronder ES cellen van muis en mens ongedifferentieerd blijven delen verschillen, is het te verwachten dat deze condities van groot belang zijn voor de derivatie van ES cellen van andere diersoorten.. Verschillen in de vroeg-embryonale ontwikkeling tussen diersoorten zijn mogelijk van invloed op de derivatie van ES cellijnen van deze dieren. Terwijl embryo's van de muis en mens bij voorbeeld invasief implanteren in de baarmoederwand, ondergaat het trofectoderm (de cellen die later de extra-embryonale structuren vormen) van varkensembryo's een elongatie gevolgd door non-invasieve implantatie van het embryo. Op moleculair celbiologisch niveau zijn verschillende genen geïdentificeerd welke van invloed zijn op

de pluripotentie (Nanog, Oct4, Sox2) en cellulaire differentiatie (Cdx2, Gata4/6) bij embryo's van muizen. Om het optimale embryonale stadium te bepalen voor derivatie van ES cellen van het varken, zijn de expressiepatronen van deze genen gedurende de vroeg embryonale ontwikkeling [embryonale dag (E)6.5-E10.5] bestudeerd en vergeleken met de expressiepatronen in embryo's van muis en mens (**hoofdstuk 2** van dit proefschrift). Expressie van zowel NANOG als SOX2 werd gedetecteerd in de ICM en epiblast van varkensembryo's. Scheiding van het primitief endoderm van de ICM in blastocysten van muizen is afhankelijk van de expressie van GATA transcriptiefactoren in combinatie met een verminderde expressie van NANOG. Gedurende het vroege blastocystenstadium (E5.5) van het varken komt NANOG niet tot expressie, terwijl sommige cellen van de ICM wel GATA6 tot expressie brengen. Dit laat zien dat in eerste instantie de scheiding van primitief endoderm bij het varken niet afhankelijk is van NANOG, in tegenstelling tot bij de muis. Immunofluorescentie studies die in dit proefschrift zijn gerapporteerd tonen aan dat op E8.5 in het varken alle ICM cellen NANOG tot expressie brengen en dat in dit ontwikkelingsstadium de scheiding van primitief endoderm en ICM compleet is. Dus door middel van NANOG detectie kan de pluripotente celpopulatie in het varken worden geïdentificeerd. Immunofluorescentie studies laten ook zien dat OCT4-expressie in het trofectoderm van het varken vermindert rond E9. Embryo's waarvan de expressie van OCT4 beperkt is tot cellen van de ICM blijken het meest efficiënt voor de derivatie van humane ES cellijnen. Op basis van deze resultaten zou men verwachten dat varkensembryo's van E9 en E10.5 het meest geschikt zijn voor derivatie van ES cellen. Celkweken van embryo's van verschillende ontwikkelingsstadia laten echter zien dat juist ICM cellen van E6.5-E8.5 vaker primaire kolonies met een ES cel morfologie en genexpressie vormden dan E9.5-E10.5 embryo's. Hoewel we deze celkweken niet ongedifferentieerd konden houden lijkt het erop dat embryo's van E6.5-E8.5 meer geschikt zijn voor de generatie van ES cellijnen van het varken.

Celkweek van pluripotente varkenscellen

Zowel in humane ES cellen als cellijnen van de epiblast van muizenembryo's wordt 'self-renewal' activiteit behouden door signalering van de groeifactoren basic FGF en ACTIVINE en inhibitie van BMP signalering door NOGGIN. Pluripotentie van muizen-ES cellen wordt echter gereguleerd door BMP en LIF-STAT3 signalering. Wij hebben ICM en epiblast cellen van varkensembryo's gekweekt in medium waar de groeifactor bFGF al dan niet in combinatie met ACTIVINE of NOGGIN aan was toegevoegd. Deze kweekcondities bleken echter niet voldoende om onbeperkte deling van pluripotente ICM- en epiblastcellen te ondersteunen (**hoofdstuk 2**). Dit suggereert dat pluripotentie en 'self-renewal' van varkenscellen *in vitro* wordt onderhouden door signaalwegen die verschillen van de handhaving van pluripotentie in humane ES cellen

en muizen epiblast-stamcellen. Wat FGF signalering betreft lijken varkens ICM-cellen in kweek nog het meest op muizen ES cellen, waarin FGF signalering namelijk differentiatie induceert. In tegenstelling tot muizen ES cellen reageren varkens ICM cellen echter niet op LIF.
Hoewel de pluripotente varkenscellen *in vitro* differentiëren onder de kweekcondities die wij hebben gebruikt kunnen voorlopercellen worden geïsoleerd uit deze gedifferentieerde populatie van gekweekte ICM/epiblast cellen. In **hoofdstuk 3** van dit proefschrift beschrijven we de isolatie van prolifererende neurale cellen van varkens ICM cellen en de differentiatie van deze neurale cellen naar astrocyten en oligodendrocyten *in vitro*. Gedifferentieerde cellen afkomstig van humane ES cellen kunnen in principe dienen als bron voor stamceltransplantatie in de regeneratieve geneeskunde. Met behulp van deze therapieën kunnen functies - welke zijn verloren door celdood of slecht functioneren van een bepaald celtype - mogelijk worden hersteld. Hoewel de eerste humane ES cellijnen in 1998 zijn beschreven, zijn er nog geen succesvolle celtherapieën uitgevoerd bij de mens. Dit is deels te wijten aan het gebrek aan een geschikt diermodel. Een ernstig gevaar van het gebruik van ES-cellen in transplantatie-experimenten is het risico van tumorontwikkeling door deze getransplanteerde cellen. Daarom is het belangrijk om de veiligheid van deze therapieën in grote diermodellen die een levensduur, fysiologie, en immunologie hebben die vergelijkbaar zijn met die van de mens, zoals bijvoorbeeld het varken, te testen. De resultaten beschreven in **hoofdstuk 3** over de derivatie van neurale voorlopercellen van varkens ICM cellen kunnen het bestuderen van de veiligheid van celregeneratie in de menselijke geneeskunde vergemakkelijken.

CAZIP, karakterisering van een nieuw genproduct mogelijk betrokken bij de differentiatie van spieren

Het onderwerp van het tweede deel van dit proefschrift is cellulaire differentiatie. Voor de generatie van in vitro vlees moeten stamcellen efficiënt differentiëren tot skeletspiercellen. Omdat genproducten die betrokken zijn bij de vorming van een bepaald celtype/weefsel *in vivo* ook vaak betrokken zijn bij de *in vitro* differentiatie van een bepaald celtype, hebben we ons gericht op de identificatie en karakterisering van genen die betrokken zijn in de spierdifferentiatie.

In **hoofdstuk 4** bespreken we de initiële karakterisering van een nieuw gen dat mogelijk betrokken is bij spierdifferentiatie, door ons Cazip genoemd. Cazip is in eerste instantie door middel van micro-array analyse op humane ES cellen die differentiëren naar cardiomyocyten geïdentificeerd als mogelijk betrokken bij spierdifferentiatie. Bij het bestuderen van de voorspelde aminozuursequentie bleek dat CAZIP een ‘leucine zipper’ domein bevat aan de C-terminus, vandaar de naam CAZIP (‘cardiac zipper protein’). Door middel van database-analyse hebben we twee

isovormen van CAZIP gevonden in muizencellen, die we de naam CAZIPa (358 aminozuren) en CAZIPb (1354 aminozuren) hebben gegeven. Met behulp van RT-PCR onderzochten we de expressie van deze isovormen in weefsels van volwassen muizen en we hebben aangetoond dat deze isovormen differentieel tot expressie komen in het hart en de hersenen van muizen. CazipA komt hoog tot expressie in neurale weefsels en op een veel lager niveau in het embryonale en volwassen hart, terwijl het tegenovergestelde expressiepatroon werd gevonden voor CazipB. 'Whole mount in situ hybridisatie' studies op embryo's van de muis en de kip bevestigden een mogelijke rol voor CAZIP in hart-en hersenweefsel. Cazip-expressie werd niet gedetecteerd in de somieten of in volwassen skeletspierweefsel, wat duidt op een specifieke rol voor CAZIP in de hartspier, maar niet in skeletspieren. Overexpressie van CAZIPb eiwit in COS-1 cellen toonde aan dat CAZIPb gelokaliseerd is in het cytoplasma, in de peri-nucleaire en sub-nucleaire structuren, en in niet nader geïdentificeerde structuren in het cytosol. De sub-nucleaire lokalisatie van CAZIPb kan worden geassocieerd met RNA-verwerking en de regulatie van transcriptie. Onze bevindingen suggereren een rol voor CAZIP in de ontwikkeling en functie van het hart en zenuwstelsel bij gewervelde dieren. Toekomstige over-expressie en 'knock-down' studies van CAZIP in cardiomyocyten en neurale cellen kunnen informatie verschaffen over de rol van CAZIP in deze cellen. Identificatie van bindingspartners van CAZIP door middel van immunoprecipitatie en massaspectrometrie kan inzicht geven in de cellulaire processen waarbij CAZIP is betrokken. Tenslotte zal de generatie van CAZIP knockout-muizen of muizen waarin CAZIP tot overexpressie is gebracht inzicht kunnen geven in de rol van CAZIP in het hart en zenuwstelsel.

De rol van SARCOSIN in skeletspierdifferentiatie

SARCOSIN is oorspronkelijk beschreven als een eiwit dat uitsluitend tot expressie komt in dwarsgestreept spierweefsel en mogelijk betrokken is bij de fusie van myofibrillen van sarcomeren. Toch blijft de functie van SARCOSIN in skeletspierontwikkeling en differentiatie onbekend. We onderzochten de expressie van SARCOSIN tijdens de embryonale ontwikkeling en in volwassen spierweefsel, en de rol van SARCOSIN in skeletspierdifferentiatie (**hoofdstuk 5**). Met behulp van 'whole mount in situ hybridisatie' toonden we aan dat Sarcosin mRNA tot expressie komt in het myotoom van somieten in muizenembryo's vanaf E9,5. Verrassend genoeg werd Sarcosin mRNA niet gedetecteerd in het embryonale hart, terwijl in dit ontwikkelingsstadium het reeds functionele sarcomeren bevat. In volwassen skeletspierweefsel werd SARCOSIN eiwit waargenomen tussen en onder lateraal fuserende myofibrillen, hetgeen wijst op een rol voor SARCOSIN in fusie van myofibrillen. Door RNA-interferentie gemedieerde 'knock-down' van SARCOSIN in de C2C12 myoblast-cellijn waren we in staat om de functionele rol van SARCOSIN in

myoblastdifferentiatie te bestuderen. SARCOSIN komt tot expressie in delende myoblasten en wordt sterk opgereguleerd tijdens de differentiatie. SARCOSIN 'knock-down' had geen invloed op myoblastfusie en vorming van 'myotubes' en er werd geen duidelijk effect op de vorming van myofibrillen waargenomen. In C2C12 cellen, waarin expressie van SARCOSIN was verminderd, was de eiwitexpressie van α-ACTININ, myosine en MYOGENINE verhoogd op dag 2 van differentiatie. Dit suggereert dat een vermindering van SARCOSIN expressie de differentiatie versnelt. Het is beschreven dat SARCOSIN word geassocieerd met het Cul3-RBX E3 ubiquitine ligase complex. Mogelijk speelt SARCOSIN een rol bij de bestemming van eiwitten voor de afbraak en vertraagt daardoor de start van differentiatie. Zoals vermeld voor CAZIP zullen *in vivo* studies bij muizen waarin SARCOSIN wordt uitgeschakeld of tot overexpressie wordt gebracht helpen om de rol van SARCOSIN in de skeletspierontwikkeling en -differentiatie te begrijpen.

Slotopmerkingen en perspectieven

Na de derivatie van de eerste muizen ES cellijnen in 1981 duurde het meer dan 17 jaar totdat ES cellijnen van humane blastocysten werden geïsoleerd. Terwijl de vroege embryologie van muizen en ratten zeer vergelijkbaar is, ondersteunen de kweekcondities onder welke muizen ES cellen onbeperkt blijven delen niet de derivatie van ES cellijnen van rattenembryo's. Pas onlangs werden ES cellijnen van de rat ontwikkeld met behulp van kleine molecuul-remmers. Het is daarom misschien niet verwonderlijk dat wij en andere onderzoekers niet in staat waren om pluripotente cellen van het varken in kweek te houden. Het onderzoek beschreven in dit proefschrift naar diverse kweekomstandigheden en naar de expressie van genen in varkensembryo's die een rol spelen in pluripotentie bij de muis draagt echter bij tot de uiteindelijke ontwikkeling van ES cellijnen van het varken.

Karakterisering van genen zoals Cazip en het onderzoek naar de functionele rol van eiwitten zoals SARCOSIN, die betrokken zijn bij spierontwikkeling en -differentiatie, is belangrijk voor de ontwikkeling van therapieën voor de spierziektes. Ook voor de productie van in vitro vlees is kennis op het gebied van spierdifferentiatie essentieel. De generatie van in vitro vlees is geen nieuw idee, in 1932 stelde Winston Churchill al dat het absurd was om hele kippen te houden wanneer je ook de kippenboutjes apart zou kunnen kweken, en dat men binnen 50 jaar slechts delen van kippen zou kweken voor voedselproductie. Het volstaat te zeggen dat deze bewering enigszins overmoedig was en meer fundamenteel onderzoek nodig is om de productie van gekweekt vlees te bereiken.

Acknowledgements

Graag wil ik iedereen bedanken die, ieder op zijn/haar eigen manier, een bijdrage heeft geleverd aan de totstandkoming van dit proefschrift. Enkelen wil ik met name noemen:

Allereerst mijn promotores Henk Haagsman en Ben Colenbrander voor de begeleiding en inzet tijdens de afgelopen jaren. Bedankt voor het vertrouwen dat jullie mij geschonken hebben. Bernard Roelen, mijn co-promotor en praktische begeleider: ik heb heel veel van je geleerd en heb veel bewondering voor hoe jij je inzet voor je AIO's en de wetenschap. Ik wil je bedanken voor de werkelijk fantastische begeleiding, ook tijdens de voor mij wat moeilijkere uurtjes. Ik had me geen betere begeleider kunnen wensen.

Christine Mummery, dank dat ik op je lab mocht werken. De periode bij je groep heeft mijn onderzoek een belangrijke impuls gegeven. Robert Passier, ook van jou heb ik veel mogen leren; ik ben blij dat we ons onderzoek naar Cazip hebben kunnen publiceren. Iedereen daar op het lab, Appie en Jantine in het bijzonder, bedankt voor alle hulp en adviezen.

Susana, je enthousiasme is aanstekelijk en je 'drive' heeft me geholpen het beste uit onze kweek-experimenten te halen. Je hebt menig uurtje met mij in het celkweeklab doorgebracht; ik waardeer je inzet enorm.

Alle (oud-)collega's van Diergeneeskunde, maar ook daarbuiten: Ewart, Leni, Eric, Christine, Elly, Jurriaan, Ineke, Arend, Mabel, Edita, Jeffrey, Hilde, Karin, Damien, Marleen, Astrid, Edwin, Martin, Albert, Peter, Esther, Juliette, Kristel en Marloes; bedankt voor de interesse die jullie toonden, de hulp op het lab en – last but not least – de gezelligheid tijdens uitjes en borrels. Anko de Graaf en Richard Wubbolts: bedankt voor de begeleiding op de confocal microscoop. Dick van der Ploeg, Arie van Nes, Johan van Amerongen, Louis van der Boom en de dierverzorgers van de Tolakker: jullie stonden altijd paraat om me te helpen met het verkrijgen van embryo's. Dank daarvoor, dat maakte het plannen van experimenten zo veel gemakkelijker.

(Ex-)Roomies! Regiane, Michael (from a distance), Chachote, Jason, Karlijn; thank you so much for the good times, nice breaks, the candy pot, 'lifting-up the spirit' moments, swimming, diner parties and the other stuff we did when avoiding to work.

Vrienden: Joyce, Femke, Martine, Laura, Anne, Misja, Cédric, Ilse, Milou, Pleuni, Annemarie, Maartje, Frederike, Rosanne, Kim, Barbara, Harrie en Roger; bedankt voor de nodige afleiding in de vorm van dinertjes, ‘eighties parties’ en wijntjes in de kroeg.

Lieve pap en mam, ik vind het knap dat jullie nog steeds de telefoon opnemen elke avond rond etenstijd om mij gezelschap te houden tijdens mijn fietstochtje naar huis! Maar nu serieus: dank voor alle steun en vertrouwen die jullie me geven. Kim en Tom: bedankt dat jullie altijd tijd voor me vrij maken om af te spreken wanneer ik een bezoekje aan zeeland breng. Oma: ook jij bedankt voor alle liefde en steun tijdens mijn studies.

Lieve Melvin, had ik je al verteld hoe blij ik ben dat wij samen zijn? Dankjewel voor je aanmoedigende woorden, je geduld, je knuffels, het vele treinen en je uiteindelijke verhuizing naar Utrecht en nog zoveel meer. Ik kijk uit naar onze toekomst samen.

Curriculum Vitae

Leonie du Puy werd geboren op 18 april 1981 te IJzendijke, Zeeuwsch-Vlaanderen. In 1999 behaalde zij haar VWO-diploma aan het ZwinCollege te Oostburg. Vervolgens studeerde zij Biologie aan de Universiteit Utrecht en specialiseerde zich in de Moleculaire Celbiologie. Tijdens deze specialisatie voerde ze twee onderzoeksstages uit. Gedurende haar eerste stage deed zij onderzoek naar de toxiciteit van gebromeerde vlamvertragers bij het Institute for Risk Assessment Sciences (IRAS); vervolgens onderzocht ze de gevolgen van prenatale dexamethason behandeling op de ontwikkeling van de hippocampus bij het Rudolph Magnus Instituut (RMI). Deze studie werd in april 2005 succesvol afgesloten met het behalen van het doctoraalexamen. In mei 2005 werd zij aangesteld als assistent in opleiding (AIO) aan de Hoofdafdeling Gezondheidszorg Landbouwhuisdieren van de faculteit Diergeneeskunde. Het onderzoek dat zij daar uitvoerde staat beschreven in dit proefschrift.

Leonie du Puy was born on April 18th 1981 in IJzendijke, The Netherlands. In 1999 she completed her secondary education at the 'ZwinCollege' in Oostburg. Thereafter, she studied Biology at Utrecht University, where she specialized in Molecular Cell Biology. Her specialization comprised two research internships: the first was conducted at the Institute for Risk Assessment Sciences (IRAS) where she investigated the toxicity of brominated flame retardants. For her second research internship, she studied the effects of prenatal dexamethasone treatment on hippocampal development in mice at the Rudolph Magnus Instituut (RMI). She obtained her biology degree in 2005, after which she started her PhD project at the Department of Farm Animal Health of the Faculty of Veterinary Medicine, which resulted in this thesis.

Publications

Du Puy L, Beqqali A, Haagsman HP, Roelen BAJ, Passier R.
CAZIP, a novel protein expressed in the developing heart and nervous system.
Developmental Dynamics, 238:2903–2911, 2009

Du Puy L, Chuva de Sousa Lopes SM, Haagsman HP, Roelen BAJ
Differentiation of porcine ICM cells into proliferating neural cells
Stem cells and development, in press.

Kuijk EW, du Puy L, van Tol HT, Haagsman HP, Colenbrander B, Roelen BAJ.
Validation of reference genes for quantitative RT-PCR studies in porcine oocytes and preimplantation embryos.
BMC Developmental Biology, 2007 May 31;7:58.

Kuijk EW, Du Puy L, Van Tol HT, Oei CH, Haagsman HP, Colenbrander B, Roelen BAJ.
Differences in early lineage segregation between mammals.
Developmental Dynamics, 2008 Apr;237(4):918-27.